Distribution and Function of Soil *Thaumarchaeota*

by

Xinda Lu

A thesis
presented to the University of Waterloo
in fulfillment of the
thesis requirement for the degree of
Doctor of Philosophy
in
Biology

Waterloo, Ontario, Canada, 2018

Examining Committee Membership

The following served on the Examining Committee for this thesis. The decision of the Examining Committee is by majority vote.

External Examiner	Dr. Jeanette Norton Professor, Utah State University
Supervisor(s)	Dr. Josh Neufeld Professor, University of Waterloo
Internal Member	Dr. Andrew Doxey Assistant Professor, University of Waterloo Dr. Barbara Butler Continuing Lecturer, University of Waterloo
Internal-external Member	Dr. Maren Oelbermann Associate Professor, University of Waterloo

Author's Declaration

This thesis consists of material all of which I authored or co-authored: see Statement of Contributions included in the thesis. This is a true copy of the thesis, including any required final revisions, as accepted by my examiners.

I understand that my thesis may be made electronically available to the public.

Statement of Contributions

Chapter 2

Brent Seuradge collected soil samples and extracted DNA.

Chapter 3

Graeme Nicol assisted with experimental design and data interpretation.

Chapter 4

Katherine Heal, Anitra Ingalls, and Andrew Doxey assisted with experimental design and data interpretation. Katherine Heal measured soil cobalamin.

Abstract

Despite the importance of ammonia-oxidizing archaea (AOA; *Thaumarchaeota*) to soil nitrification (Chapter 1), their biogeography in terrestrial environments and relative contributions to nitrification remain unclear. Leveraging the close proximity of forest, field, and agricultural plots at the ***rare*** Charitable Research Reserve (Cambridge, Ontario), thaumarchaeotal biogeography was examined at three different depths (0-15, 15-30, and 30-45 cm) from plots within areas of contrasting land usage (Chapter 2). High-throughput sequencing of thaumarchaeotal 16S rRNA gene sequences demonstrated that OTU richness was affected significantly by depth and land-use type. Specifically, thaumarchaeotal diversity was higher in soils from forest sites than from field sites, and lower within 0-15 cm soils than either 15-30 cm or 30-45 cm soils. Soil land use type influenced the relative abundance of the Soil Crenarchaeota Group (SCG), with a lower relative abundance of SCG in forest sites compared to field sites. At the OTU level, thaumarchaeotal communities changed with increasing soil depth for agricultural soils, in contrast to homogeneous depth profiles generated from forest site samples. Soil pH was the strongest factor impacting thaumarchaeotal community composition and, the evenness of archaeal taxa. Nitrogen, carbon, and soil texture shaped thaumarchaeotal community composition among field site samples.

Selected sites within the ***rare*** Charitable Research investigateg for temperature- and depth-dependence of AOA and ammonia-oxidizing bacteria (AOB) activities (Chapter 3). This work applied the recently discovered AOB inhibitor, octyne, to soil microcosms incubated at different temperatures (20, 30, 40°C) in order to differentiate ammonia-oxidation potential and N_2O production by AOA and AOB, in soils from different land uses and depth. The results showed that surface soils (0-15 cm) possessed significantly greater ammonia oxidation potential

than subsurface soils (30-45 cm) at all temperatures tested, and that AOA-associated nitrification potential dominated at higher temperatures for both summer- and autumn-collected soils. The accumulation of N_2O was only detected in surface agricultural soil at 30°C and positively correlated with nitrite accumulation within the incubation period. The detected N_2O production, along with most nitrification potential activity, were attributed to AOB, implicating AOB as major producers of this greenhouse gas in the tested agricultural soil. If consistent for other sites and land usages, higher ammonia-oxidation activity and N_2O production within surface agricultural soil reinforces the importance of agricultural surface soils as sources of nitrification and N_2O production, with potential implications for land management practices and responses to climate change.

In order to explore other functions of soil *Thaumarchaeota* besides ammonia oxidation, thaumarchaeotal cobalamin producing potential was targeted, and expanded to a broader range of cobalamin-producing and consuming microorganisms in soils (Chapter 4). Vitamin B_{12} (cobalamin) is the most structurally complex coenzyme known and its availability is thought to influence microbial diversity and community composition. Although previous studies have investigated marine cobalamin synthesis, the producers, remodelers, and consumers of cobalamin in terrestrial habitats are unknown. Here 155 globally distributed soil metagenomes were surveyed for cobalamin-producing microorganisms by quantifying and classifying cobalamin biosynthesis marker genes (*cob*/*cbi*) with profile hidden Markov models (HMMs). Complementing this sequence-based analysis, different forms of cobalamin (CN-, Me-, OH-, Ado-B_{12}) were measured, as well as the cobalamin lower ligand (5,6-dimethylbenzimidazole; DMB), in an independent set of 40 diverse soil samples. Metagenomic analysis revealed that less than 10% of soil microbial taxa are capable of complete cobalamin biosynthesis, predominantly

encoded by taxa affiliated with *Proteobacteria*, *Actinobacteria*, *Firmicutes*, *Nitrospirae*, and *Thaumarchaeota*. Consistent with vitamin production being a keystone community function, a larger proportion of soil genera possessed genes for cobalamin transport and lacked biosynthesis genes. In addition, cobalamin-dependent genes outnumbered cobalamin synthesis genes in all tested soil metagenomes. A significant positive correlation between cobalamin concentration and microbial biomass was observed, consistent with the metagenomic results showing that cobalamin-producing potential (*cob*/*cbi*) correlated positively with microbial community size (*rpoB*). Chemical measurements demonstrated that free water-leachable cobalamin was a relatively small portion of total cobalamin, compared to non-water-leachable cobalamin (associated with microbial biomass or tightly bound to minerals). The cobalamin lower ligand, DMB, was more abundant than intact cobalamin, in agreement with metagenome data showing a higher relative abundance of DMB synthesis *cob*/*cbi* genes than corrin ring synthesis or final assembly *cob*/*cbi* genes, suggesting an important role for cobalamin remodeling in terrestrial habitats. With broad implications for soil nutrient cycling and primary productivity (Chapter 5), these combined metagenomic and biochemical data implicate microbial cobalamin production as a keystone function that may influence total microbial community size, diversity, and associated biogeochemistry of terrestrial ecosystems.

Acknowledgements

I would like to express my sincere gratitude to my advisor Dr. Josh Neufeld for his patience and encouragement throughout my research and graduate program. Josh was always quick in responding to emails and willing to talk science. Also, he encouraged me to network with a broad range of scientists at conferences and on social media. I am also grateful to my committee members, Drs. Andrew Doxey and Barbara Butler, for their help and dedication to improving my research.

I would like to thank staff of the ***rare*** Charitable Research Reserve for providing access to soil sample sites, especially Jenna Quinn and John MacDonald who assisted me with my field work. I am so grateful to Jackson Tsuji, Dr. Michael Lynch, and Dr. Wei Qin for their endless help and encouragement throughout my whole program, Katja Engel for her training, and all the Neufeld lab members for the casual and creative working atmosphere. I appreciate all collaborators, Dr. Anitra Ingalls, Dr. Katherine Heal, and Dr. Graeme Nicol for helping with my research in many ways. Undergraduate volunteers, Ola Oni and Norman Tran, are thanked for help with soil incubation experiments.

Finally, I would like to thank my parents for their constant and solid support, and friends back in Oregon, Dr. David Myrold, Dr. Peter Bottomley, Trang Nguyen, Dr. Fumiaki Funahashi, Rosa Hill, and Matthew McClintock, for their help and encouragement.

Table of Contents

List of Figures

List of Tables

List of Abbreviations

Ado-B_{12}	Adenosylcobalamin
amoA	Gene encoding alpha subunit of ammonia monooxygenase
AMO	Ammonia monooxygenase
ANOVA	Analysis of variance
AOA	Ammonia-oxidizing archaea
AOB	Ammonia-oxidizing bacteria
ATU	Allylthiourea
btuB	Gene encoding vitamin B_{12} transporter
CCA	Canonical correspondence analysis
CN-B_{12}	Cyanocobalamin
cob/*cbi*	Cobalamin biosynthesis genes
comammox	Complete ammonia oxidation
db-RDA	Distance-based redundancy analysis
DCA	Detrended correspondence analysis
DCD	Dicyandiamide
DMB	5,6-dimethylbenzimidazole
HAO	Hydroxylamine oxidoreductase
HMM	Hidden Markov model
Me-B_{12}	Methylcobalamin
metH	Gene encoding methionine synthase
MS	Mass spectrometry
mutA	Gene encoding methylmalonyl-CoA mutase
NirK	Nitrite reductase
NMDS	Non-metric multidimensional scaling
NO	Nitric oxide
N_2O	Nitrous oxide

NorB	Nitric oxide reductase
NOB	Nitrite-oxidizing bacteria
NP	Nitrification potential
NXR	Nitrite oxidoreductase
nxrB	Gene encoding beta subunit of nitrite oxidoreductase
OC	Organic carbon
OH-B_{12}	Hydroxocobalamin
PCR	Polymerase chain reaction
PTIO	2-phenyl-4,4,5,5-tetramethylimidazoline-1-oxyl 3-oxide
RDA	Redundancy analysis
rpoB	Gene encoding beta subunit of RNA polymerase
rRNA	Ribosomal RNA
rsmB	Gene encoding ribosomal small subunit methyltransferase
UPLC	Ultra performance liquid chromatography
VIF	Variance inflation factor

Chapter 1

From ammonia-oxidizer to comammox: a review of soil nitrification

1.1 Introduction

Nitrogen is a key element controlling terrestrial productivity and an estimated 170 Tg yr^{-1} of anthropogenic nitrogen is applied to terrestrial surfaces and the corresponding microbially driven nitrogen cycle (Schlesinger 2009). Nitrification, ammonia oxidation to nitrate via nitrite, plays a critical role in linking reduced with oxidized pools in the global nitrogen cycle (Prosser 1990). Nitrification is economically important for agricultural practices because it can decrease fertilizer efficiency by converting ammonium (NH_4^+) into water-leachable nitrate (NO_3^-) (Allison 1966), causing groundwater and surfacewater contamination. The conventional view of nitrification divides the process into two steps, ammonia oxidation and nitrite oxidation, and the first step is generally considered rate-limiting (Prosser 1990). Ammonia oxidation has been regarded traditionally as being catalyzed solely by ammonia-oxidizing bacteria (AOB), chemoautotrophs within the *Proteobacteria* (Purkhold *et al.* 2000; Kowalchuk and Stephen 2001), since the first isolation of *Nitrosomonas europaea* by Sergei Winogradsky in 1892 (Winogradsky 1892; Dworkin and Gutnick 2012). Starting with the pioneering phylogenetic analyses of AOB (Woese *et al.* 1984, 1985), the phylogenetic framework of AOB now includes two distinct monophyletic groups. One group includes *Nitrosospira* and *Nitrosomonas*, belonging to *Betaproteobacteria*, and the other includes *Nitrosococcus* species from the *Gammaproteobacteria* (Koops *et al.* 2006). Most soil AOB affiliate with *Betaproteobacteria*, whereas marine AOB typically associate with the *Gammaproteobacteria*. However, a recently discovered *Nitrosococcus* strain TAO100 (*Gammaproteobacteria*) is an exception to this rule, obtained from an acidic soil (Hayatsu *et al.* 2017). The *Nitrosospira* lineage is subdivided into

clusters 0-4, on the basis of 16S rRNA sequence analysis, and *Nitrosomonas* fall into clusters 5-7 (Stephen *et al.* 1996; Purkhold *et al.* 2000), although this subdivision is somewhat controversial (Aakra *et al.* 2001). In soil environments, AOB distributions have been well linked with pH. In acidic soils, where ammonia availability is reduced by conversion to ammonium, *Nitrosospira* dominate, especially those from cluster 2 (Stephen *et al.* 1998; Kowalchuk and Stephen 2001). Members of the *Nitrosospira* associate with moderately acidic soils and *Nitrosomonas* spp. are reported to dominate neutral soils (Koops and Pommerening- Röser 2001). However, pH might not be always the only factor that influences the distribution of these microorganisms (Norton 2011). In a study of 23 soil samples, temperature appeared to be the best predictor of AOB community composition, with higher proportion of *Nitrosospira* cluster 2 in soils from lower annual temperature sites (Fierer *et al*. 2009). A similar pattern was reported by Avrahami and Conrad (2005), who observed more *Nitrosospira* taxa in cold soils than warm ones.

Although much research on AOB has demonstrated their importance in the soil nitrogen cycle (Kowalchuk and Stephen 2001), a disconnect was observed between AOB abundance estimations and nitrification rates in the ocean (Watson 1965), suggesting that something was missing. This AOB-centric understanding of nitrification was upended early in the 21st century, when metagenomic studies of marine (Venter *et al.* 2004) and soil (Treusch *et al.* 2005) samples revealed crenarchaeotal ammonia monooxygenase (*amoA*) genes on archaeal scaffolds, shedding light on potential archaeal ammonia oxidation in non-extreme environments, although archaea were still largely considered as extremophiles. Mesophilic *Crenarchaeota* (currently *Thaumarchaeota*; Spang *et al*. 2010) are now recognized as being ubiquitous in marine water (DeLong 1992; Fuhrman 1992), freshwater sediments (Hershberger *et al.* 1996; MacGregor *et al.* 1997; Schleper, Holben and Klenk 1997), and soil (Ueda, Suga and Matsuguchi 1995; Bintrim *et*

al. 1997; Ochsenreiter *et al.* 2003), indicating an important role for archaeal ammonia oxidation globally.

The hypothesis that some archaea catalyze ammonia oxidation was confirmed by the first isolation of *Nitrosopumilus maritimus* from a marine aquarium, which provided incontrovertible evidence for chemoautotrophic growth while oxidizing ammonia into nitrite, with bicarbonate as the sole carbon source (Könneke *et al.* 2005). It took several more years before isolation of the first soil ammonia-oxidizing archaea (I.1b AOA), *Nitrososphaera viennensis*, from a garden soil in Vienna (Tourna *et al.* 2011). Another I.1b AOA enrichment, *Candidatus* Nitrososphaera gargensis originated from a hot spring (Hatzenpichler *et al.* 2008); a pure culture was obtained recently (Palatinszky *et al.* 2015). Enrichment cultures of I.1b AOA originate from an even broader range of environments where these archaea contribute to ammonia oxidation. For example, *Candidatus* Nitrosotalea devanaterra was enriched from an acidic agricultural soil, demonstrating optimal growth at pH 4-5 (Lehtovirta-Morley *et al.* 2011), *Candidatus* Nitrosocosmicus franklandus originated from a fertilized soil (Lehtovirta-Morley *et al.* 2016), and *Candidatus* Nitrocosmicus oleophilus MY3 was obtained from a coal tar contaminated sediment (Jung *et al.* 2016). These I.1b AOA are very similar to *Candidatus* Nitrosocosmicus exaquare G61, which was enriched recently from rotating biological contactors of a municipal waste water treatment plant (Sauder *et al.* 2017). Together, these isolates and enrichment cultures provide a valuable way to look into AOA physiology under varying physical and chemical gradients relevant to soils.

Unlike ammonia oxiders, very little is known about nitrite-oxidizing bacteria (NOB), partially due to the fact that they are more difficult to grow in the lab (Daims, Lücker and Wagner 2016). As a result, the classification and characterization of NOB and their

environmental distributions depend heavily on culture-independent 16S rRNA gene sequence analysis. Soil-associated NOB typically belong to the genera *Nitrococcus*, *Nitrotoga*, *Nitrobacter*, and *Nitrospira* (Daims, Lücker and Wagner 2016), and *Nitrobacter* and *Nitrospira* often dominate in soils (Bartosch *et al.* 2002; Freitag *et al.* 2005; Poly *et al.* 2008; Wertz *et al.* 2008; Pester *et al.* 2014; Stempfhuber *et al.* 2016). Interactions between soil NOB and ammonia oxidizers are still poorly characterized, but transient NO_2^- accumulation in soil has been demonstrated (Chapman and Liebig 1952; Nelson 1982; Burns *et al.* 1995; Maharjan and Venterea 2013; Müller *et al.* 2014; Giguere *et al.* 2017). The classical concept of nitrification proposes that NOB rely on ammonia oxidizers for nitrite (Prosser 1990), thus ammonia oxidizers can benefit from nitrite detoxification. Observations of nitrite accumulation contradict the widely accepted view that ammonia oxidation is the rate-limiting step in nitrification and opens up an opportunity for follow-up studies that focus on nitrite accumulation and its ecological effects in soils.

Members of the *Nitrospira* have recently been discovered that catalyze complete ammonia oxidation ("comammox") to nitrate, which changes the conventional two-step nitrification paradigm (Daims *et al.* 2015; van Kessel *et al.* 2015). The hypothetical presence of comammox microorganisms was predicted because the energy yield from complete nitrification is higher than from either of ammonia oxidation or nitrite oxidation, and thus comammox microorganisms should be able to outcompete canonical nitrifiers (Costa, Pérez and Kreft 2006). The first comammox bacterial isolate, *Nitrospira inopinata*, confirms an oligotrophic lifestyle with high substrate affinity and high growth yield. (Kits *et al.* 2017).

1.2 Distribution, diversity, and activity of soil ammonia oxidizers

Soil represents an immense and complex habitat for an enormous diversity of microorganisms (Tiedje *et al.* 1999; Bardgett and van der Putten 2014; Thompson *et al.* 2016; Delgado-Baquerizo *et al.* 2018; Richter and Markewitz 1995; Frey 2007). Ammonia-oxidizers are ubiquitous and abundant in soils, including agricultural (Jia and Conrad 2009; Ouyang *et al.* 2016), forest (Taylor *et al.* 2010; Lu, Bottomley and Myrold 2015), estuary (Li *et al*. 2015), grassland (Daebeler *et al*. 2015), desert (Marusenko *et al*. 2014), and Arctic tundra (Alves *et al*. 2013) soils, with the detection of either 16S rRNA gene or the functional marker gene, *amoA*, which encodes subunit A of the key enzyme, ammonia monooxygenase (AMO). The *amoA* gene is the most extensively used functional marker for ammonia oxidizer biogeography studies (Rotthauwe, Witzel and Liesack 1997; Purkhold *et al.* 2000; Pjevac *et al.* 2017). Soil AOA, estimated to account for up to 5% of all terrestrial prokaryotes (Leininger *et al.* 2006), outnumber their AOB counterparts in most soils by as much as several orders of magnitude (Leininger *et al.* 2006; He *et al.* 2007; Taylor *et al.* 2010; Alves *et al.* 2013) with only a few exceptions (Bates *et al.* 2011; Petersen *et al.* 2012; Li *et al.* 2015). A survey studying 713 soil samples from the National Soil Inventory of Scotland reported a dominance of AOA over AOB in all samples across different land-uses types (Yao *et al.* 2013), which is consistent with another survey of samples spanning forest, cropland, and pasture soils in Oregon, in which the highest reported AOA to AOB *amoA* gene ratio was 396:1 in pasture samples (Zeglin *et al.* 2011). This numerical dominance of AOA over AOB in soils implies a greater role for ammonia oxidation by AOA than AOB. Environmental gradients of temperature, soil C:N, and moisture influence AOA and/or AOB abundances (Adair and Schwartz 2008), as do factors linked to soil depth (Leininger *et al.* 2006; Jia and Conrad 2009), such as nitrogen and carbon availability (Leininger

et al. 2006). Although AOB *amoA* abundances are correlated with soil physiochemical factors (percent sand, C:N ratio), precipitation, and temperature, no such relationship was established between AOA populations and any of these environmental factors, although AOA dominated all sampling sites (Adair and Schwartz 2008). Orders of magnitude higher AOA and AOB *amoA* gene abundances were recorded from top 20 cm soils than from 40-50 cm at the same agricultural site (Jia and Conrad 2009) and the same pattern was observed as deep as 60-70 cm in a sandy soil (Leininger *et al.* 2006). The abundances of AOA and AOB vary along environmental gradients, and this variation might be a key strategy for ammonia oxidizers, as a whole, to survive and function in such a diverse and heterogeneous soil habitat and, sometimes, extreme conditions (low pH and high temperature) where AOA are more likely to thrive.

Both pH and temperature emerge as key factors that affect niche differentiation of AOA and AOB, and thus impact activity responses of these two group in soils. In a study of agricultural soils, greater AOA-associated activity was observed in warmer seasons (Taylor *et al.* 2012), and temperature optima of AOA are typically higher than AOB (Tourna *et al.* 2008, 2011; Duan *et al.* 2018; Lu, Nicol and Neufeld 2018), with cases where this optimal temperature difference could be greater than 10°C (Ouyang, Norton and Stark 2017; Taylor *et al.* 2017). A quantitative study reported that 16S rRNA genes representing members of the *Crenarchaeota* from non-hyperthermal environments (-1.5 to 32°C) accounted for as much as ~1.5% of all 16S rRNA genes detected in several soil samples (Buckley, Graber and Schmidt 1998). The two phylogenetic clusters of these environmental mesophilic-crenarchaeotal sequences are groups I.1a (mainly marine or freshwater sequences), and I.1b (mainly terrestrial sequences), characterized both by phylogenetic distance and correlating relatively well with the predominant habitats where they were detected (Schleper, Jurgens and Jonuscheit 2005). Group I.1c

Thaumarchaea are not associated with ammonia oxidation (Weber *et al*. 2015), despite their high abundance in acidic forest soils (Jurgens, Lindström and Saano 1997; Bomberg and Timonen 2009) and close relation with groups I.1a and I.1b (DeLong 1998). Soil AOA and AOB isolates and enrichment cultures showed different optimal growth temperatures. For instance, thaumarchaeotal *Candidatus* Nitrosotalea devanaterra grows optimally at 25°C (Lehtovirta-Morley *et al.* 2011), *Candidatus* Nitrosocosmicus franklandus at 40°C (Lehtovirta-Morley *et al.* 2016), and *Candidatus* Nitrososphaera gargensis at 46°C (Hatzenpichler *et al.* 2008). In contrast, AOB representatives usually grow at temperatures between 20-30°C (Groeneweg, Sellner and Tappe 1994; Jiang and Bakken 1999; Avrahami and Conrad 2005; Avrahami and Bohannan 2007), with some reported to grow even at temperatures between 0-4°C (Jones *et al.* 1988; Groeneweg, Sellner and Tappe 1994; Jiang and Bakken 1999).

Among soil edaphic factors, pH is a strong environmental selector for different ammonia oxidizing groups (Nicol *et al.* 2008). Culture-independent surveys detect *Nitrosospira* as the dominant AOB in acidic agricultural (Stephen *et al.* 1996, 1998) and forest (Laverman *et al.* 2001; Jordan *et al.* 2005; Schmidt *et al.* 2007; Nugroho *et al.* 2009) soils, whereas *Nitrosomonas* sequences dominated an acid forest soil (Carnol, Kowalchuk and De Boer 2002). Members of the *Nitrosospira* also dominated neutral pH fields that received fertilization (Bruns *et al.* 1999; Mendum, Sockett and Hirsch 1999). A dominance switch from *Nitrosospira* cluster 2 in acidic pH to *Nitrosospira* cluster 3 in neutral pH has been generalized in both short- and long-term studies (Stephen *et al.* 1996, 1998; Nicol *et al.* 2008). Cultivation of acid-tolerant soil AOB has been successful and activity was observed at pH 4 (De Boer *et al.* 1991) and 5 (Hayatsu *et al.* 2017). As for soil AOA, cluster distributions show the influence of pH. For instance, AOA in neutral pH soils are usually dominated by *Nitrososphaera*, with presence of *Nitrosopumilus*, and

Nitrosocosmicus (Gubry-Rangin *et al.* 2011; Lu, Seuradge and Neufeld 2017), whereas in acidic soils, *Nitrososphaera* and *Nitrosotalea* both are abundant (Gubry-Rangin *et al.* 2011; Lehtovirta-Morley *et al.* 2011). Little is known about nitrification in alkaline soils, and no obligately alkalinophilic ammonia oxidizers have been cultivated, although *amoA* sequences were detected in these soils with pH values over 7 (Shen *et al.* 2008; Gubry-Rangin *et al.* 2011). Soil pH can influence the equilibrium between ammonia and ammonium ($pK_a = 9.27$), which is relevant because ammonia serves as the substrate for AOB (Suzuki, Dular and Kwok 1974) and presumably also for AOA. Acidic soils favor the presence of ammonium, rather than ammonia, and can potentially decrease ammonia availability by orders of magnitude with a small pH change. AOB pure cultures typically do not grow on ammonium below pH 6.5 (Allison and Prosser 1993), but ureolytic AOB such as *Nitrosospira* can grow at pH 4 (Burton and Prosser 2001). Urea hydrolysis has also been demonstrated in AOA from two acidic soils (Lu *et al.* 2012). Another mechanism applied by acid-tolerant ammonia oxidizers is forming aggregates, where internal cells are protected against unfavorable conditions such as toxic nitrous acid (De Boer *et al.* 1991).

Ammonia concentration can also select for AOA or AOB (Bates *et al.* 2011; Verhamme, Prosser and Nicol 2011), independent of a pH-ammonia interaction. With lower substrate affinities, compared to their AOA counterparts (Prosser and Nicol 2012; Lehtovirta-Morley 2018), AOB dominate fertilized agricultural soils based on several reports (Prosser and Nicol 2008; Jia and Conrad 2009; Xia *et al.* 2011; Ouyang *et al.* 2016; Zhong *et al.* 2016). In general, AOB are stimulated by high ammonia concentrations, whereas AOA prefer low ammonia concentrations (Di *et al.* 2010; Höfferle *et al.* 2010; Schleper 2010; Tourna *et al.* 2011; Verhamme, Prosser and Nicol 2011; Daebeler *et al.* 2015; Carey *et al.* 2016), with the exception

of *Nitrosocosmicus*, which are also adapted to high ammonia concentrations (Lehtovirta-Morley *et al.* 2016; Sauder *et al.* 2017). One possible explanation for high ammonia tolerance of *Nitrosocosmicus* is the lack of S-layer (Sauder *et al.* 2017), which is a major cell surface structure for general rigidity and protection (Albers and Meyer 2011), and common in other AOA (Qin *et al.* 2017a). Computational simulations demonstrated the pseudo periplasmic space and a charged S-layer in AOA effectively concentrated NH_4^+ to the membrane-associated AMO in AOA (Li *et al.* 2018). When this S-layer is absent, AMO will not be easily exposed to pre-concentrated NH_4^+, thus increasing cell ammonia tolerance. Substrate source seems to be another substrate-linked filter for AOA and AOB. Several AOB populations responded when ammonium was added directly to soil (Jia and Conrad 2009), whereas archaeal ammonia oxidation in soils might be fueled by ammonia derived from other compounds, such as urea and cyanate (Stopnišek *et al.* 2010; Levičnik-Höfferle *et al.* 2012; Palatinszky *et al.* 2015). However, AOB can also grow on fructose and pyruvate (Hommes, Sayavedra-Soto and Arp 2003), and AOA responded positively to direct nitrogen addition (Marusenko, Garcia-Pichel and Hall 2014).

Because AOA and AOB coinhabit soils, with varying relative abundances, an important research goal is to determine the relative contributions of these two groups to soil ammonia oxidation. Nitrification inhibitors such as dicyandiamide (DCD), allylthiourea (ATU), and nitrapyrin (2-chloro-6-[trichloromethyl] pyridine) are used to reduce nitrogen fertilizer loss and also commonly used for research where differential inhibition is required (Bédard and Knowles 1989; Subbarao *et al.* 2006; Lehtovirta-Morley *et al.* 2013). Both ATU and octyne have been used as differential inhibitors to distinguish between the activities of AOA and AOB (Hatzenpichler *et al.* 2008; Taylor *et al.* 2010, 2013; Jung *et al.* 2014b). The differential inhibition effect depends on inhibitor concentration. For example, all ammonia oxidation of *N.*

europaea (AOB) was inhibited by 10 μM ATU (Hooper and Terry 1973), 85% of the ammonia oxidation activity of *N. devanaterra* (AOA) was inhibited at a concentration of 100 μM (Lehtovirta-Morley *et al.* 2013), and 100% of *N. viennensis* (AOA) activity was inhibited at 300 μM (Shen *et al.* 2013). As an AOB inhibitor, octyne does not inhibit ammonia oxidation by either *N. viennensis* or *N. gargensis* at a concentration of 10 μM, which is sufficient to inhibit AOB fully (Taylor *et al.* 2010). However, AOA-associated ammonia oxidation can be inhibited by 20 μM octyne (Taylor *et al.* 2015). In addition to ATU and octyne inhibiting AOB activity, 2-phenyl-4,4,5,5-tetramethylimidazoline-1-oxyl 3-oxide (PTIO) has been used as an AOA inhibitor. The differential effect of PTIO on AOA and AOB was proposed given that AOA might use a pathway that does not produce hydroxylamine, but rather nitroxyl, and PTIO acts as an NO scavenger (Walker *et al.* 2010). However, with the demonstrated ability to produce hydroxylamine by *N. maritimus* (Vajrala *et al.* 2013), it is currently proposed that NO might act as an electron shuttle rather than a direct intermediate in the AOA ammonia oxidation pathway (Jung *et al.* 2014b; Sauder, Ross and Neufeld 2016).

In addition to catalyzing the conversion of ammonia to nitrate, greenhouse gas emission linked to ammonia oxidation is another important environmental implication of nitrification. Nitrous oxide (N_2O) is a trace gas with ~300 fold greater global warming potential than CO_2, and also a reactant causing ozone destruction (Ravishankara, Daniel and Portmann 2009), with soil being the largest N_2O source (Syakila and Kroeze 2011; Schreiber *et al.* 2012). Ammonia oxidation is a major contributor of N_2O produced aerobically, accounting for up to 80% of soil N_2O emissions (Gödde and Conrad 1999; Wrage *et al.* 2001; Kool *et al.* 2011; Zhu *et al.* 2013). Although AOB-associated N_2O could be produced through either incomplete hydroxylamine oxidation to nitrite or nitrifier-denitrification (reduction of nitrite) (Arp and Stein 2003),

hydroxylamine-dependent N_2O production is thought to contribute less N_2O than nitrifier denitrification (Arp and Stein 2003; Stein 2011a). The activities of nitrite reductase (NirK) and nitric oxide reductase (NorB) enable N_2O production by AOB through nitrite reduction. Thus, nitrite accumulation has been demonstrated to stimulate aerobic N_2O production in soil (Venterea 2007; Maharjan and Venterea 2013; Venterea *et al.* 2015; Lu, Nicol and Neufeld 2018), and by AOB (Shaw *et al.* 2006). Although the mechanism of AOA-associated N_2O production has not been fully elucidated, an abiotic reaction between hydroxylamine and nitric oxide, both of which have been detected in AOA pure culture (Vajrala *et al.* 2013; Martens-Habbena *et al.* 2015), might result in N_2O formation (Stieglmeier *et al.* 2014). The potential for N_2O production by AOA through nitrifier-denitrification is still unclear, with contrasting observations on N_2O production at variable oxygen concentrations (Jung *et al.* 2011; Löscher *et al.* 2012; Mosier, Lund and Francis 2012; Stieglmeier *et al.* 2014; Qin *et al.* 2017b). With a differential inhibitor of AOA and AOB, N_2O production in soil microcosm incubations was monitored for several soil samples (Giguere *et al.* 2017; Hink, Nicol and Prosser 2017; Duan *et al.* 2018; Hink *et al.* 2018; Lu, Nicol and Neufeld 2018), demonstrating lower N_2O emissions by AOA than AOB, further suggesting an alternative enzymatic pathway for AOA (Hink, Nicol and Prosser 2017; Lu, Nicol and Neufeld 2018). Specifically, N_2O formation in acidic soils might be due to nitrosonium cation (NO^+), which is favored at low pH and reacted with hydroxylamine to produce N_2O (Spott, Russow and Stange 2011; Qin *et al.* 2017b), and might be a reason for extremely high N_2O yields reported from a soil acidophilic AOA isolate relative to other AOA (Jung *et al.* 2014b).

1.3 Distribution, diversity, and activity of soil nitrite oxidizers

In terrestrial ecosystems, nitrite is oxidized by chemolithoautotrophic nitrite-oxidizing bacteria (NOB; *Alphaproteobacteria*, *Betaproteobacteria*, *Gammaproteobacteria*, *Chloroflexi*, *Nitrospinae*, and *Nitrospirae*) (Robertson and Groffman 2007; Daims, Lücker and Wagner 2016). *Nitrobacter* and *Nitrospira* are dominant nitrite-oxidizing genera in most sampled soils (Bartosch *et al.* 2002; Freitag *et al.* 2005; Poly *et al.* 2008; Wertz *et al.* 2008; Pester *et al.* 2014; Stempfhuber *et al.* 2016), although *Nitrotoga* were recently discovered as important for active layer permafrost tundra soils (Alawi *et al.* 2007) or surface periglacial soil (Schmidt *et al.* 2009). Compared to *Nitrobacter*, *Nitrospira* have lower half saturation constants for NO_2^- (Blackburne *et al.* 2007; Nowka, Daims and Spieck 2015; Le Roux *et al.* 2016), thus their dominance in NOB communities shows responses to varied nitrite concentrations in soil (Attard *et al.* 2010; Wertz, Leigh and Grayston 2012; Daebeler *et al.* 2014). Although cultivation challenges have slowed progress in studying NOB, compared with ammonia oxidizers, they are among the most diverse and ubiquitous nitrifiers in both natural and engineering systems (Daims *et al.* 2001), and can outnumber AOA and AOB (Winkler *et al.* 2012; Gülay *et al.* 2016). Transient nitrite accumulation in soils has been demonstrated in several studies due to either an increased ammonia oxidation (Müller, Stevens and Laughlin 2006; Giguere *et al.* 2017) or a decreased NOB activity (Chapman and Liebig 1952; Burns *et al.* 1995; Shen, Ran and Cao 2003; Venterea 2007; Maharjan and Venterea 2013; Ma, Shan and Yan 2015; Venterea *et al.* 2015). In agricultural practices, NO_2^- accumulation is reported after fertilization that undergo alkaline hydrolysis, which would inhibit NO_2^- oxidation because of high pH (Smith and Chalk 1980; Burns *et al.* 1995; Van Cleemput and Samater 1995). These observations of NO_2^- accumulation implicate nitrite oxidation as the rate-limiting step of nitrification under certain conditions. The

accumulated NO_2^- may significantly impact terrestrial ecosystems, as it is toxic to soil microorganisms and plants (Court, Stephen and Waid 1962; Bancroft, Grant and Alexander 1979), and NO_2^- accumulation is also suggested to stimulate soil N_2O emission (Maharjan and Venterea 2013; Giguere *et al.* 2018; Lu, Nicol and Neufeld 2018).

The understanding of NOB biogeography mainly depends on surveys of nitrite oxidoreductase (NXR), encoded by its corresponding gene (*nxrB*), which has served as a powerful marker to detect uncultured NOB in soils (Poly *et al.* 2008; Pester *et al.* 2014). This gene is particularly useful because its phylogeny is consistent with that of the 16S rRNA gene (Pester *et al.* 2014). Based on *nxrB* gene similarity, up to 764 "species" were affiliated with *Nitrospira* in a soil sample from Namibia (Pester *et al.* 2014). NXR, a membrane-bound enzyme, initiates nitrite oxidation by adding an oxygen atom from water (Kumar, Nicholas and Williams 1983). However, the direction to which the catalytic site of NXR faces differs between *Nitrobacter* and *Nitrospira*, with cytoplasmic and periplasmic orientations, respectively (Spieck and Bock 2005). This structural difference might explain the high substrate sensitivity and affinity of *Nitrospira* in comparison to *Nitrobacter* (Spieck and Bock 2005). The reaction catalyzed by NXR can be reversible, such that *Nitrobacter* can reduce nitrate (Sundermeyer-Klinger *et al.* 1984), which enables heterotrophic growth with nitrate as alternative electron acceptor under anoxic conditions (Bock, Wilderer and Freitag 1988).

Because NOB rely on the end products of ammonia oxidizers, a classical mutualistic symbiosis between these microbial groups was proposed, where ammonia oxidizers can benefit from nitrite detoxification by NOB (Stein and Arp 1998). Consistent with this possible mutualism, soil AOA and *Nitrospira* abundances were shown to correlate with each other (Pester *et al.* 2014). In this model, ammonia oxidizers initiate nitrification, followed by nitrite oxidation.

Although ammonia oxidizers initiating symbiosis has been widely observed, there might be exceptions where NOB can initiate nitrification by releasing urease, as observed in soils where urea is available (Koch *et al.* 2015). In addition to urea, cyanate may also be a substrate for nitrifiers, from which ammonia could be generated with cyanase (Palatinszky *et al.* 2015). Metagenomes demonstrated the presence of *Nitrospira*-like cyanases in temperate forest and agricultural soils, indicating a similar reciprocal feeding between cyanase-negative ammonia oxidizers and cyanase-positive NOB (Palatinszky *et al.* 2015).

The mechanisms employed by ammonia oxidizers and nitrite oxidizers to signal and maintain efficient nitrification are not clear. However, evidence for quorum sensing (QS) among nitrifying bacteria has been emerging. QS signal molecules, acyl-homoserine lactones (AHL), have been reported produced by AOB (Burton *et al.* 2005; Gao *et al.* 2014), and NOB (Mellbye, Bottomley and Sayavedra-Soto 2015), and proposed to connect AOB with NOB (Mellbye *et al.* 2017). Nitric oxide (NO) might also function to enhance interactions between ammonia oxidizers and nitrite oxidizers (Daims, Lücker and Wagner 2016) because all sequenced NOB possess nitrite reductase (*nirK*), an indicator of NO-producing potential. In this way, NO might function as an electron flux regulator (Starkenburg, Arp and Bottomley 2008). Both AOA and AOB can produce NO (Stein 2011b; Kozlowski *et al.* 2016) and trigger biofilm formation (Schmidt *et al.* 2004; Arp and Bottomley 2006). Thus, NO release by either NOB or AOA/AOB within nitrification aggregates might potentially act to modulate the metabolisms of both ammonia and nitrite oxidizers (Daims, Lücker and Wagner 2016).

1.4 Comammox bacteria and soil nitrification

The widely accepted two step nitrification process paradigm was challenged by a thermodynamic prediction of the presence of complete ammonia oxidation (comammox), which

should be favored due to a higher energy yield (Costa, Pérez and Kreft 2006). A decade later, the first *Nitrospira* capable of oxidizing ammonia to nitrate were discovered (Daims *et al.* 2015; van Kessel *et al.* 2015). All known comammox bacteria are members of *Nitrospira* lineage II, which also contains members of the canonical NOB (Daims *et al.* 2015; van Kessel *et al.* 2015; Pinto *et al.* 2016). Three key nitrification enzymes, ammonia monooxygenase (AMO), hydroxylamine oxidoreductase (HAO), and nitrite oxidoreductase (NXR), are found in comammox *Nitrospira* (Daims *et al.* 2015). Comammox *amoA* genes form two monophyletic clades, clade A and clade B, and both share a common ancestor with betaproteobacterial AOB *amo* (Daims *et al.* 2015). Metagenomic screening for *Nitrospira*-like *amoA* genes revealed a wide distribution of commamox bacteria, including soil samples collecting under different land use types (Daims *et al.* 2015; van Kessel *et al.* 2015; Pinto *et al.* 2016). A recently developed comammox *amoA* primer set was used to survey for the presence of comammox bacteria in a wide range of environmental samples, including rice paddy soils, forest soils, and rice rhizosphere (Pjevac *et al.* 2017). Another quantitative study of 300 forest soil samples with the same primer set demonstrated a high abundance of comammox *Nitrospira* across all samples, in comparison to canonical AOB, and they found that clade A comammox bacteria were more abundant than AOA in acidic samples (Hu and He 2017). Physiological assessments revealed oligotrophic adaptations for comammox *Nitrospira*, suggesting a possibility that ammonia-depleted soils might be a fundamental niche for these organisms (Kits *et al.* 2017).

1.5 Cobalamin production and its ecological importance

Cobalamin (vitamin B_{12}) is an important coenzyme required by most organisms for the synthesis of nucleotides and amino acids (Roth, Lawrence and Bobik 1996; Romine *et al.* 2017), its biosynthesis requires more than 30 enzymatic steps (Roth *et al.* 1993; Blanche *et al.* 1995;

Raux *et al.* 1999), and it can only be produced by a limited number of bacteria and archaea (Martens *et al.* 2002). Cobalamin is present in several chemical forms, depending on its upper ligand, which includes the enzymatically active forms of methylcobalamin (Me-B_{12}) and adenosylcobalamin (Ado-B_{12}), and the less active forms of hydroxocobalamin (OH-B_{12}) and cyanocobalamin (CN-B_{12}) (Martens *et al.* 2002). Cobalamin is light sensitive. Both Ado-B_{12} and Me-B_{12} photodegrade to OH-B_{12} within seconds of light exposure (Juzeniene and Nizauskaite 2013). The challenge of accurately measuring cobalamin concentrations in marine samples was overcome by using ultra-performance liquid chromatography (Heal *et al.* 2014). Marine cobalamin research demonstrated a significant role for cobalamin in controlling microbial plankton population and primary productivity (Panzeca *et al.* 2006; Tang, Koch and Gobler 2010; Bertrand *et al.* 2011; Giovannoni 2012; Sañudo-Wilhelmy *et al.* 2014; Helliwell *et al.* 2016). Pseudocobalamin, with adenine as a lower ligand (Renz 1999), has recently been identified as another major cobalamin-like compound in the ocean that cannot be used by most cobalamin-dependent bacteria (Heal *et al.* 2017). *Cyanobacteria*, on the other hand, have the advantages of producing and using only pseudocobalamin, whereas many other cobalamin-dependent organisms can convert pseudocobalamin into cobalamin by remodeling the lower ligand with DMB (Seth and Taga 2014; Helliwell *et al.* 2016).

In marine environments, *Thaumarchaeota* have been identified as the major cobalamin producers in a metagenomic survey (Doxey *et al.* 2015). Recent research demonstrated that all sequenced *Thaumarchaeota* strains have the potential to biosynthesize cobalamin (Doxey et al. 2015, Heal *et al.* 2017), and the measured per cell cobalamin concentration for *Thaumarchaeota* can be orders of magnitude higher than recorded in other phyla (Heal *et al.* 2017, 2018). Comparatively little is known about terrestrial cobalamin sources and sinks. Stimulation of soil

microbial growth by cobalamin was reported in the 1950s (Lochhead and Thexton 1951; Lochhead, Burton and Thexton 1952; Lochhead and Burton 1956). These studies predicted that some soil microorganisms might serve as cobalamin producers because they demonstrated that a high proportion of soil bacteria rely on cobalamin, and soil contains a wide variety of vitamin auxotrophs. Lochhead and Burton (1956) estimated the proportion of soil bacteria that require vitamin B_{12} using a semi-quantitative experiment, and suggested the importance of "growth-promoting" substances to soil microorganisms. Soil eukaryotes also rely on cobalamin (Watson *et al.* 2014), but more studies are needed to better understand eukaryote cobalamin dependence in a wide range of soil habitats.

1.6 Thesis research objectives

Among the most abundant and ubiquitous microorganisms in terrestrial environments, *Thaumarchaeota* contribute substantially to soil nitrogen cycling. Efforts over the past decade have elucidated soil thaumarchaeotal biogeography, phylogeny, and activity. However, most previous studies have focused only on surface soils, which do not represent the full complexity and diversity of soil habitats. In addition, greenhouse gas production by thaumarchaeal ammonia oxidizers has not been explored in relation to depth. And although the contributions of soil thaumarchaeotes are recognized in the context of nitrogen cycling, these archaea may play other roles as well within the context of soil ecology and metabolite production, in relation to other nitrogen cycling bacteria or to the broader microbial community as a whole.

The overarching goal of this thesis was to characterize members of the *Thaumarchaeota* in soil habitats in relation to soil depth, contrasting land use, and temperature. An important objective was to assess both ammonia oxidation and nitrous oxide production within the context of thaumarchaeotal nitrification. In order to broaden the scope of soil thaumarchaeotal functions

within terrestrial environments, this thesis also combined metagenomic data and novel analytical techniques to explore thaumarchaeotal cobalamin production potential in terrestrial environments. Together, the goal of my thesis research was to better understand the distributions and functions of soil thaumarchaeotes within the context of microbial ecology.

This thesis summarizes my work by presenting two studies (chapters 2 and 3) describing soil thaumarchaeotal distributions and activity, and one study (chapter 4) on soil microbial cobalamin production. Chapter 2 describes a biogeographical survey of *Thaumarchaeota* distribution along soil vertical profiles under different land use (***rare*** Charitable Research Reserve, Cambridge, Ontario), and their community composition changes with soil physicochemical parameters. Chapter 3 describes the activity of soil *Thaumarchaeota*-associated ammonia oxidation activity under different temperatures, and assesses nitrous oxide emissions of AOA in relation to their AOB counterparts. Chapter 4 describes cobalamin-producing bacteria and archaea in a collection of 155 soil metagenomes, evaluating their keystone species significance, and quantifies soil *in situ* cobalamin concentrations as they relate to microbial biomass. Chapter 5 presents conclusions, significance of the thesis research, and discusses future research directions.

Chapter 2[1]

Biogeography of soil *Thaumarchaeota* in relation to soil depth and land usage

2.1 Introduction

Nitrogen is an important element that structures microbial communities by serving as a limiting resource for aquatic and terrestrial productivity (Galloway *et al.* 2014; Ward and Jensen 2014). The nitrogen cycle, involving transformations of nitrogen among its six redox states, includes nitrification, which is the energy-yielding conversion of reduced (ammonia/ammonium; NH_3/NH_4^+) to oxidized (nitrite/nitrate; NO_2^-/NO_3^-) forms of nitrogen. Nitrification is an important aerobic process within the global nitrogen cycle, with profound influences on the environment through greenhouse gas emissions (Frame and Casciotti 2010) and fertilizer nitrogen leaching (NO_3^-), the latter resulting in up to 70% loss of nitrogen fertilizer worldwide as well as groundwater pollution (Raun and Johnson 1999). As a result, understanding controls on the nitrogen cycle and its microbial contributors is essential for informing biogeochemical models and associated land management practices.

Although nitrification has been studied for over a century, it was only a decade ago that archaeal genes were discovered that encode ammonia monooxygenase (AMO) in soil and marine samples (Venter *et al.* 2004; Treusch *et al.* 2005). This was followed by the isolation of *Nitrosopumilus maritimus* strain SCM1, the first representative of ammonia-oxidizing archaea, from sediment of a marine aquarium (Könneke *et al.* 2005). Together, these discoveries underlined the potential importance of chemolithoautotrophic ammonia-oxidizing archaea

[1] A version of this chapter has been published as:
Lu X, Seuradge BJ, Neufeld JD. (2016). Biogeography of soil *Thaumarchaeota* in relation to soil depth and land usage. FEMS Microbial Ecology, 93(2), fiw246.

(AOA; formerly mesophilic *Crenarchaeota*, now *Thaumarchaeota*) (Treusch *et al.* 2005; Brochier-Armanet *et al.* 2008) to global nitrogen cycling. Their counterparts, ammonia-oxidizing bacteria (AOB), were formerly regarded as sole contributors to aerobic nitrification. This changed paradigm of nitrification helped solve the contradiction between the low global abundance of AOB (Hermansson and Lindgren 2001; Altmann *et al*. 2003; Harms *et al*. 2003; Limpiyakorn *et al*. 2005), despite high *in situ* nitrification activity in oligotrophic environments where ammonia concentrations were below the threshold for AOB activity (10 μM NH_4^+-N) (Bollmann *et al.* 2002; Auguet *et al.* 2011).

In terrestrial environments, archaeal *amoA* genes have been detected across a wide range of land-uses such as grassland, agricultural, pasture, and forest soils (Leininger *et al.* 2006; Boyle-Yarwood *et al.* 2008; Taylor *et al.* 2010; Zeglin *et al.* 2011). Because the abundance of archaeal *amoA* genes often exceeds that of bacterial *amoA* genes (Leininger *et al.* 2006), AOA are likely major drivers of terrestrial nitrification. Nonetheless, the factors influencing soil AOA community composition remain poorly described (Prosser and Nicol 2012), which is a limitation for a better understanding of their function. Archaeal community composition is influenced by changing environmental factors such as soil pH (Nicol *et al.* 2008; Gubry-Rangin *et al.* 2011), moisture content (Stres *et al.* 2008; Angel *et al.* 2010; Szukics *et al*. 2010), temperature (Avrahami and Conrad 2003; Stres *et al.* 2008), ammonium availability (Höfferle *et al.* 2010), and organic carbon (Pesaro and Widmer 2002; Kemnitz *et al.* 2007). In addition, a recent study demonstrated links between the phylogeny of terrestrial thaumarchaeota and soil pH (Gubry-Rangin *et al.* 2015). However, most previous studies of soil AOA have focused only on surface samples, which do not comprehensively represent terrestrial environments; the top soil layer captures only a relatively thin cross section of global soil microbial community biomass.

Although Höfferle *et al.* (2010) reported depth-related changes in archaeal communities of a peat wetland, which is a unique soil system with high soil water saturation and high organic matter content, subsequent research is needed to assess other land usage impacts on soil AOA. In particular, agricultural soils and forest soils are relevant for further study because they represent 38% (Food and Agriculture Organization of the United Nations http://faostat3.fao.org/download/E/EL/E) and 31% (Food and Agriculture Organization of the United Nations http://www.fao.org/forestry/fra/fra2010/en/) of the global land use, respectively.

Because soil chemical and physical characteristics are depth dependent, and microbial communities are strongly influenced by such factors, overall soil microbial communities display high spatial heterogeneity in relation to soil depth (Fierer *et al.* 2003). In terms of ammonia-oxidizers, the ratio of AOA to AOB has been shown to exceed 1200 as soil depth increased to 40-50 cm (Leininger *et al.* 2006), indicating that AOA are better adapted to deeper soils than AOB. Although Hansel *et al.* (2008) and Watanabe *et al.* (2010) examined changes of archaeal community composition and methanogen communities along a soil depth profile, respectively, no study has been carried out targeting thaumarchaeotal communities in relation to soil depth in agricultural and forest soils, especially correlating environmental variables with thaumarchaeotal community patterns using multivariate statistics. In addition, even though soil texture has been known to select microorganisms by means of pore size, this is the first study that tests the influence of soil texture on thaumarchaeotal community composition, and the first one comparing thaumarchaeotal communities along soil depth profile associated with both agricultural and forest soils.

Studying AOA community composition and understanding factors that influence niche specialization of individual AOA populations in soils will help to better elucidate how environmental factors impact soil nitrification and nutrient cycling. This study explored thaumarchaeotal biogeography along soil depth profiles among distinct land-use practices at the ***rare*** Charitable Research Reserve in Cambridge, Ontario. High-throughput sequencing of thaumarchaeotal 16S rRNA genes from soil samples was used to answer questions: (i) What are the dominant thaumarchaeotal taxa in field and forest sites? (ii) Do multiple land usages display similar depth-specific patterns in terms of thaumarchaeotal community composition? And (iii) what factors (e.g., pH, texture, nutrients) influence thaumarchaeotal community composition in soil profiles?

2.2 Materials and methods

2.2.1 Site selection and soil sampling

Study sites were located at the ***rare*** Charitable Research Reserve in Cambridge, Ontario (43.380^{o}N and -80.350^{o}W; Figure 2.1). Soils were collected from field sites, which included both an active agricultural site (AA, Preston Flats), three decommissioned agricultural field sites (D03, decommissioned since 2003; D07, decommissioned since 2007; D10, decommissioned since 2010), and three forest sites (IW, Indian Woods; H, Hogsback; CA, Cliffs and Alvars) (Figure 2.1A). The forest sites have been pristine for at least 100-200 years. The well-drained and calcareous soils were classified as Burford series, with relatively thin A horizons, which is typical for the area along the Grand River (Presant 1971). Soils from each site were collected by randomly selecting three 5 m x 5 m plots (Figure 2.1B), each containing three randomly dug pits to a total depth of 45 cm (includes both A and B horizons). Soil samples were collected at three

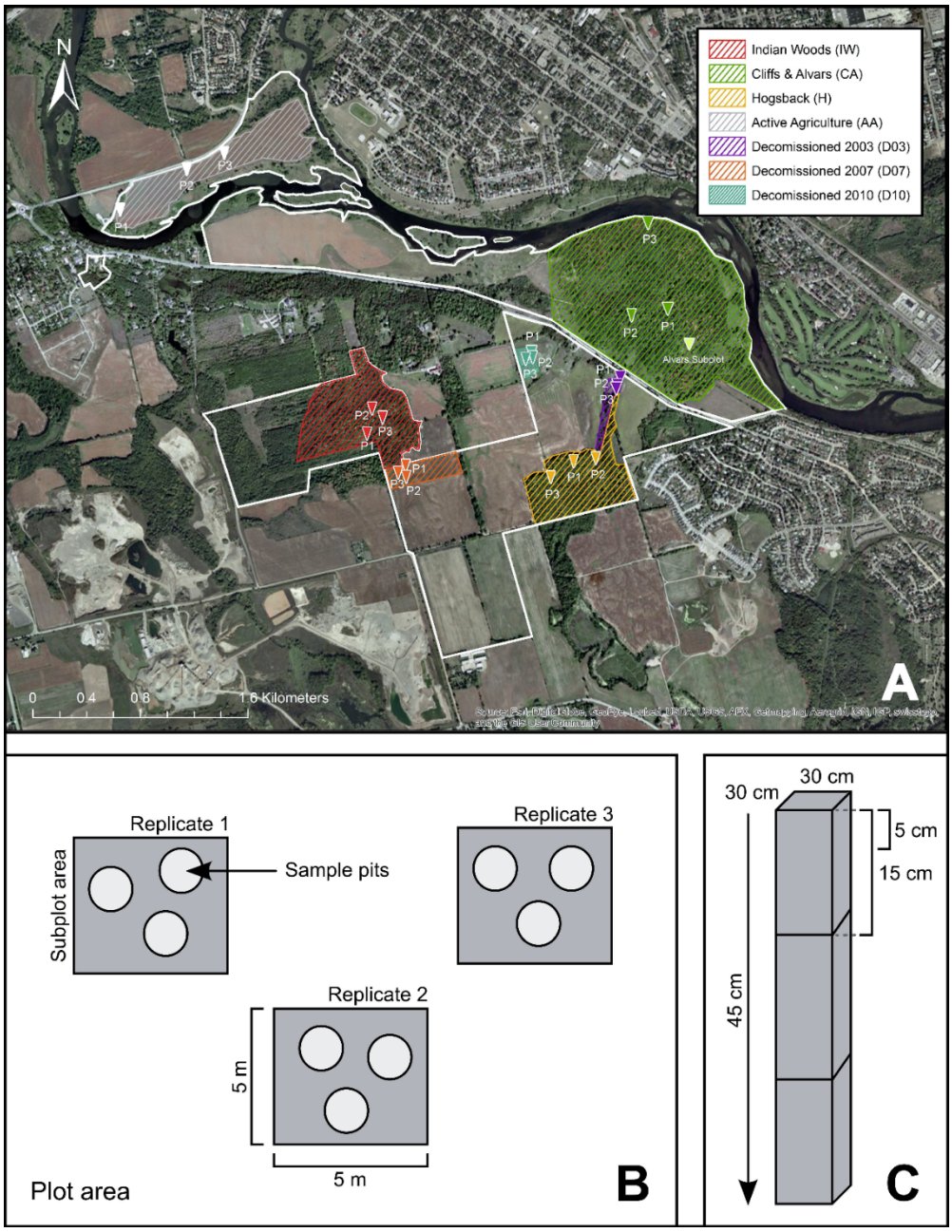

Figure 2.1 – Map of the sampling sites at the *rare* Charitable Research Reserve

Land use type is designated by color (A). Diagrams showing sampling replicates (B) and vertical sampling strategy (C). The map and diagrams are reproduced from Seuradge *et al*., (2017).

depths for each pit: 0-15 cm, 15-30 cm, and 30-45 cm (Figure 2.1C). All soils were sampled in August or September, 2013, and were also the basis of a previously described bacterial community analysis (Seuradge *et al*., 2017). Soil chemical and physical characteristics were

measured by the Agriculture and Food Laboratory at University of Guelph. Briefly, soil pH was measured using a 1:2 ratio of soil to H_2O; organic carbon (OC) measured using the combustion method (Nelson and Sommers, 1982); ammonium (NH_4^+), nitrite (NO_2^-) and nitrate (NO_3^-) measured using the KCl-extractable method (Hood-Nowotny *et al*. 2010); gravimetric soil moisture was determined by oven drying soils at 105°C for 24 h. Soil chemical and physical properties are summarized in Table 2.1, and the raw data are available in an associated bacterial community survey (Seuradge *et al*., 2017).

2.2.2 Soil DNA extraction and PCR amplification of 16S rRNA genes

Soil DNA was extracted using the PowerSoil-htp 96 Well Soil DNA Isolation Kit (MO BIO) according to the manufacturer's protocol. Thaumarchaeotal 16S rRNA genes were targeted with primers 771F (5'-ACGGTGAGGGATGAAAGCT-3') and 957R (5'-CGGCGTTGACTCCAATTG-3') (Ochsenreiter *et al.* 2003), which also contained Illumina-specific adapter and flow cell binding sequences as well as 6-base index sequences for multiplexing (Bartram *et al.* 2011). Triplicate PCR amplifications were carried out for each sample in 25 µL volumes. Each PCR contained 2.5 µL of 10X ThermoPol *Taq* buffer (New England BioLabs), 1.5 µL of 10 mg mL^{-1} bovine serum albumin, 0.05 µL of 100 mM dNTPs (New England BioLabs), 0.125 µL of 5 U μL^{-1} *Taq* DNA polymerase (New England BioLabs), 0.05 µL of 100 µM forward-indexed primer (Integrated DNA Technologies), 1 µL of 5 µM reverse-indexed primer (Integrated DNA Technologies), 1 µL normalized template DNA (1-10 ng μL^{-1}) and 19 µL of nuclease-free PCR-grade H_2O (Thermo Scientific). The PCR conditions included an initial denaturation at 95°C for 2 minutes followed by 35 cycles of (i) denaturation (95°C, 30 sec), (ii) annealing (55°C, 30 sec), and (iii) extension (68°C, 60 sec). The PCR ended

with a final extension at 68°C for 5 min. The PCR amplicons were assessed by electrophoresis on a 1% (w/v) agarose gel that was stained with 1 μg mL^{-1} ethidium bromide (Calbiochem).

2.2.3 High-throughput sequencing

Triplicate PCR products from each sample were pooled and gel quantified (stained with GelRed, 1:10,000 dilution) using AlphaView Software (Alpha Innotech Corp). All samples were pooled together into a single mixture with equal ng amounts. This final mixture was electrophoresed on a 1% (w/v) agarose gel that was stained with 1 μg mL^{-1} ethidium bromide. The correct size 16S rRNA gene amplicon band was gel extracted from primer dimers and purified using the Wizard SV Gel and PCR Clean-Up System (Promega). The purified library was diluted to 4 nM according to the Qubit 2.0 Fluorometer and the Qubit dsDNA HS Assay Kit (Invitrogen), and the concentration was confirmed by qPCR using the PerfeCTa NGS Quantification Kit for Illumina Sequencing Platforms (Quanta Biosciences). The qPCR was carried out in duplicate 20 μL volumes, using Illumina forward primer (5'-AATGATACGGCGACCACCGA-3') and Illumina reverse primer (5'-CAAGCAGAAGACGGCATACGA-3'), then mixed with 2X PerfeCTa SYBR Green SuperMix (Quanta Biosciences). The thermal cycle was as follows: 3 min initial denaturation at 95°C, followed by 35 cycles of: (i) denaturation (95°C, 10 seconds), (ii) annealing (60°C, 20 seconds), and extension (72°C, 45 seconds). The quantified library was stored at -20°C prior to sequencing. Sequencing was carried out on the MiSeq platform (Illumina) using the MiSeq Reagent Kit v2 (Illumina) with 7.5% PhiX control mixed with the library. Post-run analyses, including Phred score calculations and demultiplexing, were performed using the MiSeq Control Software v.2.3.0.3 (Illumina).

2.2.4 Sequence data processing

Paired-end reads were trimmed by removing 3' and 5' adapters from forward and reverse reads, respectively, using cutadapt v.1.8.3 (Martin 2011). This initial trim was done because amplicon lengths were shorter than the read length of the Illumina Miseq reagent kit v2 (2 x 250 bases), which can interfere with subsequent assembly of paired-end reads. Trimmed paired-end reads were further processed by Automation, eXtension, and Integration Of Microbial Ecology (AXIOME; Lynch *et al.* 2013) and Quantitative Insights Into Microbial Ecology (QIIME) pipelines (Caporaso *et al.* 2010). The PANDAseq (Masella *et al.* 2012) algorithm was used to assemble trimmed paired-end reads using a quality threshold of 0.9, and assembled sequences were clustered into operational taxonomic units (OTUs) based on 97% sequence identity by UPARSE (Edgar 2013), which removed singletons and chimeras *de novo*. An additional chimera check was performed by UCHIME (Edgar *et al.* 2011) using the RDP (ribosomal database project) classifier training database (Version 9) as a reference. Taxonomy was determined by submitting representative sequences of each OTU to SINA (SILVA Incremental Aligner, Version 1.2.11).

2.2.5 Statistical processing and multivariate analysis

The data were rarefied to 6774 reads for each sample using the phyloseq package (Version 1.10.0; McMurdie and Holmes 2013). The relationship between relative OTU abundance and environmental factors, and between diversity indices and environmental factors, were examined by Spearman correlations. The effects of land-use type and depth on diversity were examined by two-way ANOVA with Fisher's least significant difference (LSD) procedure. The difference between the relative abundance of the most abundant taxa between field sites and

forest sites was tested using the Wilcoxon rank-sum test. Community composition was visualized by non-metric multidimensional scaling (NMDS) using the Bray-Curtis dissimilarity metric. Group homogeneity (forest and field) was tested by betadisper analysis in *vegan* package (Version 2.3.0), followed by permutational multivariate analysis for variance using dissimilarity matrices (PERMANOVA; Anderson 2001) with 999 permutations to identify environmental factors that correlated significantly with community composition. These environmental factors were further tested by a variance inflation factor (VIF) to confirm that no co-linearity existed among these factors before performing redundancy analysis (RDA). Hellinger transformation was applied to the OTU table to generate a Euclidean distance matrix suitable for RDA (Legendre and Gallagher 2001). The RDA approach was preferred over canonical correspondence analysis (CCA) because the detrended correspondence analysis (DCA) result demonstrated that the greatest gradient length was less than three standard deviations (Ramette, 2007; Hill and Gauch, 1980). Distance-based redundancy analysis (db-RDA) using Bray-Curtis dissimilarity matrix was carried out to confirm the RDA results. Depth effect within field and forest samples was tested using Multi Response Permutation Procedures (MRPP). The NMDS, PERMANOVA, MRPP, RDA and db-RDA were performed using the *vegan* package (Version 2.3.0) in R v.3.1.1 (R Development Core Team. Vienna, Austria). Diversity indices including Shannon index, OUT richness, and Pielou's evenness index were calculated with *vegan* package (Version 2.3.0). Correlation and ANOVA tests were performed using StatGraphics v.16.1.03 (Statpoint Technologies, Inc., Warrenton, VA). Sequence data are available in the EBI database under project accession PRJEB12084.

2.3 Results

2.3.1 Soil conditions

Soil samples spanned a pH range of 6.03 to 8.07 across all sites, a six-fold range of organic carbon (OC), a nine-fold range for ammonium (NH_4^+), and an eleven-fold range for nitrate (NO_3^-) (Table 2.1). The soil samples differed significantly in texture (sand, silt and clay content), but showed less difference in physicochemical parameters (pH, OC, NH_4^+ and NO_3^-) (Table 2.1). Field samples (AA, D03, D07 and D10) were more similar to each other in terms of physicochemical parameters, same as forest samples (Table 2.1). Soil samples were analyzed previously for bacterial communities, with results indicating that depth, land usage, and associated physicochemical factors impacted community composition (Seuradge *et al*., 2017).

2.3.2 Soil thaumarchaeotal diversity

For the current study, the same DNA extracts used in Seuradge *et al*. (2017) were targeted with thaumarchaeotal PCR primers to identify whether the archaeal communities were also impacted by depth and land usage. A total of 5,352,508 sequences were assembled by PANDAseq and 5,147,563 high-quality assembled 16S rRNA gene sequences were obtained after removal of singletons and chimeras using UPARSE and UCHIME. Beginning with a rarefied OTU table from AXIOME, additional OTUs (56 out of 577) were removed that did not classify to the *Thaumarchaeota*, with 521 OTUs remaining. After rarefying all remaining data to 6,774 reads per sample, 1,205,772 sequences remained in the analysis. Of these, 97.9% of the sequences classified to the genus level within the *Thaumarchaeota*.

Table 2.1 – Soil physicochemical properties

Mean concentrations of soil parameters of soil samples collected from different depths and under different land use. Standard deviation of the mean in parentheses. Significant differences ($p < 0.05$) based on Tukey's HSD comparisons are indicated by superscript letters within each column. AA: active agriculture site; D03: decommissioned field since 2003; D07: decommissioned field since 2007; D10: decommissioned field since 2010; CA: forest site at Cliffs and Alvars; IW: forest site at Indian Woods; H: forest site at Hogsback. OC: organic carbon; IC: inorganic carbon; Soil moisture is calculated using gravimetric water content. * no gravel was detected in CA 0-15 cm soils. The table is based on Seuradge *et al*. (2017).

Land use	Depth (cm)	pH	OC (%)	NH_4^+ (mg/kg)	NO_3^-(mg/kg)	Moisture (%)	Sand (%)	Silt (%)	Clay (%)	Gravel (%)
AA	0-15	7.60^{ab} (0.17)	1.28^{a} (0.11)	2.71^{ac} (0.19)	7.78^{ad} (2.42)	9.12^{ab} (0.45)	71.10^{ab} (8.34)	19.53^{ace} (6.69)	9.40^{abcd} (1.67)	2.20^{ac} (1.35)
	15-30	7.80^{ab} (0.10)	0.77^{a} (0.81)	3.32^{ac} (0.32)	4.21^{def} (1.24)	8.79^{ab} (2.93)	68.63^{adh} (10.47)	21.53^{acef} (8.24)	9.83^{abcd} (3.66)	5.37^{abd} (4.72)
	30-45	7.90^{ab} (0.14)	1.05^{a} (0.83)	3.45^{ac} (1.05)	2.89^{cd} (0.05)	9.52^{ab} (1.16)	64.95^{aeg} (3.75)	23.25^{abcd} (5.59)	11.75^{abcd} (1.77)	3.75^{abd} (5.30)
D03	0-15	7.40^{ab} (0.17)	2.67^{a} (0.25)	7.68^{cde} (3.33)	10.18^{a} (3.10)	20.09^{bcde} (6.43)	33.77^{cgh} (2.29)	49.20^{bde} (3.45)	17.03^{ad} (2.06)	1.90^{a} (1.57)
	15-30	7.63^{ab} (0.15)	1.80^{a} (0.18)	4.44^{c} (1.49)	5.45^{abcd} (1.49)	20.56^{bcde} (5.24)	32.47^{chi} (2.15)	53.87^{b} (2.58)	13.70^{abcd} (1.30)	0.83^{a} (0.55)
	30-45	7.67^{ab} (0.15)	1.47^{a} (0.39)	4.45^{c} (2.35)	3.37^{cd} (1.23)	21.24^{bcde} (6.37)	36.63^{agi} (1.40)	51.33^{bf} (2.25)	12.03^{abcd} (0.85)	5.60^{abd} (2.05)
D07	0-15	7.60^{ab} (0.34)	1.23^{a} (0.48)	5.65^{cf} (2.03)	5.46^{abcd} (1.43)	9.93^{ac} (2.74)	75.13^{bdefj} (8.03)	17.00^{cg} (6.21)	7.87^{abc} (1.96)	2.03^{a} (2.08)
	15-30	7.87^{a} (0.25)	0.61^{a} (0.38)	3.44^{ac} (1.82)	1.87^{bce} (0.43)	8.05^{ae} (3.37)	79.63^{bdefk} (12.98)	14.40^{cg} (9.85)	5.97^{c} (3.25)	4.57^{abd} (4.41)
	30-45	8.00^{a} (0.26)	0.24^{a} (0.28)	2.34^{ac} (0.77)	1.59^{bce} (0.24)	7.32^{ae} (2.82)	83.50^{bdefl} (11.21)	11.70^{ch} (7.95)	4.80^{c} (3.48)	2.03^{a} (2.28)
D10	0-15	7.53^{ab} (0.06)	2.16^{a} (0.09)	2.49^{ac} (0.82)	9.31^{af} (2.66)	15.98^{bcde} (1.46)	40.33^{agij} (1.65)	43.90^{bdeg} (2.92)	15.77^{abd} (2.70)	1.00^{a} (0.36)
	15-30	7.87^{a} (0.06)	1.25^{a} (0.38)	4.38^{c} (1.42)	2.85^{cd} (0.87)	15.86^{bcde} (0.87)	42.27^{agij} (5.46)	45.03^{bdeg} (4.55)	12.70^{abcd} (1.31)	2.57^{ab} (2.45)
	30-45	8.07^{a} (0.06)	0.50^{a} (0.34)	1.67^{ac} (0.30)	1.66^{bce} (0.24)	10.30^{ac} (1.25)	63.27^{agkl} (7.38)	29.83^{abcd} (5.22)	6.90^{bc} (2.17)	12.57^{bcd} (4.25)
CA	0-15	6.03^{b} (1.46)	6.22^{b} (3.31)	15.60^{bd} (5.81)	5.83^{abcd} (5.73)	26.87^{d} (17.08)	$63.13^{aegijkl}$ (13.60)	28.03^{abcd} (11.50)	8.80^{abcd} (2.11)	0.00^{*} (0.00)
	15-30	6.40^{ab} (1.25)	1.60^{a} (0.81)	4.57^{c} (0.20)	1.66^{bce} (0.53)	14.76^{bcde} (2.80)	68.53^{adh} (16.50)	24.20^{abcd} (14.03)	7.33^{bc} (3.77)	1.30^{ac} (2.25)
	30-45	6.70^{ab} (1.01)	0.82^{a} (0.57)	4.17^{c} (0.13)	1.03^{bce} (0.43)	11.23^{ac} (2.54)	71.03^{af} (12.59)	22.77^{abcd} (12.92)	6.20^{c} (0.70)	0.33^{a} (0.58)
IW	0-15	7.07^{ab} (0.45)	1.98^{a} (0.29)	13.07^{bef} (0.71)	3.05^{cd} (1.42)	23.75^{bcd} (2.11)	54.90^{agijkl} (17.10)	36.07^{abcd} (15.38)	9.00^{abcd} (2.02)	2.47^{ab} (2.16)
	15-30	7.03^{ab} (0.65)	0.73^{a} (0.25)	6.57^{c} (1.84)	0.97^{bce} (0.33)	17.15^{bcde} (2.92)	57.10^{agijkl} (17.71)	33.13^{abcd} (16.30)	9.73^{abcd} (7.92)	3.63^{abd} (2.11)
	30-45	7.27^{ab} (0.70)	0.40^{a} (0.22)	5.44^{c} (1.83)	0.91^{bce} (0.32)	14.05^{bcde} (2.59)	61.63^{agijkl} (16.05)	26.83^{abcd} (13.17)	11.53^{abcd} (4.90)	6.63^{abd} (4.91)
H	0-15	6.73^{ab} (0.68)	2.50^{a} (0.49)	14.97^{be} (7.91)	2.62^{cd} (1.80)	13.93^{bcde} (3.33)	45.97^{agijk} (14.06)	41.37^{abcd} (14.67)	12.63^{abcd} (3.44)	6.53^{abd} (3.11)
	15-30	7.17^{ab} (0.47)	0.84^{a} (0.17)	7.29^{c} (1.20)	1.08^{bce} (0.41)	11.82^{bcde} (2.67)	49.50^{agijk} (12.95)	37.20^{abcd} (14.13)	13.33^{abcd} (1.22)	5.80^{abd} (3.29)
	30-45	7.47^{ab} (0.32)	0.50^{a} (0.15)	4.52^{c} (0.44)	1.06^{bce} (0.16)	10.36^{acde} (3.88)	52.40^{agijkl} (13.08)	30.30^{abcd} (11.98)	17.37^{d} (1.25)	14.70^{d} (12.59)

Table 2.2 – Thaumarchaeotal diversity indices and soil physicochemical properties

The effects of soil characteristics on Shannon index, OTU richness, and Pielou's evenness index using Spearman's correlations. Significant correlations ($p < 0.05$) are in bold.

Soil property	Shannon	OTU richness	Pielou's
pH	**-0.45**	-0.09	**-0.49**
OC (%)	-0.10	**-0.26**	-0.05
NH_4^+ (mg kg^{-1})	**0.22**	-0.09	**0.27**
NO_3^- (mg kg^{-1})	**-0.53**	**-0.34**	**-0.53**
Moisture (%)	0.06	-0.09	0.08
Sand (%)	0.04	0.14	0.02
Silt (%)	0.01	-0.10	0.02
Clay (%)	-0.15	**-0.18**	-0.13
Gravel (%)	-0.11	-0.07	-0.13

Thaumarchaeotal 16S rRNA gene OTU richness (i.e., number of OTUs) was influenced significantly by land-use type ($p = 0.002$) and depth ($p < 0.001$). In contrast, both the Shannon index (richness and evenness) and Pielou's evenness index (evenness) differed only among land-use type ($p < 0.001$) but not among depths ($p = 0.663$, 0.786, Shannon index and Pielou's evenness index, respectively). Specifically, the OTU richness, Pielou's evenness, and Shannon indices were significantly higher (LSD, $p < 0.05$) in forest sites (CA, H, IW) than field sites (AA, D03, D07, D10); OTU richness was lower (LSD, $p < 0.05$) within surface soils (0-15 cm) compared to subsoils (15-30 cm and 30-45 cm) (Figure 2.2). Among field sites, thaumarchaeotal OTU richness was significantly lower in surface soils (0-15 cm) than subsoils (15-30 cm or 30-45 cm) (LSD, $p < 0.05$), but not significantly different between subsoils (data not shown). Neither the Shannon index nor Pielou's evenness index differed among different soil depths. Among forested sites, only 0-15 cm soils and 30-45 cm soils showed significant differences in

OTU richness ($p < 0.05$), and no significant difference was observed for either the Shannon index or Pielou's evenness index (data not shown). The Shannon index, OTU richness, and Pielou's evenness index showed correlations with soil characteristics (Table 2.2). Soil pH and NO_3^- negatively correlated with both the Shannon index and Pielou's evenness index, whereas NH_4^+ showed a positive correlation. Using a linear regression, a clear relationship was observed between soil pH and the Shannon index, and between soil pH and Pielou's evenness, but not between OTU richness and pH (Figure 2.3).

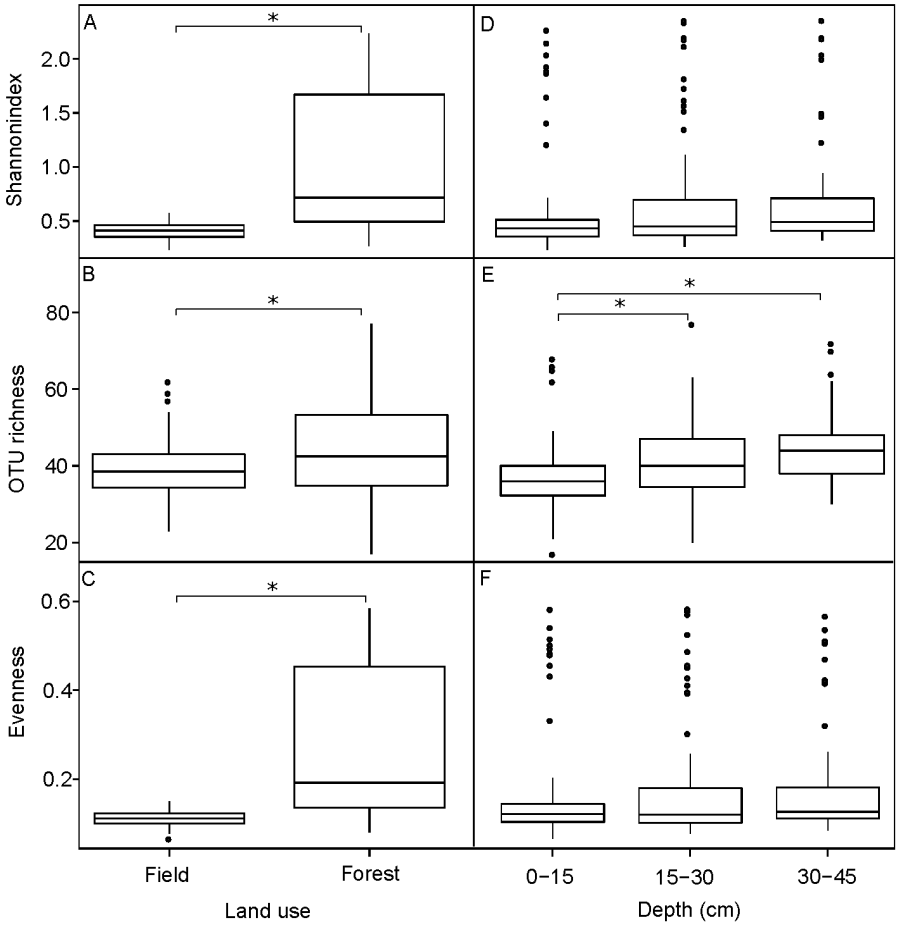

Figure 2.2 – *Thaumarchaeota* diversity in different samples

Shannon index, OTU richness and Pielou's evenness for soil samples collected from different land usages (field and forest) (A, B and C), and among different soil depths (0-15 cm, 15-30 cm and 30-45 cm) (D, E and F). * indicates significance ($p < 0.05$).

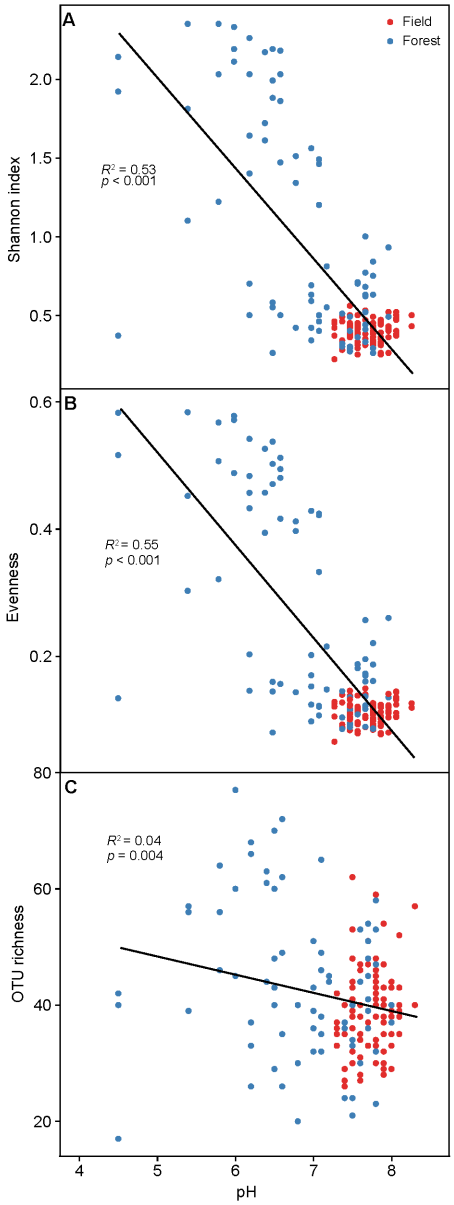

Figure 2.3 – *Thaumarchaeota* diversity with pH

Relationship between (A) Shannon index, (B) evenness, and (C) richness of thaumarchaeota among all samples and soil pH employing best fit line.

2.3.3 Soil thaumarchaeotal community composition

The majority of the 16S rRNA gene sequences were affiliated with the Soil Crenarchaeote Group (SCG; 87.0%) and the Terrestrial Group (TG; 11.0%), followed by the South African Gold Mine Group 1 (SAGMCG-1; 0.15%) and Marine Group I (MG-I; 0.02%). Both SAGMCG-1 and MG-I were primarily associated with forest site samples, except for 4 and 6 samples from the field sites with detected SAGMCG-1 and MG-I, respectively. The SCG

group dominated both field sites and forest sites, with 98.9% and 70.4% relative abundance, respectively (Figure 2.4). For the most abundant groups (SCG and TG), the relative abundance of SCG was significantly higher for field site samples than for those of forest sites ($p < 0.01$), whereas the relative abundance of TG was significantly higher in forest sites compared to field sites ($p < 0.01$). At all depths, the relative abundance of unclassified thaumarchaeotal sequences was higher in DNA extracts from forested soils in relation to those from field site soils (Figure 2.4).

Most of the forest sites had distinct AOA communities, in relation to the field sites, such that the field samples grouped distinctly within ordination space (Figure 2.5A), which was associated with visible differences in the corresponding AOA communities (Figure 2.5B).

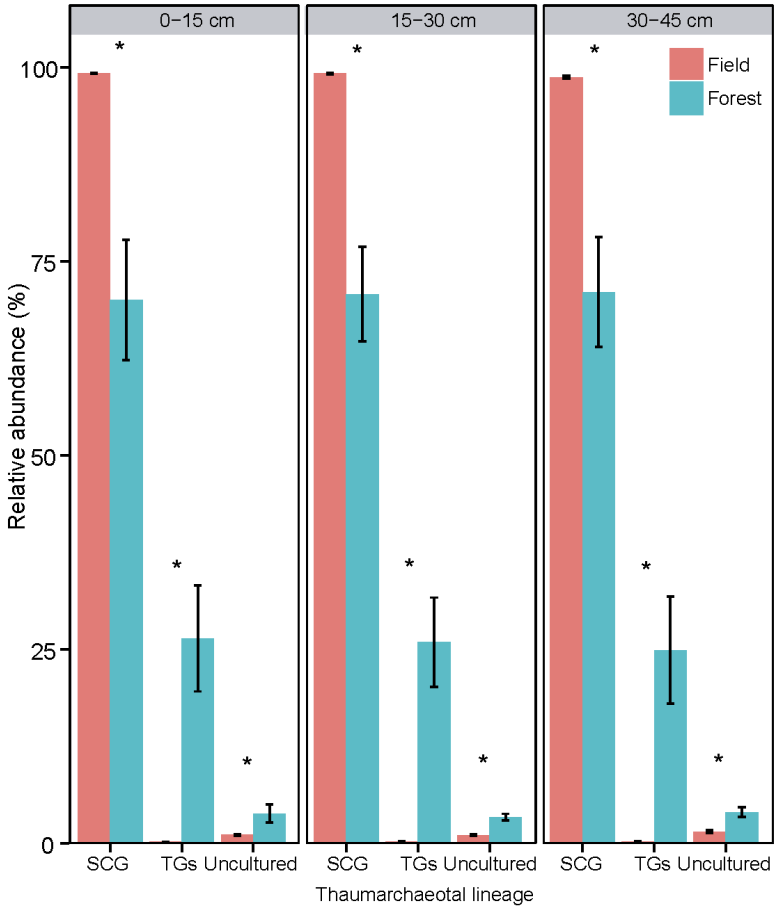

Figure 2.4 – Thaumarchaeotal dominant lineage in different samples

Relative abundance of the two most abundant thaumarchaeotal lineages with different soil depths and land usages. * indicates significance ($p < 0.05$). SCG: Soil Crenarchaeota Group; TG: Terrestrial Group.

The field sites were characterized by SCG, whereas the forest sites were associated more with TG. Besides the overall difference between forest and field sites, samples from each depth also separated by land-use type within ordination space when data were analyzed at the OTU-level (Figure 2.6). The AOA community composition of individual sites associated with distinct land usages showed distinct depth profiles (Figure 2.7). For example, topsoil samples (0-15 cm)

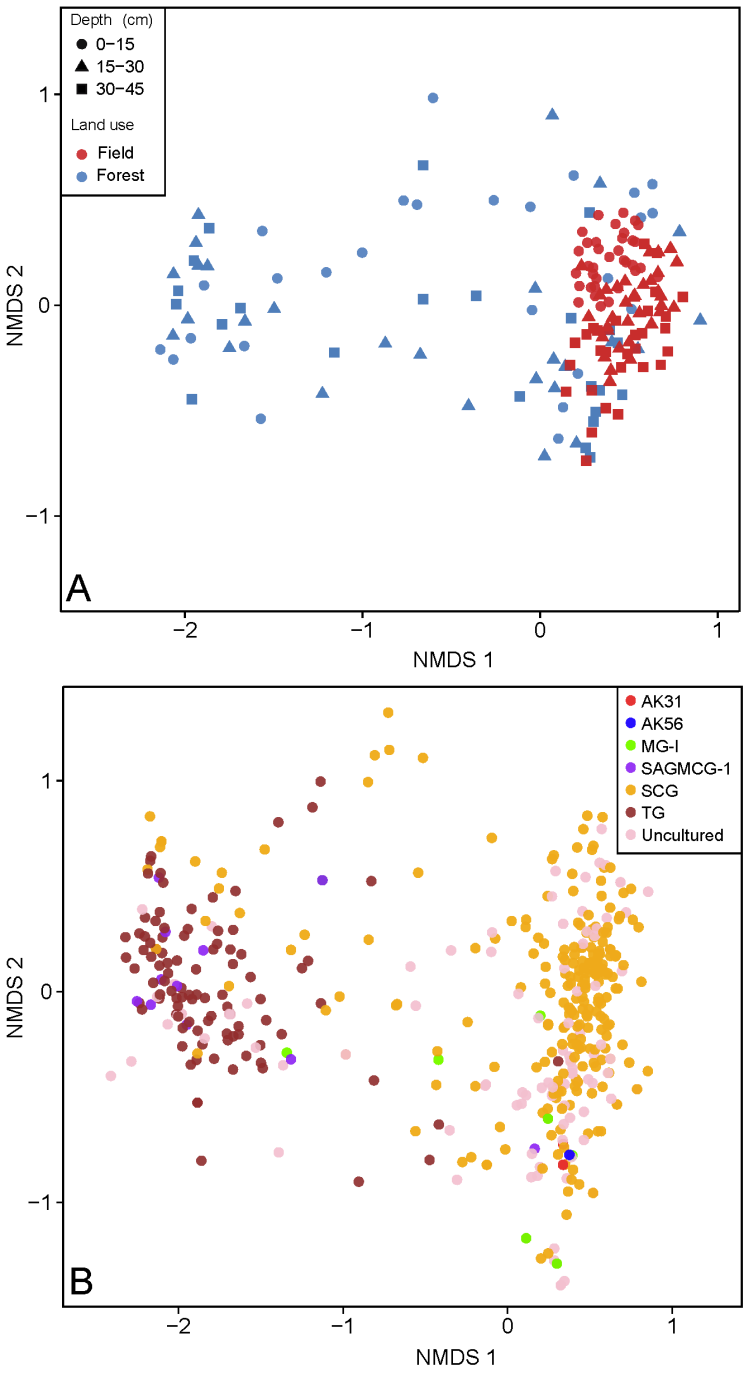

Figure 2.5 – *Thaumarchaeota* structure in different samples.

Non-metric multidimensional scaling (NMDS; stress value: 0.14) ordinations of (A) all samples under different land usage and depth based on 16S rRNA gene OTUs (97% sequence identity) and (B) thaumarchaeotal taxa of all samples within the same ordination space.

separated from subsoil samples (15-45 cm) for all field sites, although site D03 showed a clearer separation between 15-30 cm and 30-45 cm depths than other field sites. Samples from the active agriculture site were similar to those of the samples from decommissioned sites, so all field site

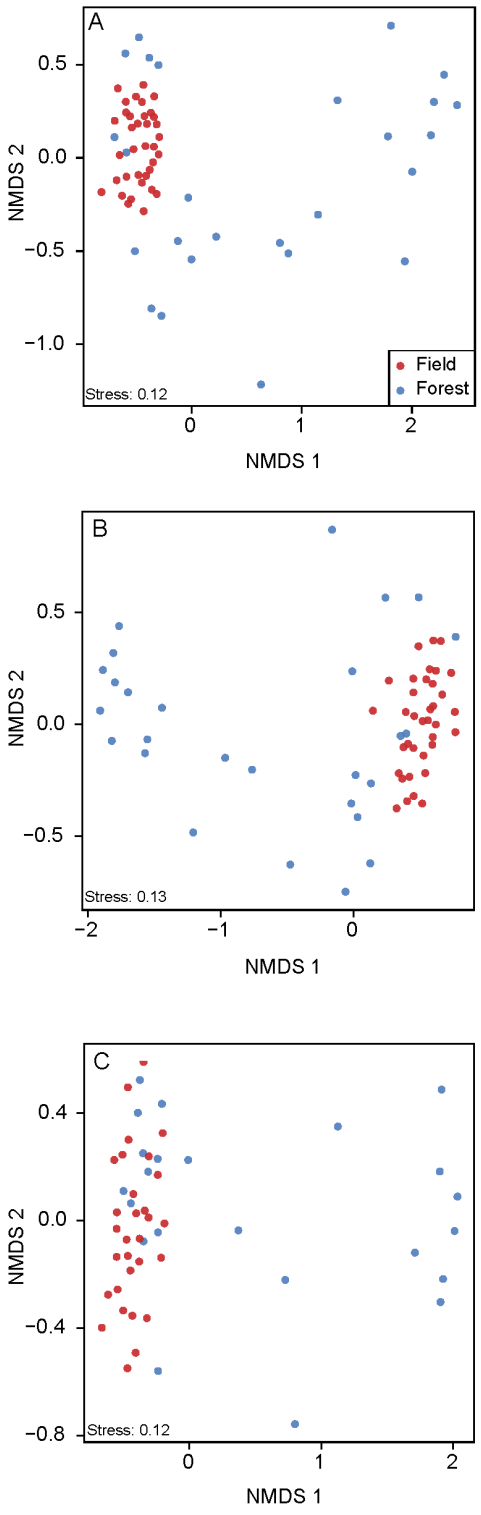

Figure 2.6 – Soil sample characterization by *thaumarchaeota* community composition

Non-metric multidimensional scaling (NMDS) plots of thaumarchaeotal community composition (based on 16S rRNA gene OTUs at 97% sequence identity) across all sites for the (A) 0-15 cm, (B) 15-30 cm, and (C) 30-45 cm depth increments.

samples (AA, D03, D07 and D10) were grouped together for further analysis, given the homogeneity among field samples, in order to reduce the complexity of data presented. For the three forest sites, AOA community sample profiles were more homogeneous at all depths. Relating the relative abundance of thaumarchaeotal groups with environmental variables, OTUs affiliated with the TG correlated negatively with pH (Figure 2.8A), whereas SCG showed a positive correlation with pH (Figure 2.8B).

In terms of samples from the same land-use type (forest or field), the field samples formed distinct groups based on soil depth (MRPP; $A = 0.09$, $p < 0.001$), whereas samples from forest sites did not show such separation (MRPP; $A = -0.01$, $p = 0.61$) (Figure 2.7). By performing PERMANOVA, pH, NO_3^-, OC, NH_4^+ and silt content impacted total sample profiles (Figure 2.9). For field samples, depth, OC, NO_3^-, NH_4^+ and soil texture (silt, clay and gravel content) impacted community composition, whereas only pH and NO_3^- explained community composition dissimilarity among forest samples (Figure 2.9). Using RDA analysis, the distribution of thaumarchaeotal communities in different soil samples and their relationship with soil environmental variables were examined and visualized (Figure 2.10; db-RDA, Figure 2.11). Across all samples analyzed in this study, thaumarchaeotal communities were mainly distributed along soil pH and NH_4^+ gradients, with higher pH for field samples and higher NH_4^+ for forest

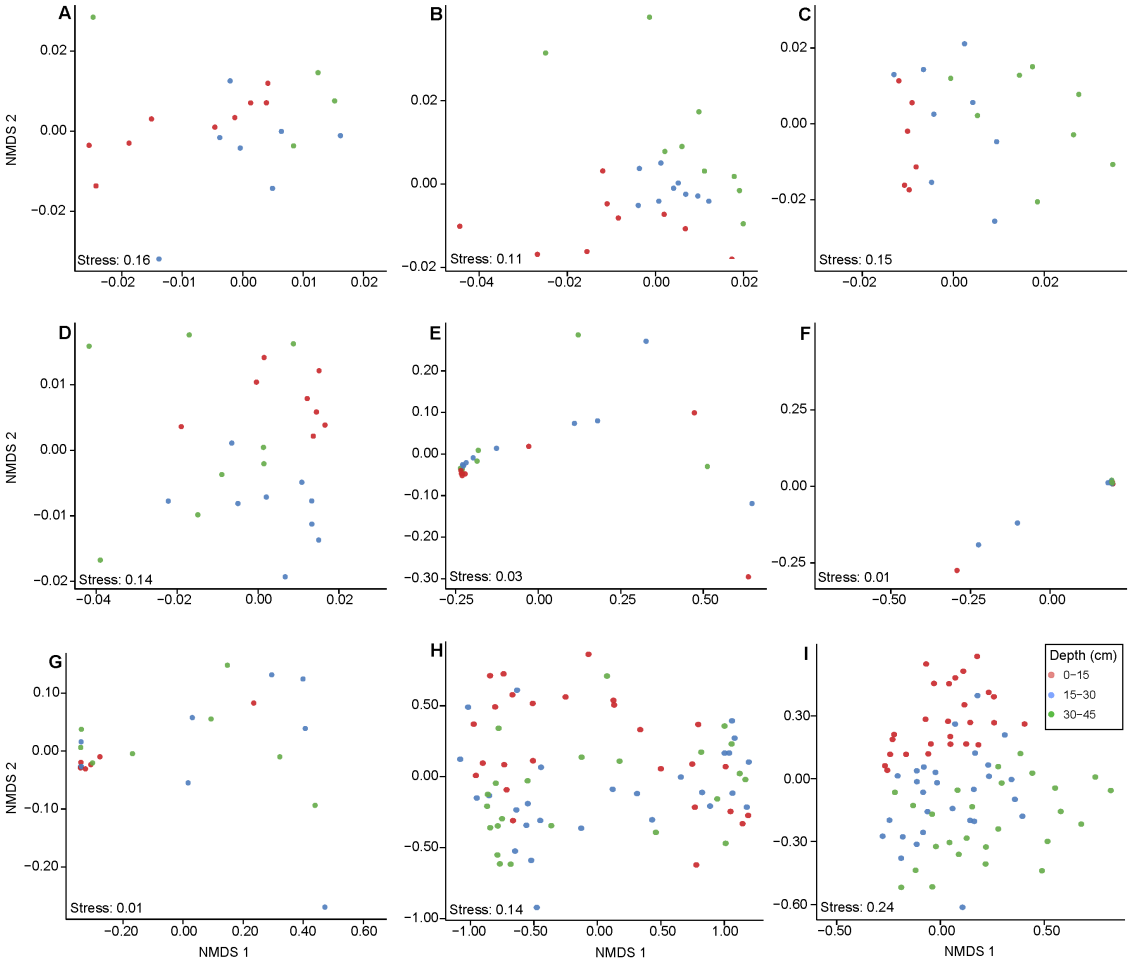

Figure 2.7 – Thaumarchaeotal community composition for all individual sites

Non-metric multidimensional scaling (NMDS) plots of thaumarchaeotal community composition (based on 16S rRNA gene OTUs at 97% sequence identity) across all depths of different sites and land usage. A: active agriculture; B: decommissioned since 2003; C: decommissioned since 2007; D: decommissioned since 2010; E: Cliffs and Alvars; F: Indian Woods; G: Hogsback; H: all forest sites; I: all field sites.

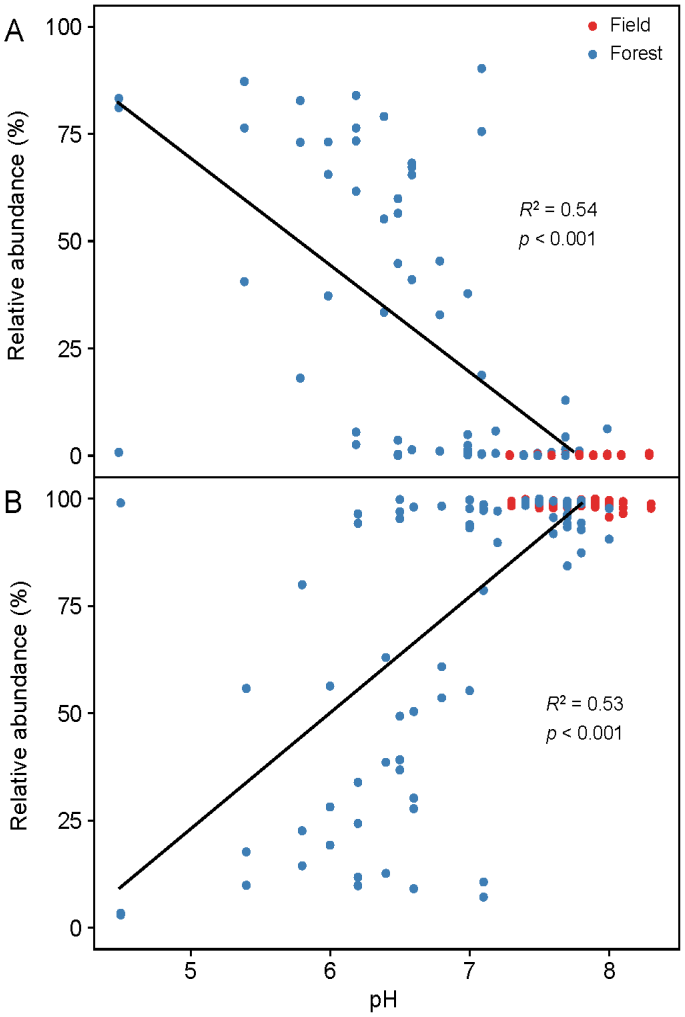

Figure 2.8 – Relationship between thaumarchaeotal dominant lineage and pH.

Relationship between relative abundance of (A) TG and (B) SCG with soil pH employing best fit line.

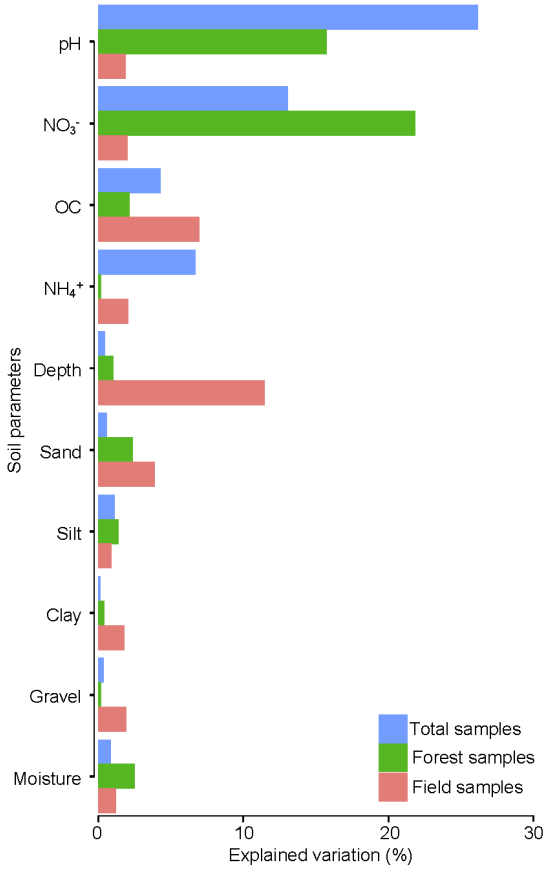

Figure 2.9 – Environmental factors influencing thaumarchaeotal community strucutre

Variation in community dissimilarity of all samples, forest samples, and field samples explained by the major environmental factors using PERMANOVA.

samples (Figure 2.10A, Figure 2.11A). Forest samples were affected by soil pH and NO_3^- concentration, but there was no consistent separation among forest soils by depth or site (Figure 2.10B, Figure 2.11B). In terms of field sites, subsoil samples (15-30 cm or 30-45 cm) separated from surface samples (0-15 cm), likely due to the decrease of NO_3^-, NH_4^+, and OC content, and the increase of gravel content with deeper samples. The D07 and active agriculture site samples were separated from all other field sites mainly along the sand gradient. The D03 site

corresponded to increased clay content and decreased sand content, suggesting the importance of soil texture in shaping thaumarchaeotal community composition for samples from this site (Figure 2.10C, Figure 2.11C).

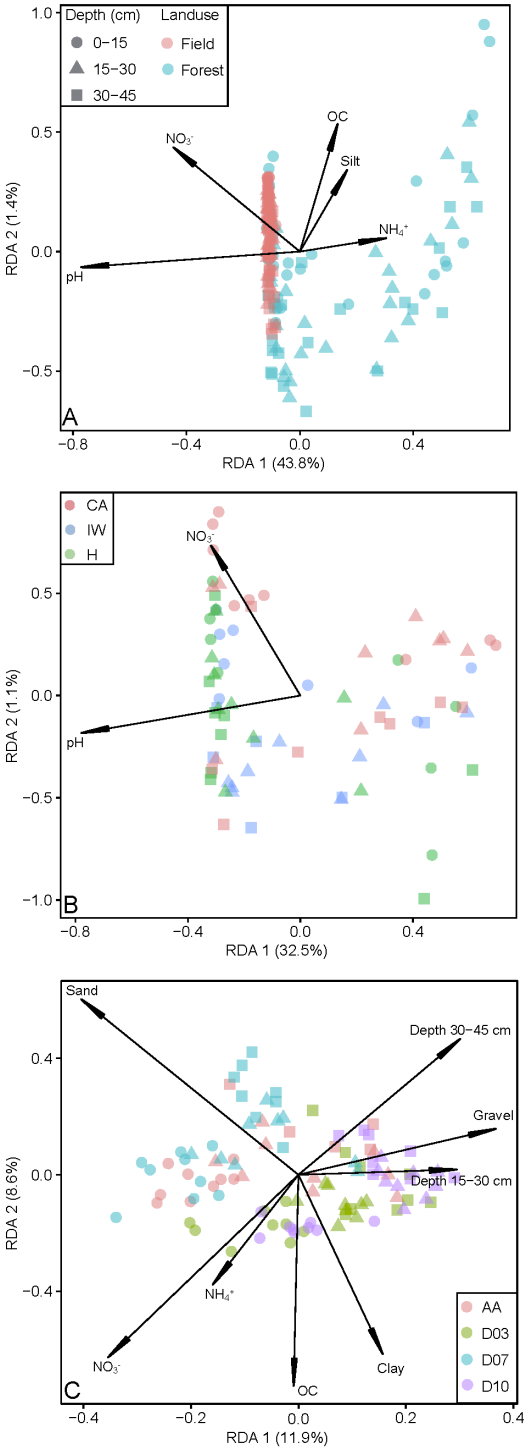

Figure 2.10 – Redundancy analysis of thaumarchaeotal community composition and environmental factors

Redundancy analysis (RDA) plots of thaumarchaeotal community composition (based on 16S rRNA gene OTUs at 97% sequence identity) of (A) all samples among different depth and land usage, (B) forest samples among different depth and sites, and (C) field samples among different depth and sites.

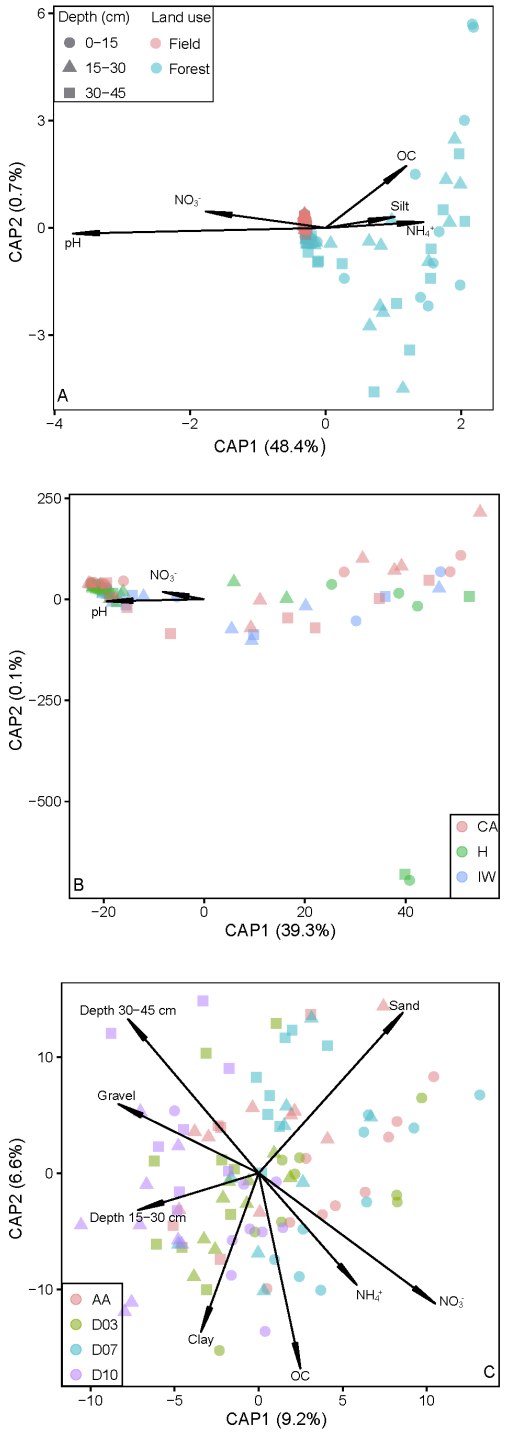

Figure 2.11 – Distance-based redundancy analysis of thaumarchaeotal community composition and environemtnal factors

Distance-based redundancy analysis (db-RDA) plots of thaumarchaeotal community composition (based on 16S rRNA gene OTUs at 97% sequence identity) of (A) all samples among different depth and land usage, (B) forest samples among different depth and sites, and (C) field samples among different depth and sites.

2.4 Discussion

Based on high-throughput 16S rRNA gene sequence results, both field and forest sites were dominated by the Soil Crenarchaeote Group (SCG; soil group 1.1b), which agreed with previous findings showing group 1.1b as the main archaeal lineage in soils (Auguet *et al.* 2009; Bates *et al.* 2011; Tripathi *et al.* 2015; Höfferle *et al.* 2010). However, this result might also be influenced by the commonly used thaumarchaeotal primer set (e.g., Lehtovirta, Prosser and Nicol 2009; Gubry-Rangin, Nicol and Prosser 2010; Sauder *et al*. 2012), which has a high specificity for members of the *Thaumarchaeota* (771F) and the soil 1.1b group (957R) (Hong, Kim and Cho 2014). Nonetheless, the relative abundance of SCG was higher at field sites than forest sites, indicating that although group 1.1b dominated most soil samples, land-use type could influence the relative abundance of this group. In contrast, group 1.1a archaea are less common in soils sampled previously (Ochsenreiter *et al.* 2003; Nicol *et al.* 2005). A recent study by Tripathi *et al.* (2015) reported a higher abundance of group 1.1a archaea in acidic soils (mean pH = 5.4). However, Marine Group I (marine group 1.1a) archaea were detected in forest soils with pH ranges higher than this previous work (pH ranges 6.4-8.0). This pattern demonstrates that group 1.1a thaumarchaeota are not limited to acidic soils, but can adapt to neutral or slightly alkaline soils. Considering that *Candidatus* Nitrosotenuis chungbukensis (soil cultivated representative of group 1.1a) is neutrophilic (optimum pH: 7-7.5) (Jung *et al.* 2014a), it is not surprising to find 1.1a thaumarchaeota in neutral forest soils. However, it is interesting to note that *Ca.* N. chungbukensis was cultivated from a C horizon soil (Jung *et al.* 2014a) whereas in this study, group 1.1a 16S rRNA genes were detected at all sampled depths (0-45 cm), including samples from horizons A and B, indicating the capability of group 1.1a to adapt to not only oligotrophic deep soil horizons but also a wider range of soil niches along a depth profile.

The sequences classified as Terrestrial Group (TG) in this study were associated with the 1.1c group. This group, being reported in association with acidic forest soils (Bomberg and Timonen 2007), was found in all soil depths (including A and B horizons) at the forest sites in this study, contrasting with previous results demonstrating an absence of the 1.1c group thaumarchaeota in the A horizon (Hansel *et al.* 2008). Since the first report of group 1.1c in a Finnish boreal soil (Jurgens *et al.* 1997), Weber *et al.* (2015) recently reported that, unlike group 1.1a or 1.1b, 1.1c does not use ammonia as an energy source. Given that group 1.1c sequences were found in relatively high abundance in forest soils (Kemnitz *et al.* 2007; Stopnišek *et al.* 2010; Catão *et al.* 2013), as well as in acidic agricultural soil (Lehtovirta, Prosser and Nicol 2009), they may contribute a unique metabolism other than nitrification, which expands the possibility for discovery of more potential keystone roles for members of the *Thaumarchaeota*.

One drawback of the primers used in this study is relatively poor coverage of group 1.1c thaumarchaeota (Hong, Kim and Cho 2014), which might underestimate the abundance of this group in these soil samples. Nonetheless, the successful detection of abundant 1.1c group thaumarchaeota among all soil samples indicates a potential high relative abundance of this group *in situ*. Indeed, a previous study by Yarwood and colleagues (2010) reported that the 1.1c group accounted for 20-25% archaeal abundance in Oregon forest soils. The inability to detect 1.1c-associated *amo* genes (Yarwood, Bottomley and Myrold 2010; Weber *et al.* 2015) raised the question of their biogeochemical roles *in situ*. As pointed out by Weber *et al.* (2015), the possibility of possessing novel *amoA* genes by members of the 1.1c group cannot be ruled out, and it might be interesting to test the effect of AOA *amoA*-specific inhibitors on the growth and activity of this group.

Thaumarchaeotal OTU richness and diversity were significantly affected by soil pH, which is also known to alter bacterial community composition and diversity (Fierer and Jackson 2006). Similar results of pH affecting thaumarchaeotal communities were reported by Tripathi *et al.* (2015) in a large scale survey of tropical and temperate soils. In this study, both the Shannon index and OTU richness negatively correlated with soil pH (Table 2.2, Figure 2.3). However, a peak in OTU richness around neutral pH was reported previously (Gubry-Rangin *et al.* 2011; Pester *et al.* 2012; Tripathi *et al.* 2015). This negative correlation could be due to the relatively narrow range of pH in this study, which did not include many acidic soils with pH below 4, resulting in a linear relationship instead of unimodal relationship. But the slightly higher OTU richness around pH 5-6 than that around alkaline pH suggested that more of the AOA taxa in this study were adapted to slightly acidic conditions. AOA may be more tolerant to low pH than their counterparts, the AOB, in terms of relative abundance (e.g., Leininger *et al.* 2006; Gubry-Rangin, Nicol and Prosser 2010; Lu, Bottomley and Myrold 2015), and Nicol *et al.* (2008) reported AOA *amoA* gene copy numbers decreased as pH increased. This study found a significant decrease of thaumarchaeotal OTU evenness with pH, indicating a greater variation in the number of OTUs in alkaline soils than neutral or acidic soils. This pattern suggested that at least the abundance of some OTUs changed as pH increased. To date, little evidence supports the presence of AOA in soils with pH values exceeding 8 (Wuchter *et al.* 2006; Zhang *et al.* 2008).

Importantly, this study demonstrates that thaumarchaeotal OTU richness was lower in surface soil (0-15 cm) than in subsoils (15-30 cm and 30-45 cm), which agreed with previous observations that archaeal OTU richness was lowest in the B horizon and highest in the C horizon (Hansel *et al.* 2008). Thaumarchaeotal OTU richness changed with depth differently in field site soils in comparison to forest site soils. In field site soils, thaumarchaeotal OTU richness

within shallow soil samples was significantly lower than that within either 15-30 cm or 30-45 cm soils. In forest soils, richness only differed between 0-15 cm soil and 30-45 cm soils. In terms of thaumarchaeotal community composition, however, depth was a significant variable only for field sites. Based on RDA results, NH_4^+, NO_3^-, and OC content decreased with depth (15-30 cm and 30-45 cm). This pattern indicates the importance of nitrogen and carbon in shaping AOA communities, supporting the niche hypothesis that indicates the importance of physical and chemical properties in supporting the growth and activity of a particular nitrifying taxon (Schleper 2010). All available AOA cultures possess an autotrophic metabolism (Könneke *et al.* 2005; De La Torre *et al.* 2008; Hatzenpichler *et al.* 2008; Jung *et al.* 2011; Lehtovirta-Morley *et al.* 2011; Tourna *et al.* 2011; Lebedeva *et al.* 2013), but some also demonstrate heterotrophic or mixotrophic growth (Tourna *et al.* 2011). The results suggest an OC effect on AOA community composition within field sites, suggesting differences in potential carbon source preferences among different AOA subgroups along the depth profile. Previous research with acidic forest soils also showed the effect of OC on archaeal community composition (Pesaro and Widmer 2002; Kemnitz *et al.* 2007). Overall, thaumarchaeotal community composition was more homogeneous throughout the entire 45 cm depth profile for the forest sites than field sites, with pH and NO_3^- as the most significant variables shaping community composition. On the other hand, although NO_3^- accumulation can be contributed by both AOA and AOB, this study shows that the AOA community of field and forest sites, together with higher NO_3^- accumulation at field sites, might suggest activity differences corresponding to distinct AOA communities. Similarly, for the field sites only, the NO_3^- vector indicates that surface soils might have a higher nitrification activity than subsoils due to distinct AOA communities (Figure 2.10).

The total microbial community composition has been shown to shift along soil depth profiles within the top 40 cm by measuring microbial C-to-N ratio in a spruce forest (Matejek *et al.* 2010). Although changing soil environmental factors along the soil profile, such as temperature and moisture, were suggested to cause the shift in detected microbial communities, no analysis was done to correlate these proposed environmental factors with the changing C-to-N ratio. In this study, soil moisture was also measured, but was not shown as a significant factor influencing thaumarchaeotal community composition or diversity.

The thaumarchaeotal community composition differences along soil profiles for field samples were also shown to be influenced by soil particle size. Based on RDA results, for example, the vector for 15-30 cm showed an acute angle with clay content and gravel content, suggesting that clay and gravel increased within depth 15-30 cm. The gravel content increased as soil depth increased to 45 cm, but not clay content. Soil aggregates can support different microbial communities by physically excluding certain types of microbes in favor of others (Bales *et al.* 1989), or by changing water tension (Treves *et al.* 2003) and oxygen diffusion flux rates (Greenwood and Goodman 1967), which are essential for microbial metabolism. Given differing soil texture profiles due to parent material among geological locations, the distribution of ammonia oxidizers may vary by location, suggesting texture-associated nitrification potential. This pattern might also imply that studying niche separation of AOA should also take into account the interactions of soil texture with other physicochemical characteristics such as soil organic matter content, making interpretation of the underlying constraints on AOA biogeography more complex.

2.5 Conclusion

This study demonstrated that soil thaumarchaeotal community composition is closely related to soil pH, and that soil pH is the variable that best explained the separation of thaumarchaeotal communities among field and forest sites. Soil land-use type impacted thaumarchaeotal community composition with depth for field samples, but not for forest samples collected in this study. Nitrogen and organic carbon content also influenced AOA community composition. To my knowledge, this is the first study showing the effects of soil mineral structure on thaumarchaeotal community composition, and the first one comparing thaumarchaeotal communities along soil depth profile associated with both agricultural and forest soils with consistent underlying geology. Considering the community differences along different soil depths, and the ubiquity of soil thaumarchaeota, it will be important for future research to clarify the relative contributions of these nitrifier groups to ammonia oxidation as a function of soil depth.

Chapter 3[2]

Differential responses of soil ammonia-oxidizing archaea and bacteria to temperature and depth under two different land uses

3.1 Introduction

Nitrification is traditionally considered a two-step microbially driven process for oxidizing ammonia (NH_3) to nitrate (NO_3^-) via nitrite (NO_2^-). This process links reduced and oxidized nitrogen pools by the combined activities of ammonia-oxidizing bacteria (AOB; (Prosser 1990), ammonia-oxidizing archaea (AOA; Könneke *et al.* 2005), nitrite-oxidizing bacteria (NOB; Prosser 1990), and the newly discovered complete ammonia oxidation "comammox" bacteria (Daims *et al.* 2015; van Kessel *et al.* 2015).

Although ammonia oxidation to nitrite, the first and often rate-limiting step in nitrification, has been studied intensively, the relative contributions of AOA and AOB to this process and factors that may influence their contributions are still unclear (Schleper 2010; Hatzenpichler 2012; Prosser and Nicol 2012). The isolation of AOA and AOB cultures from different environments suggests that temperature may have a role in niche separation between AOA and AOB. Specifically, cultured AOA range from mesophiles to hyperthermophiles, with optimum growth temperatures ranging from 25°C for *Candidatus* Nitrosotalea devanaterra Nd1 (Lehtovirta-Morley *et al.* 2014) to 74°C for *Candidatus* Nitrosocaldus cavascurensis (Abby *et al.* 2018), with others in between these extremes (De La Torre *et al.* 2008; Jung *et al.* 2011, 2014a; Kim *et al.* 2012; Stieglmeier *et al.* 2014a; Lehtovirta-Morley *et al.* 2016; Sauder *et al.* 2017; Daebeler *et al.* 2018). Isolated AOB appear to have a narrower range, with the optimum

[2] A version of this chapter has been published as:
Lu X, Nicol GW, Neufeld JD. (2018). Differential responses of soil ammonia-oxidizing archaea and bacteria to temperature and depth under two different land uses. Soil Biology and Biochemistry, 120, 272-282.

temperatures for most strains ranging from 20 to 30°C (Groeneweg, Sellner and Tappe 1994; Jiang and Bakken 1999; Avrahami and Conrad 2005; Avrahami and Bohannan 2007), but with growth of several also possible at 4°C (Jones *et al.* 1988).

The influence of temperature on AOA and AOB community composition (Tourna *et al.* 2008) and activity (Horak *et al.* 2013; Wu *et al.* 2013; Taylor *et al.* 2017) has been assessed for various environmental samples. In soil, an increase of AOA-associated activity was observed for an agricultural soil in the warmer seasons of late summer and early fall (Taylor *et al.* 2012), with differential inhibition during soil incubations indicating that AOA possessed at least a 10°C higher optimal temperature than AOB (Ouyang, Norton and Stark 2017; Taylor *et al.* 2017). Whether these patterns are observed in contrasting land-use types and at different soil depths remains unclear. In addition, the effect of temperature on AOA- and AOB-associated nitrous oxide (N_2O) production associated with soil nitrification is poorly understood. Because previous studies examining the effect of temperature on N_2O production (Conrad, Seiler and Bunse 1983; Slemr, Conrad and Seiler 1984; MacDonald *et al.* 1997; Mogge, Kaiser and Munch 1998, 1999; Avrahami, Liesack and Conrad 2003) were conducted before the discovery of AOA, and a recent one only focused on greenhouse agricultural soils (Duan *et al.* 2018), the temperature-dependent relative contributions of AOA and AOB to soil N_2O production activity in a natural system requires further study.

Nitrous oxide, a trace gas with a ~300 fold greater global warming potential than CO_2, is a reactant capable of causing stratospheric ozone destruction (Ravishankara, Daniel and Portmann 2009). Soil is considered the largest source of N_2O emissions (Syakila and Kroeze 2011; Schreiber *et al.* 2012), of which microbial ammonia oxidation contributes approximately

80% (Gödde and Conrad 1999; Wrage *et al.* 2001; Kool *et al.* 2011; Zhu *et al.* 2013). AOB produce N_2O enzymatically through two mechanisms: incomplete oxidation of hydroxylamine (NH_2OH) to NO_2^- and sequential reduction of NO_2^- to NO and N_2O by "nitrifier-denitrification" (Arp and Stein 2003). Although the N_2O-producing mechanism within AOA has not been fully resolved, it is thought that AOA produce N_2O during NH_3 oxidation through an abiotic reaction between NH_2OH and NO, an intermediate of the AOA ammonia oxidation pathway (Stieglmeier *et al.* 2014b), which has been demonstrated for pure cultures (Jung *et al.* 2011; Stieglmeier *et al.* 2014b; Kozlowski *et al.* 2016; Qin *et al.* 2017b). AOA-associated N_2O production in environmental samples has been reported in several studies (Santoro *et al.* 2011; Löscher *et al.* 2012; Hink, Nicol and Prosser 2016; Peng *et al.* 2016; Giguere *et al.* 2017; Hink *et al.* 2018). Although some studies have determined the relative contributions of AOA and AOB to soil nitrification using selective inhibitors (Taylor *et al.* 2010, 2013; Daebeler *et al.* 2015; Giguere *et al.* 2015; Lu, Bottomley and Myrold 2015; Ouyang *et al.* 2016; Duan *et al.* 2018), and examined the relative contributions of AOA and AOB to nitrifier-dependent N_2O production in agricultural or non-cropped soils (Shi *et al* 2017.; Hink, Nicol and Prosser 2016; Wang *et al.* 2016; Giguere *et al.* 2017), no microcosm study has yet examined the influence of temperature on N_2O production by AOA and AOB along a soil depth profile.

In Chapter 2, the influence of depth and land-use on thaumarchaeotal and bacterial community composition was characterized within soil samples collected at the ***rare*** Charitable Research Reserve (Lu, Seuradge and Neufeld 2017; Seuradge, Oelbermann and Neufeld 2017). Using this knowledge of thaumarchaeotal and bacterial biogeography, site-specific heterogeneity, and depth profiles, the aim of this study was to perform a targeted investigation into how AOA and AOB at different soil depths and under different land uses respond to

temperature with respect to their relative contributions to ammonia oxidation and N_2O production.

3.2 Material and methods

3.2.1 Site selection and soil sampling

Soil samples were taken from the ***rare*** Charitable Research Reserve (Cambridge, Ontario) in early September ("summer" samples) and early November ("autumn" samples) in 2015. Soil samples were collected at two depths (0-15 and 30-45 cm) from either an agricultural site (Preston Flats; A) or forest site (Hogsback; F). Previous research determined sites A and F possessed distinct bacterial and thaumarchaeotal communities, with distinct profiles also associated with the two depth ranges sampled (Lu, Seuradge and Neufeld 2017; Seuradge, Oelbermann and Neufeld 2017). A composite soil sample from each depth at each site was generated by randomly collecting 3-5 replicates from the same location as previous sampling plots used for a bacterial and thaumarchaeotal biogeography survey (Lu, Seuradge and Neufeld 2017; Seuradge, Oelbermann and Neufeld 2017). The agricultural site has been under no-till management since 2002, operated under a rotation of corn (*Zea mays*) and soybeans (*Glycine max*) from 2002 to 2011, and a corn monocrop since 2011. The forest site is a mixture of northern hardwood and Carolinian tree species, maintained as pristine forest for over 100 years, and is thus classified as a mature forest. Soils from both sites are classified as Burford series, which is typical for the area along the Grand River. The soils are well-drained and calcareous, with a relatively thin A horizon. The B horizons of both soils have a sandy clay loam texture, wavily extending into a C horizon that contains over 50% gravel (Presant and Wicklund 1971). Soil samples for the incubation experiment were sieved (4.75 mm) and stored at 4°C prior to

establishing microcosms, or at -20°C prior to physicochemical analysis at the Agriculture and Food Laboratory (University of Guelph).

3.2.2 Whole soil nitrification assay

A modified 8-day whole soil assay (Lu, Bottomley and Myrold 2015) was used to measure the nitrification potential (NP) attributed to AOA and AOB in composite soil samples. Triplicate subsamples from each composite soil were pre-incubated for two days in a 120-mL serum bottle (15 g field moisture soil per replicate) at room temperature (22°C) with a loosely capped stopper prior to microcosm incubation. This room temperature pre-incubation minimized the influence of 4°C storage (Giguere *et al.* 2015). An NH_4Cl solution was added to each microcosm, resulting in a final concentration of 200 mg-N kg^{-1} $soil_{dry}$ and a gravimetric water content of 30%. Serum bottles were sealed with silica stoppers and incubated in the dark at 20°C, 30°C, or 40°C. At the beginning of the incubation, triplicate bottles were amended with either acetylene (0.02% v/v) or octyne gas (1.9% v/v) following a protocol published elsewhere (Taylor *et al.* 2013). Acetylene was used to irreversibly inactivate ammonia monooxygenase of both AOA (Offre, Prosser and Nicol 2009; Vajrala *et al.* 2013) and AOB (Hyman and Wood 1985), whereas octyne is a specific inhibitor of AOB only (Taylor *et al.* 2013, 2015; Giguere *et al.* 2015, 2017; Lu, Bottomley and Myrold 2015; Hink, Nicol and Prosser 2016). To monitor net nitrification potential, the incubated soils were sampled at 0, 2, 4, 6, and 8 d by removing 2.5 g of soil, and then re-establishing inhibitor concentrations. Nitrification potential rates were determined by measuring the accumulation of NO_2^-+NO_3^- at each sampling point (Taylor *et al.* 2010). Total net nitrification potential rates were determined by the accumulation of NO_2^-+NO_3^- without inhibitors (i.e., acetylene or octyne). Nitrification potential in octyne-amended

microcosms was attributed to AOA, with the difference between no inhibitor and octyne-amended microcosms attributed to AOB activity. To determine NO_2^-+NO_3^- production from autotrophic nitrification in the forest soil, NO_2^-+NO_3^- concentrations in acetylene-amended microcosms at each time point were subtracted from those in uninhibited microcosms, as described previously (Lu, Bottomley and Myrold 2015). As forest soil microcosms showed a decrease in NO_2^-+NO_3^- concentrations after six days of incubation, indicating a possible increase in denitrification activity and/or immobilization (data not shown), only the first six days of data were used for analysis.

3.2.3 Analysis of N_2O, NO_2^- and NO_2^-+NO_3^-

N_2O concentrations were determined in the headspace of microcosms immediately before each sampling event, as described previously (Coyotzi *et al.* 2017), with 1 mL gas sampled using a disposable syringe and injected into a GC-2014 gas chromatograph (Shimadzu Scientific Instruments, Columbia, MD) equipped with a Porapak Q 80-100 column and an electron capture detector (ECD).

Soil NO_2^- concentrations were measured directly with Griess reagents, whereas soil NO_2^-+NO_3^- accumulation was determined using a vanadium reduction assay to convert NO_3^- to NO_2^- before adding Griess reagents to measure NO_2^- (Miranda, Espey and Wink 2001; Sauder *et al.* 2017). All assays were conducted in clear flat bottom 96-well plates (Greiner, Frickenhausen, Germany) and absorbance measured at 550 nm using a Filtermax F5 Multi-Mode Microplate Reader (Molecular Devices, Sunnyvale, CA).

3.2.4 DNA extraction and qPCR

Soil genomic DNA was extracted using the PowerSoil DNA Isolation Kit (MO BIO, Carlsbad, CA) according to the manufacturer's instructions. Ammonia-oxidizing archaea (AOA) and bacteria (AOB) were quantified by determining *amoA* gene abundance using recently developed primer sets GenAOAF/R and GenAOBF/R, respectively (Meinhardt *et al.* 2015). All qPCR amplifications used SsoAdvanced Universal SYBR Green Supermix (Bio-Rad, Hercules, CA) and were performed on a CFX96 Real-Time PCR Detection system (Bio-Rad, Hercules, CA). All qPCR amplifications were carried out in duplicate 10 µL volumes. Each reaction contained 5 µL of 2× SsoAdvanced Universal SYBR Green Supermix, 1 µL of template DNA, 0.4 µL of a 10 mg mL^{-1} bovine serum albumin solution, and 0.025 µL of each primer at 100 µM concentrations. Thermal cycling conditions were as follows: 3 minutes of initial denaturation at 98°C, followed by 39 cycles of denaturation at 98°C for 15 seconds and annealing/extension at 55°C for 30 seconds. The standard curves for both AOA and AOB *amoA* genes were constructing with 10-fold serial dilutions of PCR amplicons generated from the same soil samples with the same primers. Efficiencies were 91.2% and 95.8% for AOA and AOB *amoA* qPCR data, respectively. Standard curve R^2 values were all >0.99.

3.2.5 Statistics

A three-way ANOVA (analysis of variance) was used to identify the effects of land-use, depth, and temperature on activity measurements (NO_2^-+NO_3^- or N_2O accumulation), followed by a Tukey's test. Two-way ANOVA was used to assess the influence of depth and temperature on NO_2^- accumulation. Spearman's rank order correlation was used to test the relationship

between environmental factors and activity measurements or ammonia oxidizer gene abundances. All statistical tests were carried out using R 3.2.3 (R Core Team, Vienna).

3.3 Results

3.3.1 Soil sample characteristics

Measured NH_4^+ concentrations were influenced by land-use, with higher concentrations in composites from forest soil than those from agricultural soil (Table 3.1). The NO_3^- concentrations were influenced by depth, higher for subsurface agricultural composites than subsurface forest soil composites (Table 3.1). The pH of the soil samples spanned a relatively narrow range (pH 6.7-8.2). The C:N ratio was highest among subsurface soil samples collected from forest sites in autumn (Table 3.1).

3.3.2 Dynamics of NO_2^-+NO_3^- accumulation

Background soil nitrification rates were determined for all soil samples, without additional NH_4^+ at 30°C, by measuring net accumulation of NO_2^-+NO_3^-. The background nitrification rate was highest (1.44 mg N kg^{-1} soil d^{-1}) in autumn surface agricultural soils across all samples (Figure 3.1). All subsurface soils showed nitrification rates below 0.20 mg N kg^{-1} soil d^{-1}. In all soils, background nitrification rates were attributed primarily to AOA, with octyne-resistant activity ranging from 63 to 100% of the uninhibited samples (Figure 3.1). Acetylene-resistant activity was not observed for any soil samples.

When additional NH_4^+ was added to soil samples, detectable NO_2^-+NO_3^- did not accumulate during the six-day incubation time for agricultural soil microcosms in the presence of acetylene, indicating that the accumulation of NO_2^-+NO_3^- in acetylene-free microcosms was

Table 3.1 – Soil physicochemical properties

Properties of soil samples from active agricultural (A) and forest (F) sites. Soils were composites of field replicates.

Site	Sampling season	Depth (cm)	NH_4^+ (mg N kg $soil^{-1}$)	NO_3^- (mg N kg $soil^{-1}$)	Inorganic C (%)	Organic C (%)	Total N (%)	C:N ratio	pH
A	Summer	0-15	1.22	6.85	1.25	1.59	0.12	23.7	8.0
		30-45	0.60	3.95	0.29	1.21	0.08	18.8	7.7
F		0-15	10.6	14.3	0.00	5.94	0.33	18.0	6.8
		30-45	8.70	2.98	2.66	1.55	0.08	52.6	7.7
A	Autumn	0-15	0.59	9.41	0.85	1.90	0.13	21.2	7.8
		30-45	0.63	1.53	0.40	0.60	0.05	20.0	7.9
F		0-15	3.39	9.14	0.00	2.89	0.16	18.1	6.7
		30-45	0.95	0.62	5.91	0.47	0.05	127.6	8.2

dominated by autotrophic nitrifiers. However, a relatively small amount of acetylene-resistant activity (up to 9.2% in surface soil and 12.2% in subsurface soil) was detected in autumn forest soils after four days of incubation, suggesting heterotrophic nitrification. The overall nitrification potential (NP) ranged from 0.72±0.16 to 6.73±0.11 mg N kg^{-1} soil d^{-1} for summer surface soils

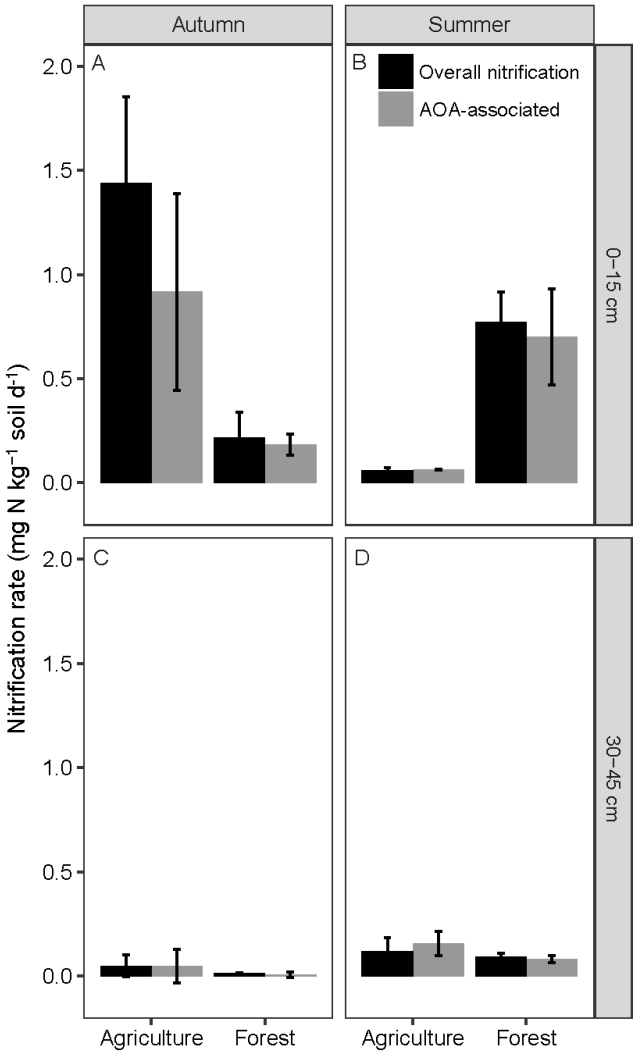

Figure 3.1 – Soil background nitrification rates

Background nitrification rates in autumn (A and C) and summer (B and D) soil samples with (grey)/without (black) octyne. Surface soils (A and B) are in general more active than subsurface soils (C and D), except for summer agricultural soils. Nitrification rate was measured as the accumulation of NO_2^-+NO_3^-. The soils were incubated at 30°C.

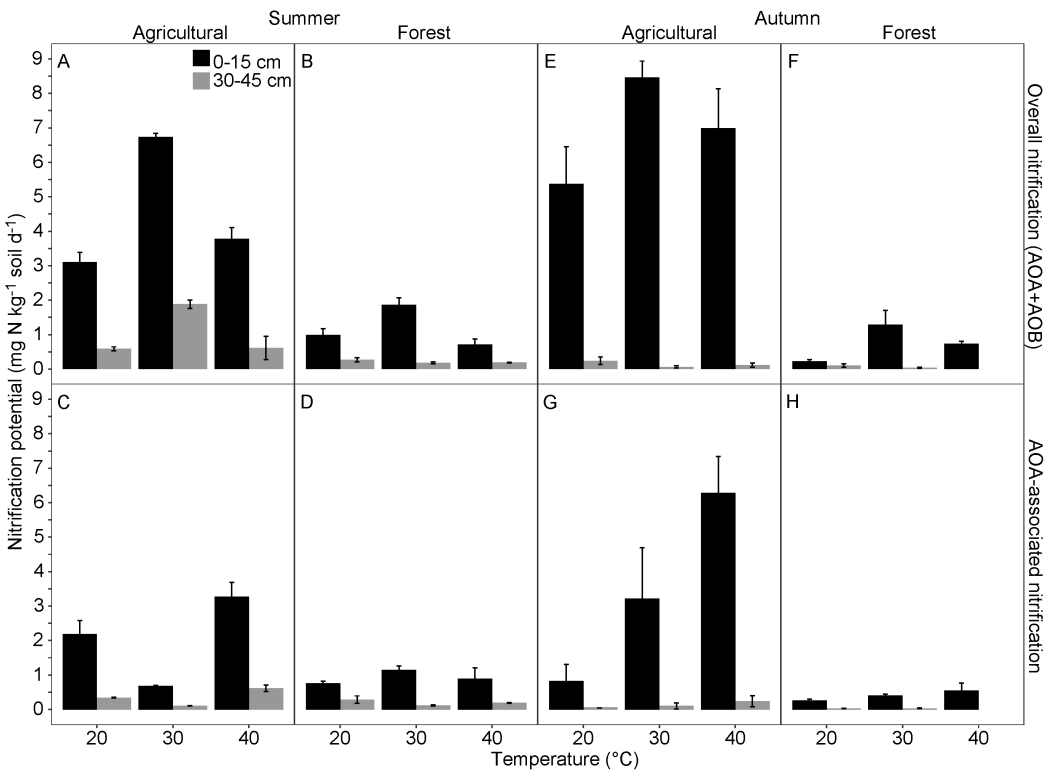

Figure 3.2 – Nitrification potential

Overall nitrification potential (A, B, E, and F) and AOA-associated nitrification potential (C, D, G and H) of a six-day whole soil incubation for both agricultural (A and C, E and G) and forest (B and D, F and H) soils at three different incubation temperatures (20, 30, and 40°C) and depths (0-15 and 30-45 cm). Summer (A-D) and autumn (E-H) soils are included. The NP was measured as nitrite and nitrate accumulation per gram of soil per day. No activity was detected in subsurface forest soils collected in autumn.

and 0.18±0.03 to 1.88±0.12 mg N kg^{-1} soil d^{-1} for summer subsurface soils (Figures 3.2A and B), and 0.22±0.05 to 8.46±0.48 mg N kg^{-1} soil d^{-1} for autumn surface soils and 0.04±0.02 to 0.24±0.11 mg N kg^{-1} soil d^{-1} for autumn subsurface soils (Figures 3.2E and F). No NP was detected in the subsurface forest soil (autumn) replicates incubated at 40°C (Figures 3.2F and H). The overall NP was influenced by land use type ($p < 0.001$), depth ($p < 0.001$), and temperature ($p < 0.001$). Interactions among the three factors were detected by a three-way ANOVA and, as a result, the overall NP was analyzed independently for each soil type. In general, agricultural soils had a higher overall NP than forest soil, and surface soils higher than subsurface soils, at the

same incubation temperature (Figures 3.2A, B, E, and F). Surface soils under both land uses reached greatest activity at 30°C for soils collected in both seasons but statistical analysis indicated no significant difference between nitrification activity measured at 30 and 40°C (p = 0.18), nor between 20 and 40°C (p = 0.13) among agricultural soils collected in autumn. For subsurface soils, higher nitrification activity was observed at 20°C across autumn agricultural and forest site samples, but not significantly different from other temperatures ($p > 0.05$). Agricultural subsurface soil sample collected in summer reached highest activity at 30°C ($p <$ 0.01), and its NP was even higher than summer forest surface soil sample incubated at 40°C ($p <$ 0.01).

The AOA-associated (octyne-resistant) NP increased with incubation temperature in surface soils for both agricultural and forest samples collected in autumn (Figures 3.2G and H). In autumn agricultural soil, the lowest and highest rates were observed at 20 and 40°C for surface samples, respectively (Figure 3.2G). Within surface forest soils, the highest AOA-associated NP was 0.55±0.22 mg N kg^{-1} soil d^{-1} (Figure 3.2H), which was only 8.8% of highest rate observed for the agricultural soil. No statistical difference was detected among AOA-associated NP in subsurface soils (autumn) from either agricultural or forest sites, respectively. Agricultural soils collected in summer showed different temperature responses in terms of AOA-associated activity. The lowest AOA-associated activity for surface soil was detected at 30°C, with similar NP as that of autumn samples at 20°C (Figure 3.2C). Similar to autumn samples, no significant difference was detected among forest surface soils collected in summer under different temperatures ($p > 0.05$; Figure 3.2D).

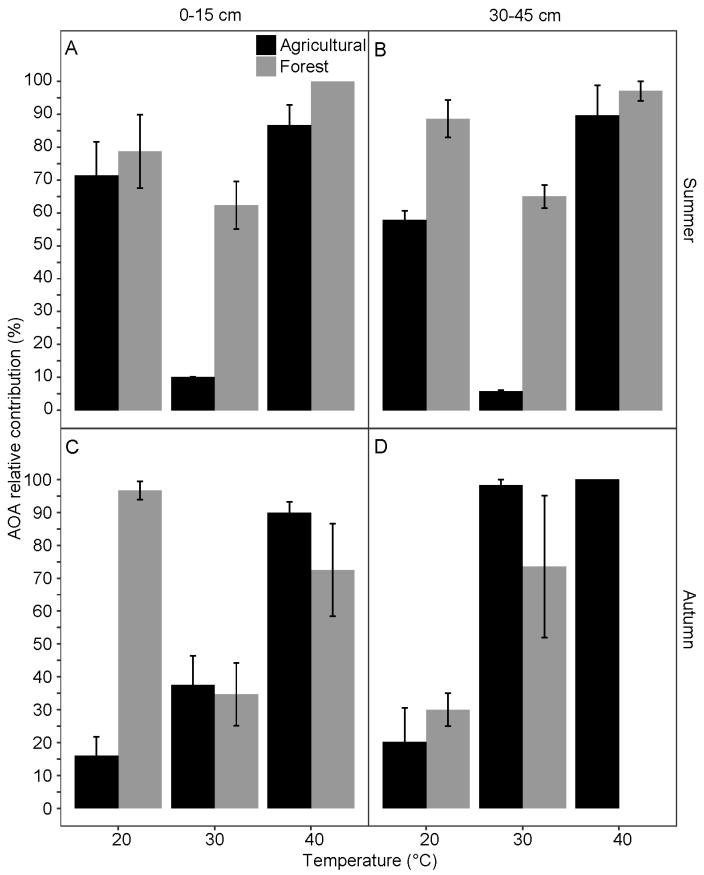

Figure 3.3 – AOA contribution to nitrification

Relative contribution of AOA to total nitrification activity in summer (A and B) and autumn (C and D) soil samples collected from both agricultural (black) and forest (gray) sites, incubated at three different incubation temperatures (20, 30, and 40°C). Two depths were included: surface (0-15 cm; A and C) and subsurface (30-45 cm; B and D). The AOA contribution is calculated by dividing octyne-resistant activity over total activity. No activity was detected in subsurface forest soils collected in autumn.

In order to evaluate the relative contribution of AOA to total (AOA- and AOB-associated) nitrification, the proportion of AOA-supported nitrification to total nitrification activity was calculated (Figure 3.3). AOA relative activity ranged from ~5 to 98% across all microcosms from the agricultural and forest sites, and across multiple depths and temperatures (Figure 3.3). When incubated at 40°C, nitrification in all soils was dominated by AOA (mean percentage > 50%), except for autumn subsurface forest soils where no activity was detected.

The AOA-associated activity was 100% in surface forest soil collected in summer (Figure 3.3A) and subsurface agricultural soil collected in autumn (Figure 3.3D). At 20°C, agricultural soils and subsurface forest soil replicates were dominated by AOB-associated nitrification among autumn samples, but switched to AOA-dominance in summer samples. The only two summer soil samples with activity dominated by AOB were agricultural soils from both depths incubated at 30°C (Figures 3.3A and B). Furthermore, two-way ANOVA showed that the proportion of AOA-associated activity for agricultural soils was influenced significantly by temperature (p = 0.003 summer soils, $p < 0.001$ autumn soils) and depth ($p = 0.01$ summer soils, no significant difference among autumn soils). For AOA-associated forest soil proportions, no significant depth effects were detected for samples collected in both seasons, whereas temperature ($p < 0.001$) showed a significant influence on autumn samples, but not on summer samples. Three-way ANOVA detected significant land-use effect on AOA-associated activity percentage only among autumn samples ($p < 0.001$), but land use effect was insignificant among summer samples (p = 0.103).

3.3.3 AOA and AOB amoA gene abundance

Overall AOA *amoA* gene abundance decreased with depth in all samples (Figure 3.4), with significant differences only detected among autumn samples ($p = 0.59$ summer soils, $p <$ 0.01 autumn soils). AOB *amoA* gene abundance were similar at each depth among summer samples ($p = 0.98$), as well as autumn forest samples ($p = 0.83$). A significant decrease of AOB *amoA* gene abundance with increasing depth was only detected among autumn agricultural samples ($p < 0.01$). Temporal change was detected among AOA *amoA* gene abundance in subsurface soils from both land-use type ($p = 0.04$ agricultural soils, $p = 0.02$ forest soils), but no

significant change was detected in surface soils. In contrast, AOB *amoA* gene abundance was relatively stable in both seasons, with no significant change detected in either surface or subsurface soils.

When correlated with environmental factors, summer and autumn samples showed a different trend. AOA *amoA* gene abundance decreased with pH ($p < 0.001$, rho = -0.85) and increased with soil NO_3^- content ($p < 0.001$, rho = 0.89) in autumn samples, but not in summer samples. Summer soil AOA *amoA* gene abundance increased with total carbon ($p = 0.04$, rho = 0.68). AOB *amoA* gene abundance decreased with total carbon ($p = 0.03$, rho = -0.69, autumn; $p = 0.02$, rho = -0.76, summer) and soil NH_4^+ content ($p = 0.03$, rho = -0.82, autumn), and increased with NO_3^- ($p = 0.02$, rho = 0.70, autumn) and pH ($p = 0.03$, rho = 0.71, summer).

3.3.4 N_2O production dynamics with NO_2^-+NO_3^- accumulation

Across all microcosm incubations, N_2O production was only detected in surface agricultural soil replicates incubated at 30°C. The overall six-day average N_2O production rate for autumn replicates was 0.02 mg N_2O-N kg $soil^{-1}$ d^{-1}, and 0.14 mg N_2O-N kg $soil^{-1}$ d^{-1} for summer. Proportional yields of N_2O were calculated as accumulation of N_2O-N divided by NO_2^-+NO_3^--N accumulation. The six-day average yield for the whole soil incubation was 0.28±0.14% for autumn samples and 2.18±0.53% for summer samples (Table 3.2).

Table 3.2 – Nitrification dynamics during incubation

Ammonia oxidation and N_2O production in surface agricultural soil incubated for 2, 4, or 6 days. All values are given mean with standard deviation (n=3). Soils were composites of field replicates.

	Incubation time (day)	N_2O accumulation (mg N kg^{-1} soil)	Total NO_2^-+NO_3^- accumulation (mg N kg^{-1} soil)	AOB NO_2^-+NO_3^- accumulation (mg N kg^{-1} soil)	Total N_2O yield (%)*	AOB N_2O yield (%)†
Autumn soils	2	0.05 (0.05)	33.5 (6.07)	12.3 (3.96)	0.16 (0.21)	0.53 (0.72)
	4	0.13 (0.08)	38.5 (3.06)	26.3 (2.15)	0.36 (0.22)	0.51 (0.29)
	6	0.15 (0.08)	50.8 (2.87)	31.5 (6.25)	0.28 (0.14)	0.51 (0.36)
Summer soils	2	0.05 (0.02)	14.3 (0.72)	11.5 (1.08)	0.37 (0.12)	0.46 (0.13)
	4	0.53 (0.11)	22.3 (1.65)	19.6 (1.66)	2.43 (0.62)	2.77 (0.73)
	6	0.88 (0.21)	40.4 (0.64)	36.3 (0.57)	2.18 (0.53)	2.43 (0.59)

Percentage yields of N_2O were calculated as accumulation of N_2O-N divided by NO_2^-+NO_3^--N accumulation. * Total N_2O yield was calculated by dividing N_2O accumulation by total NO_2^-+NO_3^--N accumulation; † AOB N_2O yield was calculated by dividing N_2O accumulation over AOB NO_2^-+NO_3^--N accumulation.

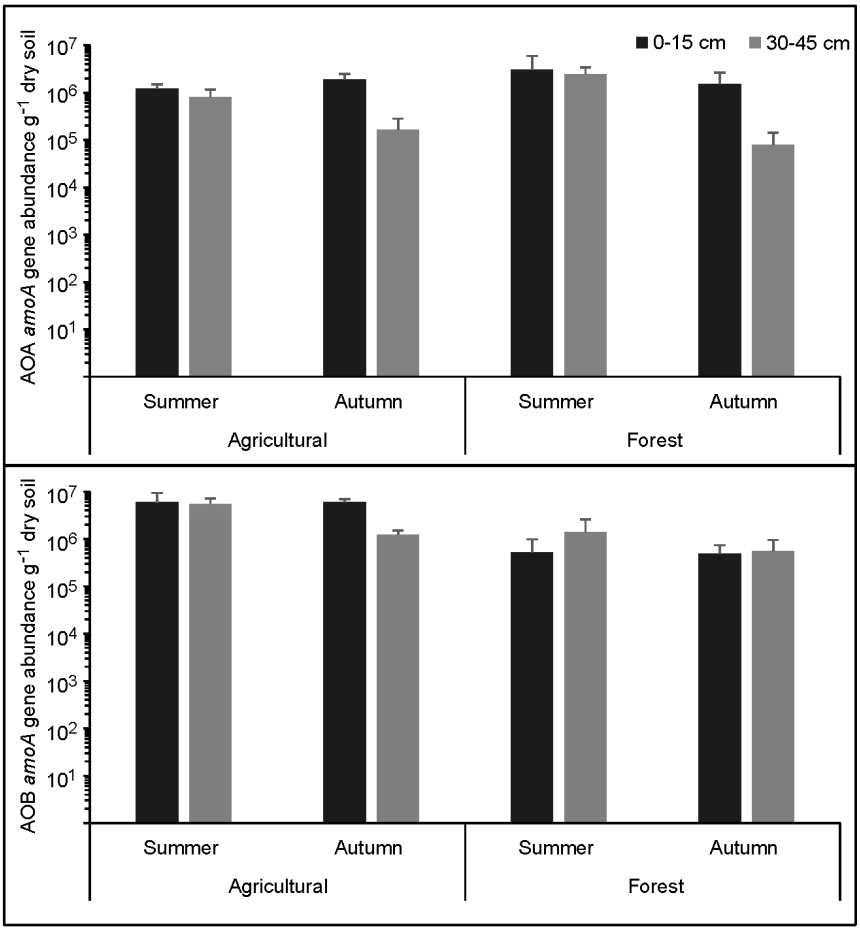

Figure 3.4 – AOA and AOB abundance in soil samples

Abundance of *amoA* genes from ammonia-oxidizing archaea (upper) and bacteria (bottom) in active agricultural and forest soils.

By day six, 2.33 and 5.46 nmol g soil^{-1} N_2O was recorded in the acetylene-treated replicates for autumn and summer soils, respectively, which was likely not associated with nitrification because detectable levels of NO_2^-+NO_3^- did not accumulate in the acetylene treatments in these agricultural soils. An additional 5.24 nmol N_2O g soil^{-1} production was measured in the absence of acetylene for autumn samples, which was inferred to be associated with nitrification. The N_2O concentration detected in summer soils in the absence of acetylene was 31.4 nmol N_2O g soil^{-1}, six times higher than that of autumn soils. Octyne-treated agricultural soil had no detectable N_2O production, indicating that AOA (octyne-resistant) were

not responsible for the N_2O production. The six-day average N_2O yield for AOB only was 0.51±0.36% for autumn soils and 2.43±0.59% (Table 3.2) for summer soils. The six-day average N_2O production rate per cell was estimated to be 1.44×10^{-7} nmol cell^{-1} d^{-1} for AOB-supported nitrification in autumn soils and 8.84×10^{-7} nmol cell^{-1} d^{-1} for summer soils.

N_2O yields after 2, 4, and 6 days of incubation were calculated for both AOB-dominated (octyne-sensitive) and total activity (Table 3.2). The N_2O yield correlated significantly with incubation time ($p < 0.05$) for both AOB-dominated and total activity, indicating the production of N_2O together with NO_2^-+NO_3^- accumulation was not independent of incubation time. A comparison of the N_2O yields in the AOB-dominated versus total activity at each sampling point (days 2, 4, and 6) confirmed that AOA did not contribute significantly to N_2O production. The statistical analysis did not detect any significant differences between N_2O yields for AOB-dominated and total activity at the three time points ($p > 0.05$).

3.3.5 Dynamics of NO_2^- accumulation and N_2O production

NO_2^- accumulation was detected only in surface and subsurface agricultural soil microcosms without any inhibitor (octyne or acetylene), collected either in summer and autumn (Figure 3.5), with accumulation rates ranging from 0.002 to 5.82 mg N kg^{-1} soil d^{-1}. In surface agricultural soil microcosms, NO_2^- was detected after 2 days incubation, and the percentage of NO2- relative to total NO_2^-+NO_3^- concentrations increased with incubation time reaching 45.9% and 68.8% in summer and autumn soil microcosms, respectively, after incubation at 30°C for 6 days (Figures 3.5A and C). In subsurface soil microcosms incubated at 30°C, this proportion

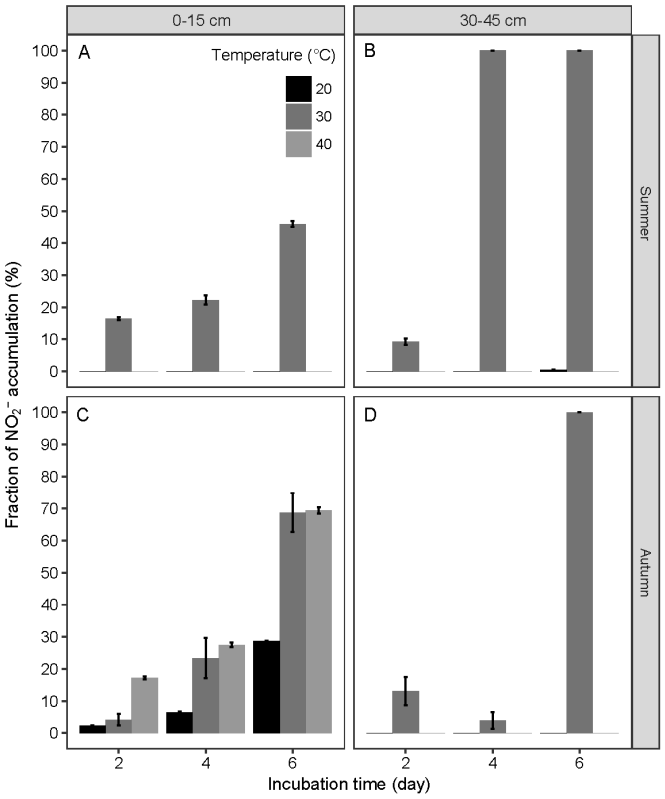

Figure 3.5 – Nitrite accumulation in soils during incubation.

Fraction of NO_2^- in NO_2^-+NO_3^- accumulation in agricultural surface (A and C) and subsurface (B and D) soils collected in summer (A and B) and autumn (C and D) at 20, 30, and 40°C measured after 2, 4, and 6 days of incubation. NO_2^- accumulation in surface summer soil and subsurface autumn soil was detected only at 30°C.

reached 100% after 4-and 6-days incubation in summer and autumn samples, respectively (Figures 3.5B and D). NO_2^- accumulation was also observed in autumn surface agricultural soils incubated at 20 and 40°C (Figure 3.5C) and summer subsurface soils at 20°C (Figure 3.4B). Both temperature ($p < 0.001$) and incubation time ($p < 0.001$) influenced the NO_2^- proportion significantly in surface autumn samples (Figure 3.5C).

For surface agricultural soil microcosms where N_2O production was detected, NO_2^- accumulation started at 2.29 mg N kg^{-1} soil after 2 days incubation, and reached 18.5 mg kg^{-1} and 34.9 mg N kg^{-1} soil after 6 days incubation in summer and autumn soil microcosms, respectively. The N_2O accumulation rate in summer agricultural soils correlated significantly with NO_2^- accumulation ($R^2 = 0.67$, $p = 0.004$), but no significant correlation was observed in autumn agricultural soils ($R^2 = 0.13$, $p = 0.19$) (Figure 3.6).

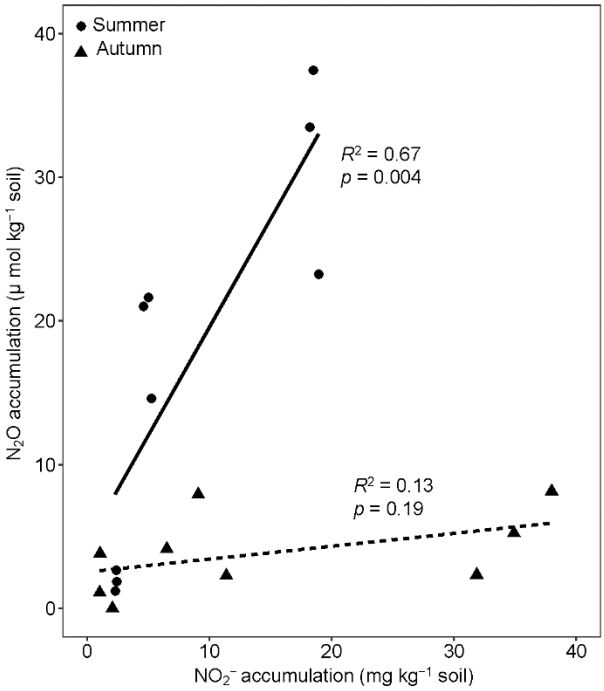

Figure 3.6 – Nitrous oxide emission under different nitrite accumulation.

Correlation between N_2O and NO_2^- accumulation in agricultural surface soils throughout 6 days incubation at 30°C. Circles: summer soil; triangles: autumn soil. Significant ($p < 0.05$) correlation was only observed in summer soil.

3.4 Discussion

3.4.1 Relative contributions of AOA and AOB to soil nitrification

The effect of temperature on short-term (≤6 days) AOA-associated (octyne-resistant) and AOB-associated (octyne-sensitive) ammonia oxidation activity in surface (0-15 cm) and subsurface (30-45 cm) agricultural and forest soils were examined. At the same time, N_2O produced during ammonia oxidation was measured together with NO_2^-+NO_3^- accumulation. Although several studies have reported the activity of AOA isolates at 35-72°C (De La Torre *et al.* 2008; Tourna *et al.* 2011; Lehtovirta-Morley *et al.* 2016), the influence of temperature on *in situ* ammonia oxidation was not clear prior to this study.

During the soil microcosm incubations, additional NH_4^+ increased the octyne-sensitive (AOB-associated) contribution to overall activity compared to no addition, except for autumn subsurface agricultural soil and autumn subsurface forest soil. This NH_4^+-induced AOB activity

was reported in several studies (Jia and Conrad 2009; Taylor *et al.* 2010, 2012; Xia *et al.* 2011; Giguere *et al.* 2015; Ouyang *et al.* 2016; Hink *et al.* 2018). Absolute AOA-associated nitrification potential was higher within agricultural soil samples than forest soils at each incubation temperature (Figures 3.2C, D, G, and H). Given that AOA abundance was of the same order of magnitude among forest and agricultural soils at the same depth, this discrepancy between agricultural and forest soil AOA-associated ammonia oxidation rates is probably due to the differences in AOA community composition in these two soils.

3.4.2 Temperature effect on nitrification

In this study, temperature was identified as an important factor controlling the magnitude of AOA and AOB ammonia oxidation and N_2O production. The highest AOA-associated and AOB-associated activity in surface soils was observed at 40°C and 30°C, respectively. The highest AOA-associated activity in subsurface agricultural soils was recorded at 40°C for both summer and autumn soils, whereas 20°C and 30°C favored AOB-associated activity in autumn and summer subsurface agricultural soil, respectively. In forest subsurface soils, the optimal temperature for AOB showed seasonal variation, 20°C in autumn soil and 30°C in summer soil, but 40°C did not favor AOB activity in either soil. In general, the results showed that AOA were more active at higher temperature, whereas AOB preferred lower temperature. Several studies have reported a dominance of AOB for agricultural soil ammonia oxidation (Jia and Conrad 2009; Xia *et al.* 2011; Ouyang *et al.* 2016), within which soil microcosms were carried out at temperatures ~27°C, which agreed with the results at 30°C for both surface agricultural and surface forest soils. Recently, Taylor and colleagues (2017) reported that soil AOA and AOB contributed differently to ammonia oxidation across a temperature range of 4-42°C, with AOA

having optimal temperatures at least 12°C higher than AOB. A similar pattern was observed in a slurry incubation with greenhouse agricultural soils covering 5-45°C (Duan *et al.* 2018). It has been suggested that results from a slurry assay may not extrapolate to whole soil incubations because of disturbed homogenizing incubation and redox conditions, which can influence ammonia oxidation rates (Lu, Bottomley and Myrold 2015). However, a similar pattern was observed in this study, with AOA showing higher activity at elevated temperatures compared to AOB, as found previously by Taylor *et al.* (2017) and Gubry-Rangin *et al.* (2017). In addition, there may be a confounding influence of temperature with soil pH, which has been demonstrated to be a major factor determining thaumarchaeotal niche differentiation (Prosser and Nicol 2012). A differential temperature response of the thaumarchaeotal community varying with soil pH was similar to that observed by Gubry-Rangin *et al.* (2017), indicating a pH-dependent selection mechanism on AOA populations with different optimal growth temperatures. The different optimal temperature of soil AOA along soil depth in this study also suggested the potential that different AOA lineages may be present along the soil profile, both in forest and agricultural soils.

3.4.3 Temperature effect on soil N_2O production

The detection of N_2O production in surface agricultural soils only at 30°C provides evidence for a temperature-dependent influence on N_2O production via nitrification. However, it should be noted that an inability to detect the presence of N_2O at 20 or 40°C does not necessarily mean the absence of N_2O under those conditions. The N_2O detection limit of the method used in this study was 0.05 nmol g^{-1} soil. Based on an agricultural soil AOA pure culture, whose N_2O yield is 0.08-0.23% (Jung *et al.* 2011, 2014b), the calculated archaeal N_2O production at 40°C would be ~0.18-0.52 nmol g^{-1} soil d^{-1} for autumn agricultural soils and 0.09-0.27 nmol g^{-1} soil d^{-1}

for summer agricultural soils used in this study. This theoretical value is above the detection limit, so it is more likely that in the soil samples used here, the actual AOA-associated N_2O production was not as high as in pure cultures. Such a low *in situ* N_2O production rate by AOA was also reported by Hink et al., (2017, 2018) with inorganic N addition. In addition, soil pH may have a role in determining N_2O yields by AOA. Currently, the highest measured N_2O yield for a cultured AOA is for the acidophilic I.1a-associated archaeon strain CS isolated from acid mine sediment (original pH 3.4, grown at pH 5.0), demonstrating ~5-50 times higher N_2O production than other agricultural strains isolated from soils with neutral pH (6.5-7.5) (Jung *et al.* 2014b). These results suggest a different N_2O production mechanism in acidic soils where AOA are probably the major contributors under oxic conditions. Acidic AOA might produce N_2O via the formation of nitrosonium cation (NO^+) from nitrous acid (HONO) under acidic conditions (Hughes 1999). However, this process might rely more on abiotic hybrid via nucleophilic nitrosation of NH_2OH (Spott, Russow and Stange 2011), and it still remains unclear what mechanism is used by acidophilic AOA. However, given the non-acidic pH of the soils in this study, the low AOA-associated N_2O yield is possibly due to the absence of this abiotic hybrid process. The high yield of acidophilic AOA strains is also possibly due to their high sensitivity to nitrite, which can inhibit the growth of *Nitrosotalea devanaterra* and strain CS at 40 μM and 100 μM, respectively (Lehtovirta-Morley *et al.* 2011; Jung *et al.* 2014b), whereas *Nitrososphaera viennensis*, isolated from neutral pH soil, can tolerate a nitrite concentration ~100 times higher than *N. devanaterra* (Tourna *et al.* 2011). The detected N_2O in the headspace represented net N_2O accumulation, with N_2O consumption processes potentially occurring simultaneously. Denitrification is considered the major N_2O consumption pathway in soil (Vieten *et al.* 2008; Hu *et al.* 2015) and although oxic conditions were maintained during microcosm incubation, it is

possible that some microsites had low oxygen concentrations during the incubation which facilitated denitrification activity. Subsurface soil samples may naturally possess higher denitrification activity due to low *in situ* oxygen concentrations and thus a greater denitrifier activity. In previous research, potential denitrifiers were identified including *Pseudomonas* and *Thiobacillus* in these ***rare*** site soils (Seuradge, Oelbermann and Neufeld 2017). Therefore, the absence of detected N_2O in some soils may be the result of relatively high denitrification activity resulting in the lowering of N_2O concentrations to less than the detection limit.

Seasonal (temporal) changes in N_2O production and nitrification were also detected in these soil samples. The summer samples showed a 10-fold higher N_2O yield than autumn soil samples, indicating the potential change of active populations in these soil samples. This difference might be due to different soil temperatures when soil samples were collected. The summer soil was 26°C when sampled and the autumn soil was 14°C; distinct ammonia oxidizer populations may have been selected during this time. Taylor and colleagues (2017) recently modeled temperature responses of AOA and AOB and demonstrated that AOA and AOB showed highest nitrification activity under different temperatures. The optimal temperature for AOA was close to 40°C for the soils samples they used, and AOB always showed highest activity below 30°C, and sometimes below 20°C. This range matched the soil temperature when sampled, and may have explained the AOB-dominant activity difference between the two sampling times. However, identification of the active lineages in these soils under different temperatures would enable comparison of their *in situ* nitrification activities to isolates or enrichments.

3.4.4 Influence of NO_2^- accumulation on soil N_2O production

The results demonstrated a positive correlation between NO_2^- accumulation and N_2O production in surface agricultural soil during a 6-day incubation period (Figure 3.6). Although this correlation was not significant for autumn soil, a strong positive correlation was found in soil samples collected from the same site in summer, indicating a possible seasonal effect on NO_2^- accumulation and nitrifier-associated N_2O production in this agricultural soil. An association between aerobic N_2O production and NO_2^- accumulation in soil has been observed in several studies (Venterea 2007; Maharjan and Venterea 2013; Venterea *et al.* 2015; Giguere *et al.* 2017; Duan *et al.* 2018). However, AOA- or AOB-dependent N_2O production was also observed in soils where NO_2^- was not detected (Hink, Nicol and Prosser 2016). Both NO_2^--dependent and independent N_2O production were observed in the same agricultural soils collected in different seasons, indicating a seasonal effect on AOA- or AOB-associated N_2O production. Indeed, both NO_2^--dependent and independent N_2O-producing mechanisms in ammonia oxidizers have been proposed in a number of studies (Cantera and Stein 2007; Jung *et al.* 2014b; Kozlowski, Price and Stein 2014; Stieglmeier *et al.* 2014b), and nitrite-dependent N_2O production might be a detoxifying mechanism to protect nitrifiers from nitrite toxicity (Jung *et al.* 2014b). Moreover, growth of the recently discovered comammox bacterium *Nitrospira inopinata* can result in transient NO_2^- accumulation during complete oxidation of NH_3 (Kits *et al.* 2017), although the accumulated nitrite was subsequently converted to nitrate. Although it is likely that transient NO_2^- accumulation was the result of a temporary differences in the capacity between active ammonia and nitrite oxidizing populations, there is a possibility that this short-term incubation covered only the period of nitrite accumulation by comammox, if they were present in these soil samples. Given the possibility of an inhibition effect of octyne on comammox bacteria, it is

possible that nitrite accumulation detected in soil samples without added octyne was produced by comammox bacteria in addition to AOB. Regardless of the NO_2^- source, the results confirmed the presence of NO_2^--dependent and independent N_2O production in the agricultural soils, and more importantly, the temperature-dependent nature of this mechanism.

3.4.5 Relative contributions of AOA and AOB to N_2O production

In these soils, AOB-associated N_2O production showed N_2O yields of ~0.50% for autumn samples and 2.43% for summer samples, a little higher than the range reported for *Nitrosomonas europaea* (Jung *et al.* 2011, 2014b), but within in the reported range of 0.02 to 7.6% (Shaw *et al.* 2006; Mørkved, Dörsch and Bakken 2007; Santoro *et al.* 2011; Zhu *et al.* 2013; Jung *et al.* 2014b; Stieglmeier *et al.* 2014b; Hink, Nicol and Prosser 2016; Hink *et al.* 2018). The per cell AOB N_2O production rate (1.44×10^{-7} nmol cell^{-1} d^{-1} autumn, 8.84×10^{-7} nmol cell^{-1} d^{-1} summer) was calculated for the six-day incubation period, using the original AOB *amoA* gene abundance as an estimation. Considering that growth may have occurred during the six-day incubation, the actual N_2O-producing rate may be lower than the calculated value. Isolated representatives of *Nitrosospira*, which are typically the dominant soil AOB group, can have N_2O production rates of 0.9-1.4×10^{-7} nmol cell^{-1} d^{-1} (Smith *et al.* 2001), and the rate of *N. europaea* can be as high as 13.9×10^{-7} nmol cell^{-1} d^{-1} (Shaw *et al.* 2006). In general, AOB cultures have higher N_2O yields than AOA cultures, particularly when compared to marine AOA (Shaw *et al.* 2006; Jung *et al.* 2011, 2014b; Santoro *et al.* 2011; Stieglmeier *et al.* 2014b). This higher rate of N_2O production by AOB compared to AOA might be explained by AOB producing N_2O via two enzymatic mechanisms (i.e. the incomplete oxidation of hydroxylamine and nitrifier-denitrifcation) whereas it has been proposed that N_2O derived from AOA is only produced via the abiotic interaction of

hydroxylamine and NO (Kozlowski *et al.*, 2016). However, although Stieglmeier *et al.* (2014b) suggested that AOA may not be capable of nitrifier-denitrification, NO_2^--dependent N_2O production was measured during AOA-supported nitrification recently by Giguere *et al.* (2017), which raises the need for further investigation into NO_2^- stimulation of N_2O production.

3.5 Conclusion

The results highlight differential temperature responses of AOA and AOB, with AOA dominating nitrification at higher soil temperatures. Soil AOB were identified as major contributors to N_2O production through ammonia oxidation in the tested agricultural samples, influenced by temperature. Surface soils were major N_2O sources, whereas subsurface soils may not contribute significantly to soil N_2O production.

Chapter 4[3]

A keystone role for soil cobalamin producers

4.1 Introduction

Vitamin B_{12} (cobalamin), once referred to as "nature's most beautiful cofactor" (Stubbe 1994), plays an important role as a coenzyme involved in the synthesis of nucleotides and amino acids, in addition to carbon processing and gene regulation within cells across all domains of life (Roth, Lawrence and Bobik 1996; Romine *et al.* 2017). Despite widespread metabolic dependency on cobalamin, only a relatively small subset of bacteria and archaea are capable of its production (Zhang *et al.* 2009; Degnan *et al.* 2014; Seth and Taga 2014). Cobalamin is present in natural systems in several chemical forms, including the enzymatically active forms of adenosylcobalamin (Ado-B_{12}) and methylcobalamin (Me-B_{12}), and the inactivated forms of hydroxocobalamin (OH-B_{12}) and cyanocobalamin (CN-B_{12}). Cobalamin biosynthesis requires more than 30 enzymatic steps (Roth *et al.* 1993; Blanche *et al.* 1995) via aerobic or anaerobic pathways (Raux *et al.* 1999) and represents a high genomic and metabolic burden for producers.

Previous research on microbial cobalamin production and its environmental significance has focused on marine systems where many eukaryotic primary producers are cobalamin dependent and limited by the availability of this short-lived cofactor, demonstrating a significant role for cobalamin in controlling ocean microbial community composition (Panzeca *et al.* 2006; Tang, Koch and Gobler 2010; Bertrand *et al.* 2011; Giovannoni 2012; Sañudo-Wilhelmy *et al.* 2014; Doxey *et al.* 2015; Helliwell *et al.* 2016; Heal *et al.* 2017; Frischkorn, Haley and Dyhrman 2018; Walworth *et al.* 2018). Metagenomes, full genomes, and biochemical analyses revealed

[3] A version of this chapter has been submitted for publication in Nature Microbiology:
Lu X, Heal KR, Ingalls AE, Doxey AC, Neufeld JD. A keystone role for soil cobalamin producers. *Under review*.

that taxa affiliated with *Proteobacteria* and *Thaumarchaeota* are major marine cobalamin producers (Doxey et al. 2015; Heal *et al.* 2017), whereas marine *Cyanobacteria* produce pseudocobalamin, a closely related compound with limited bioavailability (Heal *et al.* 2017). Recent understanding of marine cobalamin concentrations and forms has been furthered by methodological advances enabling the direct measurement of cobalamin in environmental samples (Heal *et al.* 2014). Together, the availability of metagenomic data and advances in analytical chemistry techniques provide an ideal framework for exploring cobalamin production, consumption, exchange, and interdependecies in terrestrial ecosystems.

Soils harbor high densities of microbial biomass densities and host some of the most diverse microbial communities on Earth (Richter and Markewitz 1995; Daniel 2005; Roesch *et al.* 2007). The majority of soil biogeochemical processes are mediated by microorganisms (Nannipieri *et al.* 2003) and the sustainability of agricultural soils relies on microbial communities that govern nutrient supplies to plants and crops (Kennedy and Smith 1995). Therefore, it is crucial to elucidate the factors that influence soil microbial diversity, activity, and physiology in order to understand the controls on terrestrial biogeochemical functions (Bier *et al.* 2015; Louca, Parfrey and Doebeli 2016). As a cofactor required by a majority of microorganisms (Rodionov *et al.* 2003), cobalamin availability and distribution in soils are constrained by microbial producers, which might have profound and unexplored impacts on terrestrial biogeochemical cycles. Because cobalamin-dependent enzymes include ribonucleotide reductase (Dickman 1977), methyltransferases (Banerjee 1999), and reductive dehalogenases (Janssen, Oppentocht and Poelarends 2001), cobalamin availability governs a wide range of microbial processes, such as DNA replication and repair (Blakley and Barker 1964; Blakley 1965), regulation of gene expression (Ortiz-Guerrero *et al.* 2011), amino acid synthesis (Banerjee and

Matthews 1990), CO_2 fixation (Berg *et al.* 2007), recycling of carbon to the tricarboxylic acid (TCA) cycle (Bertrand and Allen 2012), and aromatic compound detoxification (Giedyk, Goliszewska and Gryko 2015).

Nearly seventy years ago, microbial cultivation efforts showed that a high proportion of cultured soil bacteria rely on exogenous cobalamin (Lochhead and Thexton 1951; Lochhead, Burton and Thexton 1952; Lochhead and Burton 1956), with the implication that a cohort of soil microorganisms may serve as *in situ* sources of this essential cofactor. Since these early studies, there has been a lack of research into the microbiology of soil cobalamin production, presumably due to both an inability to measure soil cobalamin and the limitations of relying on cultivation-based approaches. In this study, cobalamin-producing genes in soil metagenomes are identified and quantified with profile hidden Markov models (HMMs) and relate the distribution and taxonomy of cobalamin biosynthesis genes to genes involved in cobalamin transport and utilization. Because many microorganisms require cobalamin as a cofactor, there would be a link between the relative abundances of cobalamin consumers and cobalamin producers/remodelers. In addition to metagenomic analyses, the standing stock of *in situ* cobalamin in representative soil samples were quantified and characterized and potential links between cobalamin and soil microbial community composition and abundance were assessed.

4.2 Materials and methods

4.2.1 Soil metagenomes and marker gene selection

A set of 155 soil metagenomes were retrieved from the Metagenomics RAST Server (MG-RAST; Appendix A), ensuring a diverse selection of soil habitats including grassland,

Table 4.1 – The HMMs used in the study of soil cobalamin.

For information on the whole pathway:

http://www.jcvi.org/cgi-bin/genome-properties/GenomePropDefinition.cgi?prop_acc=GenProp0113

Category	HMM	TIGRFAM/PFAM	HMM length	Group
corrin ring biosynthesis	cobI_cbiL	TIGR01467	230	A
corrin ring biosynthesis	cobJ_cbiH	TIGR01466	239	A
corrin ring biosynthesis	cobM_cbiF	TIGR01465	247	A
corrin ring biosynthesis	cbiE	TIGR02467	204	A
corrin ring biosynthesis	cbiT	TIGR02469	124	A
corrin ring biosynthesis	cobH_cbiC	PF02570	196	A
corrin ring biosynthesis	cobB	TIGR00379	449	A
final synthesis and repair	cobA	TIGR00708	177	B
final synthesis and repair	cobQ	TIGR00313	477	B
final synthesis and repair	cobD	TIGR00380	305	B
final synthesis and repair	cobS	TIGR00317	241	B
DMB synthesis and activation	bluB	TIGR02476	205	C
cobalamin transporter gene	btuB	TIGR01779	614	NA
phylogenetic marker	rpoB	FunGene	2842	NA
Methionine metabolism	metH	TIGR02082	1182	NA
methylmalonyl-CoA mutase	mutA	TIGR00642	620	NA
16S rRNA (cytosine(967)-C(5))-methyltransferase	rsmB	TIGR00563	437	NA

agriculture, forest, desert, cold desert, wetland, pasture, and tundra. A set of 12 genes were chosen to represent both aerobic and anaerobic cobalamin biosynthesis pathways (Table 4.1), minimizing a potential pathway-specific bias, as described previously for the analysis of marine metagenomes (Doxey *et al.* 2015; Heal *et al.* 2017). These marker genes for cobalamin

production were classified into three categories (group A, corrin ring biosynthesis; group B, final synthesis and repair; group C, DMB synthesis) (Bertrand *et al.* 2015; Heal *et al.* 2017). Species included in any of the three groups must show the presence of all marker genes within that group from the same soil metagenome, and the taxa with complete cobalamin synthesis pathways were assigned based on the presence of all 12 *cob*/*cbi* genes in the same taxonomic group from the same soil metagenome. Microbial community size was estimated by quantifying the amount of a single-copy gene for the RNA polymerase beta subunit (*rpoB*) (Dahllöf, Baillie and Kjelleberg 2000; Case *et al.* 2007; Kembel *et al.* 2012). The cobalamin transporter gene, *btuB* (Cadieux and Kadner 1999; Chimento *et al.* 2003), was selected as a marker for evaluating cobalamin uptake potential. Three cobalamin-dependent enzyme coding genes, *metH*, *mutA*, and *rsmB* (Romine *et al.* 2017) were included to further explore cobalamin consuming potential in addition to uptake by *btuB* transporter. The input HMM profiles (Table 4.1) for *cob*/*cbi*, *btuB*, *bluB*, *metH*, *mutA*, and *rsmB* genes were retrieved from TIGRFAM (Haft, Selengut and White 2003) or Pfam (Finn *et al.* 2016), and the phylogenetic marker, *rpoB*, from FunGene (Fish *et al.* 2013).

4.2.2 Taxonomic classification using functional genes

MetAnnotate (Petrenko *et al.* 2015), was used to mine for selected marker genes (Table 4.1) in soil metagenomes. Each HMM is searched via HMMsearch (Eddy 1998) against RefSeq release 80 (O'Leary *et al.* 2016) for reference homologs, and against the 155 soil metagenomes for metagenomic homologs, with an *E*-value threshold of 10^{-6}. Taxonomic classifications were made based on the best hits in the NCBI RefSeq database release 80, as predicted using USEARCH (Edgar 2010) with a 50% minimum amino acid identity threshold. Metagenome HMM hit counts were normalized by HMM length.

Table 4.2 – List of all soil sample used for cobalamin measurement.

For ***rare*** Charitable Research Reserve soils, depth is denoted as follows: L1 is 0-15 cm, L2 is 15-30 cm, and L3 is 30-45 cm.

Sample	Project	Land use
10AS	CM^2BL	Agricultural soil - soy
11AW	CM^2BL	Agricultural soil - wheat
13CO	CM^2BL	Compost
1AT	CM^2BL	Arctic Tundra
20CG	CM^2BL	UW community garden
2ATN	CM^2BL	Arctic Tundra
4TS	CM^2BL	Sand
5BF	CM^2BL	Boreal coniferous forest
6TD	CM^2BL	Temperate deciduous forst
7TR	CM^2BL	Temperate rain forest
8NP	CM^2BL	Northern peatlands
9WLM	CM^2BL	Wetland soil
pH4-5	Scotland pH plot	Agricultural
pH5-0	Scotland pH plot	Agricultural
pH5-5	Scotland pH plot	Agricultural
pH6-0	Scotland pH plot	Agricultural
pH6-5	Scotland pH plot	Agricultural
pH7-0	Scotland pH plot	Agricultural
pH7-5	Scotland pH plot	Agricultural
AA_L1	***rare***	Agricultural 0-15 cm
AA_L2	***rare***	Agricultural 15-30 cm
AA_L3	***rare***	Agricultural 30-45 cm
D03_L1	***rare***	Decommissioned agricultural 0-15 cm
D03_L2	***rare***	Decommissioned agricultural 15-30 cm
D03_L3	***rare***	Decommissioned agricultural 30-45 cm
D07_L1	***rare***	Decommissioned agricultural 0-15 cm
D07_L2	***rare***	Decommissioned agricultural 15-30 cm
D07_L3	***rare***	Decommissioned agricultural 30-45 cm
D10_L1	***rare***	Decommissioned agricultural 0-15 cm
D10_L2	***rare***	Decommissioned agricultural 15-30 cm
D10_L3	***rare***	Decommissioned agricultural 30-45 cm
CA_L1	***rare***	Forest 0-15 cm
CA_L2	***rare***	Forest 15-30 cm
CA_L3	***rare***	Forest 30-45 cm
HB_L1	***rare***	Forest 0-15 cm
HB_L2	***rare***	Forest 15-30 cm
HB_L3	***rare***	Forest 30-45 cm
IW_L1	***rare***	Forest 0-15 cm
IW_L2	***rare***	Forest 15-30 cm
IW_L3	***rare***	Forest 30-45 cm

4.2.3 Soil samples collection for cobalamin measurement

Soil samples for cobalamin measurements (Table 4.2) were composed of a collection of soils from three different projects: Canadian MetaMicroBiome Library (CM^2BL) soils covering wide range of soil biome across Canada (Neufeld *et al.* 2011), two distinctive land-use along soil profiles (***rare*** Charitable Research Reserve, Cambridge, Ontario) (Lu, Seuradge and Neufeld 2017), and a pH gradient (4.5-7.5) of agricultural soils (Scottish Agricultural College, Craibstone, Scotland) (Kemp *et al.* 1992). The ***rare*** soil samples were retrieved from three different depths (L1: 0-15 cm, L2: 15-30 cm, L3: 30-45 cm) for each land use type (field and forest). The microbial community compositions of these soils have been determined elsewhere (Neufeld *et al.* 2011; Bartram *et al.* 2014; Lu, Seuradge and Neufeld 2017; Seuradge, Oelbermann and Neufeld 2017), but all representative 16S rRNA gene reads from these projects were re-classified using RDP Naive Bayesian rRNA Classifier (version 2.11), with default settings (Wang *et al.* 2007). Soil DNA for biomass estimation was extracted according to manufacturer protocols with the PowerSoil DNA Isolation Kit (MoBio, Carlsbad, CA), and quantified with a Qubit 2.0 fluorometer (Invitrogen, Carlsbad, CA).

4.2.4 Soil cobalamin extraction and UPLC/MS measurement

Both water leachable cobalamins and non-water leachable cobalamins were extracted from all soil samples using a modified method developed by Heal and colleagues (Heal *et al.* 2014). Field moist soil (0.5 g) was added to 15-ml tubes (VWR, Radnor, PA), with approximately 2 mL of a mixture of 100 μm, 400 μm, 1.4 mm, and 4.0 mm diameter glass beads (OPS Diagnostics). For water leachable cobalamin extraction, each tube was filled with 7 ml of 2 M KCl solution and mixed gently every 10 minutes at room temperature for 60 minutes. The

tubes were centrifuged at 4000 rpm at 4°C for 15 minutes. Supernatants were transferred into 24-ml glass vials and stored at -20°C until desalting and downstream cobalamin analysis. Following the removal of the water leachable portion, remaining cobalamins were extracted with three solutions with decreasing polarity. Solutions used were prepared fresh and the recipe of each solution can be found at the end of this section. Samples were initially beadbeaten three times in 7 ml of solution A for 90 seconds; samples were kept at - 20°C for 30 minutes in between beadbeating rounds. Samples were centrifuged at 4000 rpm, 4°C for 15 minutes, and the supernatant was transferred to 60-ml glass vials. Next, 7 ml solution B was added into the pelleted soil subject to beadbeating for 90 seconds, stored at -20°C for 5 minutes, and centrifuged at 4000 rpm for 15 min at 4°C. Supernatants were added to the same 60-ml glass vials. Extraction was repeated with another 7 ml solution B and supernatant transferred to the same vial, adding up the final volume to 21 ml for each glass vial. Another three rounds of bead beating and centrifugation were carried out using solution C (7 ml each time, 21 ml in total), and the extracts transferred to the 60-ml vials, followed by three, 7ml MeOH extractions. Each MeOH extraction was combined with the extracts to the 60-ml vials. Samples in 60-ml vials were dried down overnight under clean N_2 at no more than 35°C. Finally, samples were reconstituted with 3 ml Milli-Q H_2O, sonicated and vortexed.

Desalting was carried out following a protocol similar to that designed for marine water samples (Heal *et al.* 2014). For each sample (water leachable or non-water leachable) a C18-500 mg SPE column (Waters Sep-Pak) was conditioned by passing through 5 ml methanol, followed by a rinse with 5 ml Milli-Q H_2O, both via gravity. Samples were loaded to SPE columns via gravity, followed by two rinses with 3 ml of Milli-Q H_2O and 3 ml of solution D, respectively. After the rinses, samples were eluted with 5 mL of solution E and collected into 12-ml

borosilicate centrifuge tubes. Eluates were dried down under vacuum at low heat (no more than 35°C). Samples were reconstituted using 380 µl solution F and 20 µl vitamin injection standard mix, sonicated for 2 minutes, and then syringe filtered into labeled amber I-class vials. Samples were analyzed using ultra performance liquid chromatography – mass spectrometry (UPLC/MS) using previously published conditions and vitamin internal standards (Heal *et al.* 2014) for the cobalamins. For DMB, MS conditions used have been reported elsewhere (Boysen *et al.* 2018), paired with the UPLC conditions for the cobalamin analysis. Data were extracted, integrated, and processed through in-house quality control and normalization as reported by Boysen and colleagues (2018). Total cobalamin is the summed value of all detected forms of cobalamin in both the water leachable and non-water leachable fractions of the soil

Solutions A-E were as follows, using Omnisolve grade solutions. Solution A: 50% methanol, 50% 0.2 M KCl (vol/vol); solution B: 50% methanol, 50% Milli-Q H_2O (vol/vol); solution C: 40% acetonitrile, 40% methanol, 20% Milli-Q H_2O, 0.1% formic acid (vol/vol); solution D: 10% methanol, 90% Milli-Q H_2O (vol/vol); solution E: 80% methanol, 20% Milli-Q H_2O (vol/vol); solution F: 20 mM ammonium formate and 0.1% formic acid in H_2O.

4.2.5 Data analysis and visualization

Soil metagenome data were transformed into sample-based relative abundance before statistical analysis. All statistical analyses were carried out using R (V 3.2.3). Analysis of variance (ANOVA) was performed to test the effect of environmental factors on gene abundance or cobalamin concentration, followed by post-hoc Tukey HSD test. A Shapiro-Wilk normality test was used to check a normality assumption prior to correlation analysis. Spearman's rank correlations were employed to compare cobalamin concentrations and microbial biomass, and a

simple linear regression was used to test for a significant linear relationship. In order to test the relationship between cobalamin-producing and consuming taxa in the soil metagenomes studied, Spearman correlation coefficient between the relative abundance of *cob*/*cbi* and *btuB* genes were calculated and compared to the coefficient through 10^5 permutations to determine significance. Package *phyloseq* (V 1.14.0) (McMurdie and Holmes 2013) was used to preprocess OTU tables and calculate diversity indices.

4.3 Results

4.3.1 Soil metagenomic survey of cobalamin producers

With selected profile HMMs and translated nucleic acid sequences, 155 soil metagenomes from diverse geographical locations and land use types were analyzed (Appendix A) to assess the contribution of different taxa to cobalamin production potential via *cob/cbi* gene taxonomic profiles (Figure 4.1). *Proteobacteria*, the dominant cobalamin-producing phylum, contributed to 45.9% of *cob*/*cbi* genes across all soil metagenomes, followed by *Actinobacteria* (24.9%), *Firmicutes* (6.2%), *Acidobacteria* (5.1%), and *Thaumarchaeota* (2.9%) (Figure 4.1A). These phyla contributed similarly to each of the *cob*/*cbi* gene groups that are defined based on the cobalamin biosynthesis pathway (Table 4.1): corrin ring biosynthesis ("Group A"; seven genes), final synthesis and repair ("Group B"; four genes), and 5,6-dimethylbenzimidazole (DMB) synthesis ("Group C"; one gene) (Martens *et al.* 2002; Campbell *et al.* 2006). Proteobacterial *cob*/*cbi* genes dominated all three groups (Figure 4.1B, C, and D). Acidobacterial *cob*/*cbi* genes represented a greater proportion to final assembly and repair (Figure 4.1C) than to

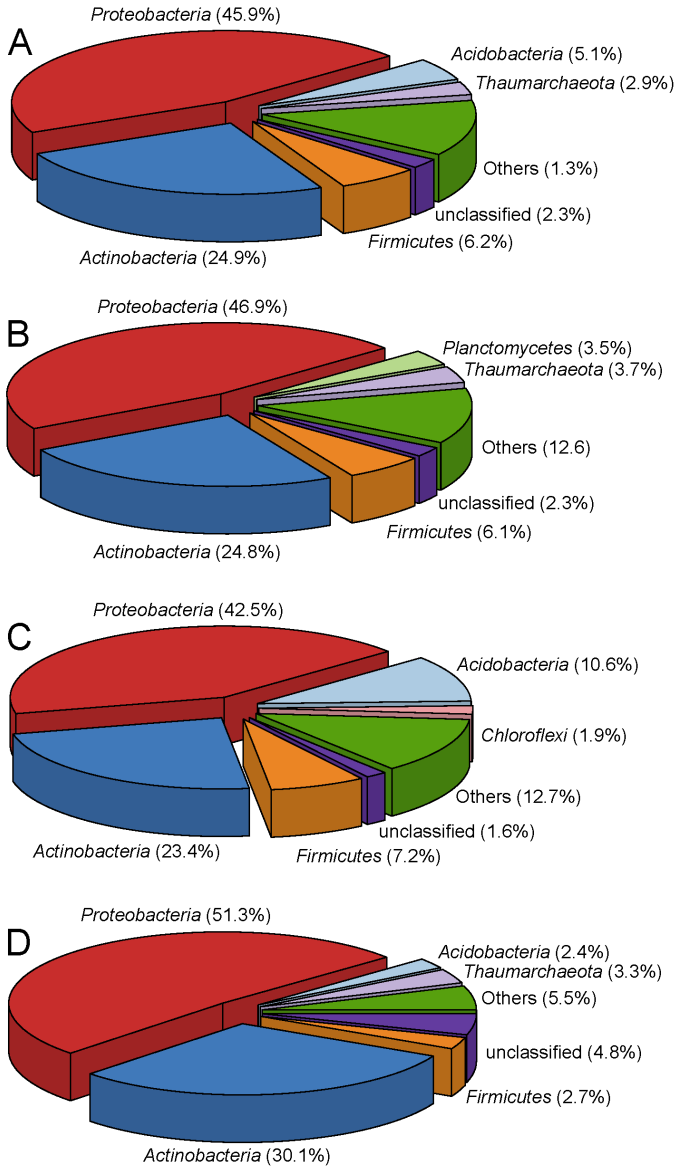

Figure 4.1 – Taxonomic composition of the HMM hits to *cob*/*cbi* genes

Taxonomic composition of HMM hits to *cob*/*cbi* genes averaged among all 155 soil metagenomes for (A) all 12 *cob*/*cbi* genes, (B) corrin ring biosynthesis genes ("Group A"), (C) final assembly and repair genes ("Group B"), and (D) the DMB biosynthesis gene ("Group C").

corrin ring (Figure 4.1B) or DMB biosynthesis (Figure 4.1D). *Thaumarchaeota* contributed similarly (~3%) to both corrin ring and DMB biosynthesis (Figure 4.1B and D), but with lower proportions associated with final synthesis and repair (Figure 4.1C).

Across all sampled metagenomes, 26 genera from five phyla (i.e., *Proteobacteria*, *Actinobacteria*, *Firmicutes*, *Nitrospirae*, and *Thaumarchaeota*) were associated with the potential complete pathway for cobalamin production, based on the presence of all 12 representative *cob*/*cbi* genes (Figure 4.2). Together, these complete cobalamin producers

constituted 8.7 ± 2.3% of the global averaged soil microbial community, estimated by comparison to *rpoB* gene relative abundances of these same genera in the surveyed soil metagenomes. Of these, only three genera exceeded 1% average abundance (*Solirubrobacter*, 1.98%; *Bradyrhizobium*, 1.22%; *Streptomyces*, 1.08%). Complete cobalamin-producing genera within the *Proteobacteria* constituted 3.6% of the average microbial community. Complete cobalamin-producing genera from *Actinobacteria* represented an average of 2.9% of the total soil microbial community across all soil metagenomes, whereas other complete cobalamin-producing genera (i.e., members of the *Firmicutes*, *Nitrospirae*, and *Thaumarchaeota*) represented less than

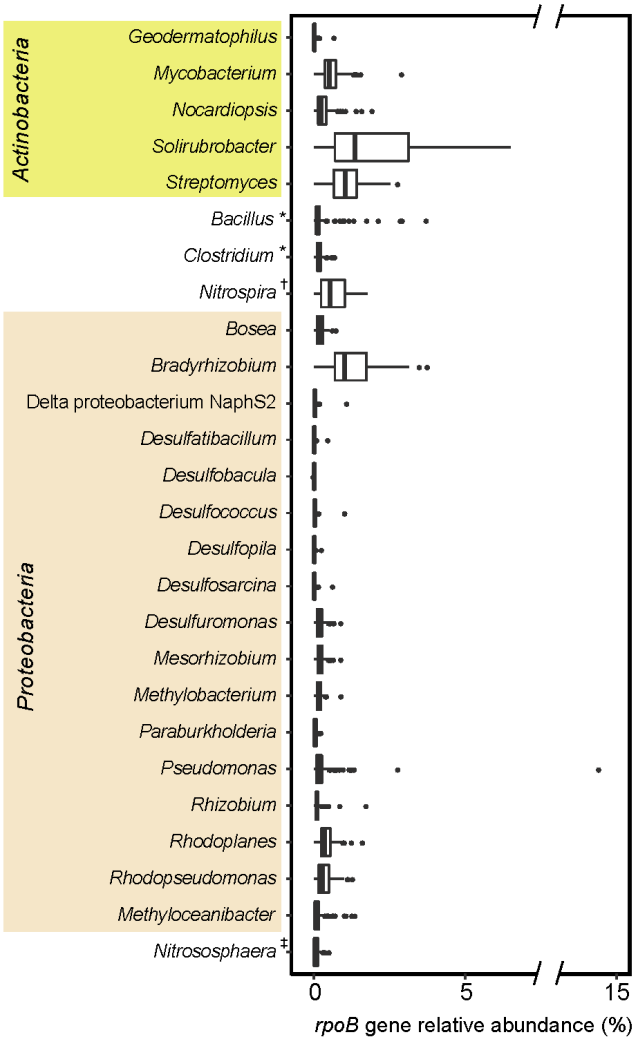

Figure 4.2 – Relative abundance of genera with potentially complete cobalamin synthesis pathways

Relative abundance of genera with potentially complete cobalamin synthesis pathways in each of the 155 soil metagenomes based on *rpoB* HMM hits. The corresponding taxa are shown on the left side. Phylum names are: **Bacillus* and **Clostridium* (phylum *Firmicutes*); *†Nitrospira* (phylum *Nitrospirae*); *‡Nitrososphaera* (phylum *Thaumarchaeota*).

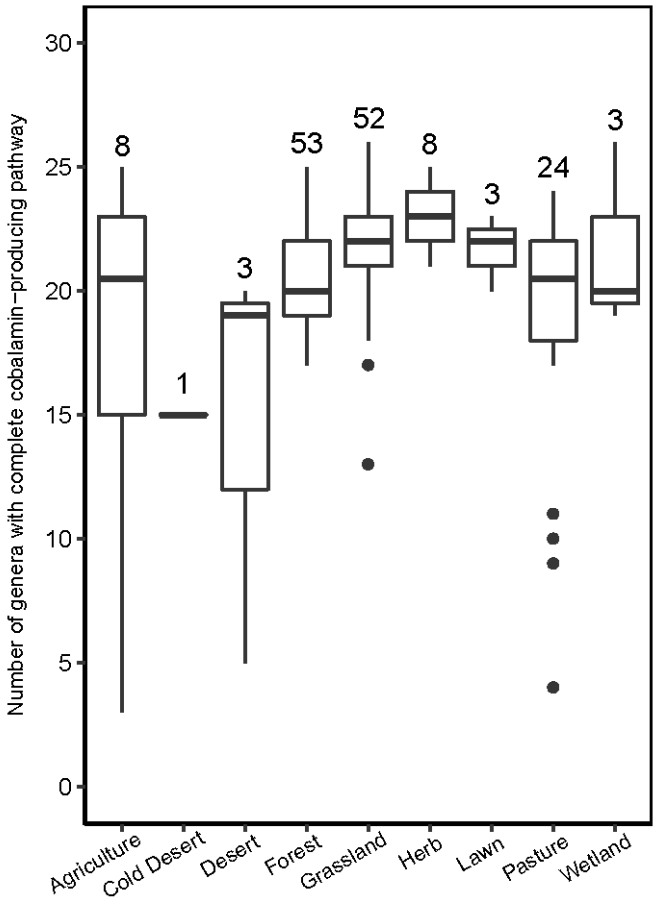

Figure 4.3 – Richness (number of genera) for potential complete cobalamin-producing genera in each of the 155 soil metagenomes

The number of soil metagenomes included in each land use is shown above each corresponding box.

1% of soil metagenomes. The number of complete cobalamin-producing genera showed a relationship with soil type (one-way ANOVA, $p < 0.001$, Figure 4.3).

At the genus level, taxonomic composition varied for the three different steps (*cob*/*cbi* gene groups) in the cobalamin biosynthesis pathway. DMB synthesis (Group C) was affiliated with 619 genera, followed by 83 genera for final assembly and repair (Group B), and 79 for corrin ring synthesis (Group A) (Appendix B). As for contribution to cobalamin producing potential (*cob*/*cbi* gene abundance), several genera played a significant genetic role based on the average relative abundance of HMM hits. For example, *Streptomyces* constituted the most (4.2%) to overall group A *cob*/*cbi* genes, followed by *Bradyrhizobium* (3.2%) and *Nitrososphaera* (2.8%) (Figure 4.4A). *Bradyrhizobium* (3.1%), *Acidobacterium* (2.9) and

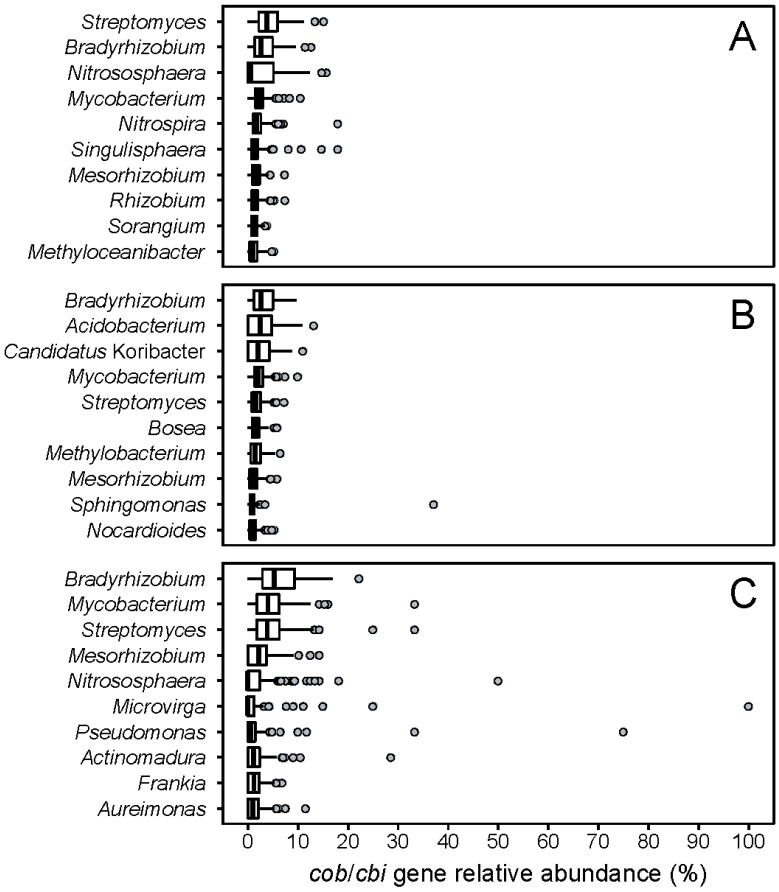

Figure 4.4 – Top genera contributing to *cob*/*cbi* gene HMM hits

From (A) to (C): Group A, corrin ring biosynthesis; Group B, final synthesis and repair; Group C, 5,6-dimethylbenzimidazole (DMB) synthesis.

Candidatus Koribacter (2.5%) were detected as the top three genera contributing most to final synthesis and repair (Figure 4.4B). DMB synthesis was attributed to *Bradyrhizobium* (6.1%), *Mycobacterium* (4.8%), *Streptomyces* (4.5%), and *Nitrososphaera* (2.1%) (Figure 4 .4C). When evaluating the corresponding *rpoB* gene abundance for these same genera, the 79 corrin ring biosynthesizing genera accounted for 23.3% of total soil microbial community, final assembly genera represented 26.3%, whereas DMB-producing genera averaged 56.7% (Table 4.3).

4.3.2 Cobalamin-producers and transporters in soil

Soil metagenome analysis revealed a significant positive correlation ($R^2 = 0.82$, $p < 0.001$) between overall microbial community size (*rpoB*) and cobalamin-producing potential

(*cob*/*cbi*) (Figure 4.5). The overall ratio of *cob*/*cbi* to *rpoB* gene reads was 0.10 across all soil metagenomes. "Rare biosphere" (i.e., < 0.1% relative abundance) microorganisms collectively contributed to the same level of cobalamin producing potential as intermediate abundance taxa (Table 4.4). When testing the correlation between the relative abundance of cobalamin-producing genes (*cob*/*cbi*) and the cobalamin transport gene (*btuB*) at the genus level across soil metagenomes, evidence for mutual exclusion (permutation test $p < 0.001$) of these two gene complements emerged for both rare biosphere members (Figure 4.6A-C) and intermediate abundance taxa (between 0.1 and 5%; Figure 4.6D-F). Thus, genera that were more represented among the cobalamin-synthesis genes were less well represented among the cobalamin transport gene pool and vice versa.

Genes encoding cobalamin-dependent reactions (methionine synthase, *metH*; methylmalonyl-CoA mutase, *mutA*; ribosomal small subunit methyltransferase, *rsmB*) were also surveyed among all 155 soil metagenomes to further confirm the potential use of cobalamin by genera that either produce (with *cob*/*cbi* genes) or transport (with *btuB* gene) this cofactor (Figure 4.7). Strong and significant ($p < 0.001$) correlations were observed between the abundances of genes encoding cobalamin-dependent reactions (R^2: *metH*, 0.77; *mutA*, 0.78; *rsmB*, 0.87) and those encoding cobalamin synthesis and transport (*cob*/*cbi* and *btuB*), indicating a corresponding requirement for cobalamin as a cofactor when cobalamin is produced and/or transported. Genera harboring cobalamin-dependent genes accounted for over 70% of the total community size (Figure 4.8A). The total encoded potential for cobalamin use, expressed as a sum of HMM hits to all three tested cobalamin-dependent genes (i.e., *metH*, *mutA*, and *rsmB*), was significantly greater (paired t-test, $p < 0.001$) than the encoded potential for cobalamin production and transport (i.e., sum of *cob*/*cbi* and *btuB* gene abundance) (Figure 4.8B).

4.3.3 Soil cobalamin measurements

Annotations of metagenome HMM hits demonstrated substantial inter-metagenome variation in taxonomic contributions to the production of cobalamin (Figure 4.9A). To investigate differences in cobalamin production further, cobalamin concentrations were measured in another 40 soil samples. Representative soil samples that were collected from different locations were tested for *in situ* cobalamin concentrations and forms, originating from both water leachable and non-water leachable (i.e., intracellular and/or mineral-binding cobalamin) extracts (Table 4.5). Total cobalamin (sum of both water leachable and non-water leachable) ranged between 0.06 to 6.84 pmol g^{-1} dry soil across all 40 soil samples tested, with

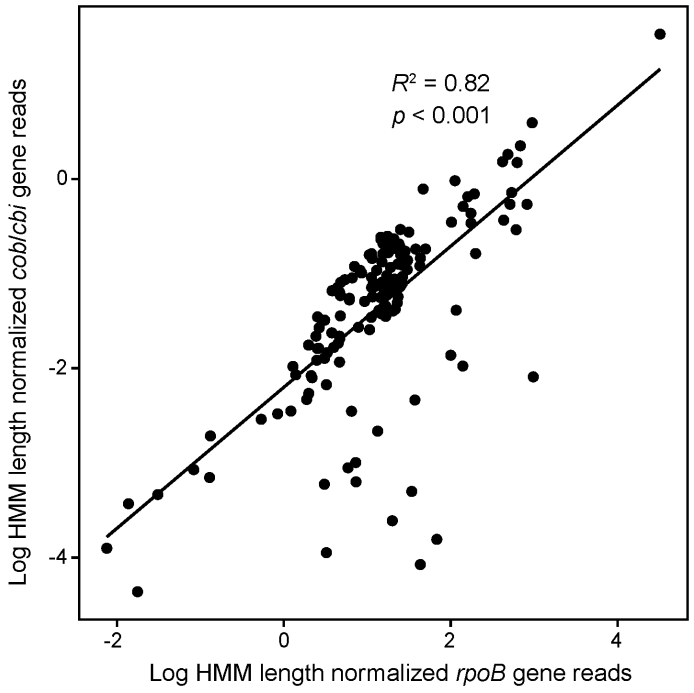

Figure 4.5 – Community cobalamin producing potential and community size

Community cobalamin producing potential (*cob*/*cbi* gene abundance) positively correlated (R^2 = 0.82, p < 0.001) with corresponding community size based on *rpoB* HMM hits for all 155 soil metagenomes. The gene reads were normalized to HMM length. Data are log transformed for visualization.

an average of 1.19 pmol g^{-1} dry soil (Figures 4.9B and 4.10, Table 4.5). Within the total cobalamin pool, the water leachable fraction only accounted

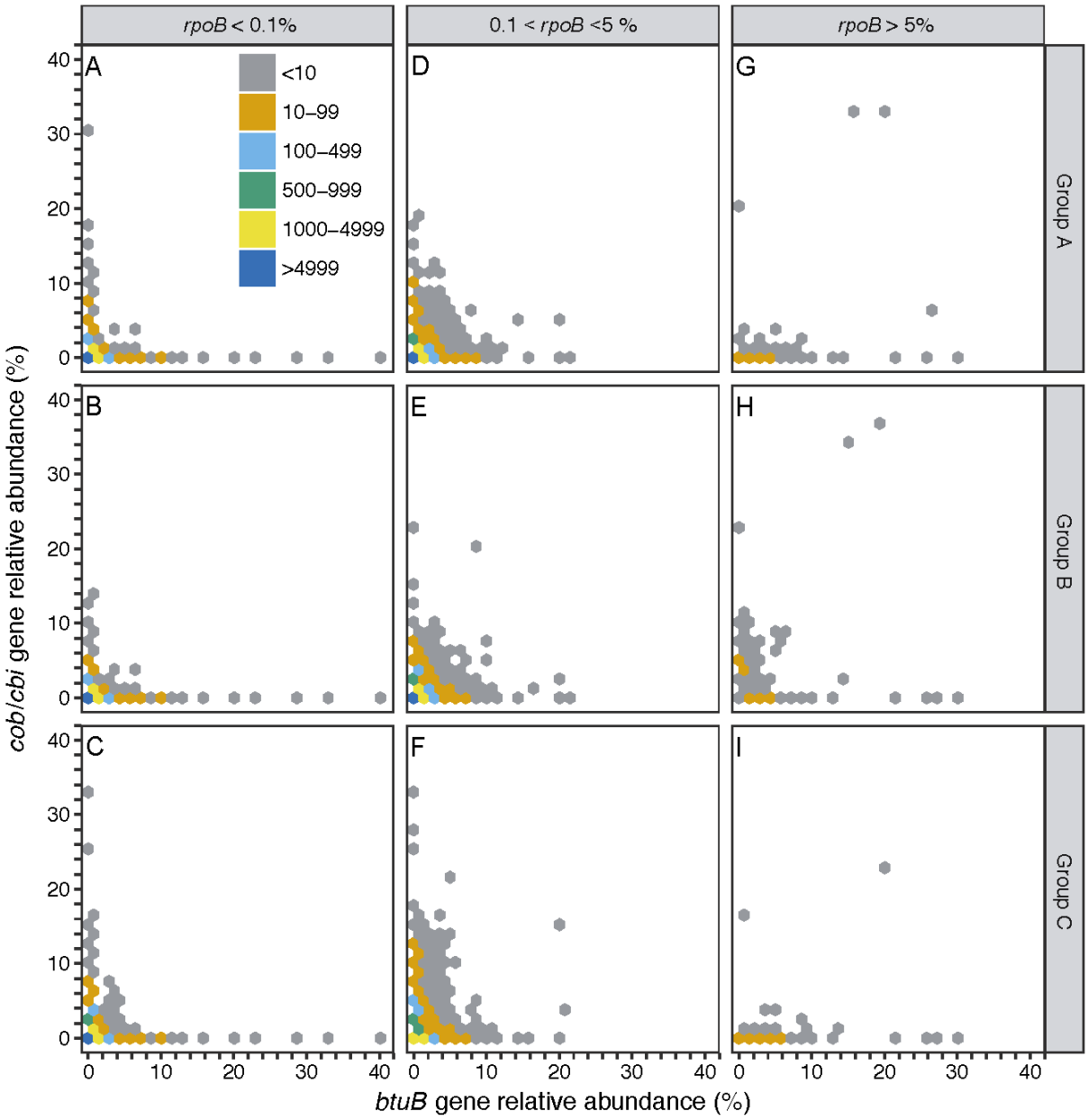

Figure 4.6– Relationship between *cob*/*cbi* gene and *btuB* gene

Hexagon heatmap based on relative gene abundance at the genus level across 155 soil metagenomes. Each point in A-C represents a genus whose *rpoB* gene relative abundances were below 0.1% (rare biosphere), D-F between 0.1 and 5% (intermediate abundance taxa), and G-I over 5% (dominant taxa). Mutual exclusion between the cobalamin transporter gene (*btuB*) and cobalamin synthesis genes (*cob*/*cbi*) for rare biosphere and intermediate abundance taxa are tested with 10^5 permutations. Occurrence numbers are denoted by hexagon color. From top to bottom: Group A, corrin ring biosynthesis; Group B, final synthesis and repair; Group C, 5,6-dimethylbenzimidazole (DMB) synthesis.

Table 4.3 – Proportions of genera associated with *cob*/*cbi* genes in each of the three abundance categories (rare biosphere, intermediate abundance, and dominant taxa).

The relative abundances of genera associated with *cob*/*cbi* and *btuB* genes, compared to the overall microbial community, were calculated by comparison to the abundance of *rpoB* genes associated with those same genera. NA is not applicable. Group A is corrin ring biosynthesis, Group B is final synthesis and repair, and Group C is 5,6-dimethylbenzimidazole (DMB) synthesis.

Abundance	Genera affiliated with *cob*/*cbi* gene (%)			Relative abundance of *cob*/*cbi* carrying genera within microbial community (%)			Relative abundance of *btuB*-associated genera within microbial community (%)
	Group A	Group B	Group C	Group A	Group B	Group C	
Rare	5.9	5.9	44.3	1.1	1.1	8.2	9.9
Intermediate	21.7	26.4	57.0	15.3	18.6	40.2	44.3
Dominant	67.6	64.7	81.4	6.9	6.6	8.3	13.2
Total	NA	NA	NA	23.3	26.3	56.7	67.4

Table 4.4 – Gene abundance breakdown (%) of each of the three microbial categories (rare biosphere, intermediate abundance, and dominant taxa).

Group A is corrin ring biosynthesis, Group B is final synthesis and repair, and Group C is 5,6-dimethylbenzimidazole (DMB) synthesis. Only annotated genera are included in this table.

	Group A *cob*/*cbi*	Group B *cob*/*cbi*	Group C *cob*/*cbi*	*btuB*
Rare	45.4	45.4	41.9	50.5
Intermediate	50.9	49.0	51.7	34.7
Dominant	1.0	3.6	0.9	3.6

Table 4.5 – Cobalamin concentration measured in soils.

Total cobalamin, DMB, Ado-, CN-, Me-, and OH-cobalamin concentrations are shown as pmol g^{-1} dry soil.

Dataset	Sample	Total cobalamin	DMB	Ado-B_{12}	CN-B_{12}	Me-B_{12}	OH-B_{12}
rare soil	IW_3	0.17	0.66	0.00	0.01	0.00	0.16
rare soil	IW_2	0.21	8.28	0.00	0.01	0.00	0.21
rare soil	IW_1	0.25	1.57	0.00	0.02	0.00	0.23
rare soil	H_3	0.13	1.26	0.00	0.01	0.00	0.12
rare soil	H_2	0.30	2.27	0.00	0.01	0.00	0.28
rare soil	H_1	1.11	2.27	0.00	0.04	0.00	1.07
rare soil	D10_3	0.18	0.03	0.00	0.01	0.00	0.17
rare soil	D10_2	0.37	1.70	0.01	0.01	0.00	0.35
rare soil	D10_1	1.00	0.44	0.00	0.02	0.00	0.97
rare soil	D07_3	0.06	0.04	0.00	0.01	0.00	0.05
rare soil	D07_2	0.13	1.04	0.00	0.01	0.00	0.12
rare soil	D07_1	0.74	0.61	0.00	0.02	0.00	0.72
rare soil	D03_3	0.69	5.12	0.04	0.01	0.00	0.64
rare soil	D03_2	0.88	2.33	0.00	0.02	0.00	0.86
rare soil	D03_1	1.09	0.47	0.00	0.04	0.00	1.05
rare soil	CA_3	0.12	0.41	0.00	0.01	0.00	0.11
rare soil	CA_2	0.24	3.06	0.01	0.01	0.00	0.22
rare soil	CA_1	0.17	0.50	0.00	0.02	0.00	0.15
rare soil	AA_3	0.09	0.04	0.00	0.02	0.00	0.07
rare soil	AA_2	0.14	1.15	0.00	0.01	0.00	0.13
rare soil	AA_1	0.52	0.50	0.00	0.04	0.00	0.47
pH soil	pH7-5	0.65	0.72	0.02	0.03	0.00	0.61
pH soil	pH7-0	0.73	1.23	0.02	0.01	0.00	0.69
pH soil	pH6-5	0.31	0.69	0.00	0.01	0.00	0.29
pH soil	pH6-0	0.33	0.71	0.00	0.02	0.00	0.31
pH soil	pH5-5	0.57	1.61	0.01	0.01	0.00	0.56
pH soil	pH5-0	0.62	1.15	0.00	0.01	0.00	0.62
pH soil	pH4-5	0.47	1.04	0.02	0.01	0.00	0.45
CM2BL	9WLM	6.21	2.45	0.00	0.02	0.00	6.19
CM2BL	8NP	5.51	61.12	0.00	3.70	0.00	1.81
CM2BL	7TR	1.18	9.01	0.09	0.01	0.00	1.09
CM2BL	6TD	2.32	0.87	0.06	0.49	0.00	1.77
CM2BL	5BF	0.30	2.20	0.00	0.02	0.00	0.28
CM2BL	4TS	1.65	3.44	0.05	0.25	0.00	1.35
CM2BL	2ATN	0.69	0.05	0.00	0.59	0.00	0.11

CM2BL	1Tundra	6.84	0.18	0.00	6.36	0.00	0.49
CM2BL	20CG	1.99	1.49	0.06	0.12	0.00	1.81
CM2BL	13CO	6.66	1.49	0.90	0.07	0.00	5.69
CM2BL	11AW	0.89	0.98	0.02	0.02	0.00	0.86
CM2BL	10ASSOY	1.09	0.52	0.02	0.02	0.00	1.04

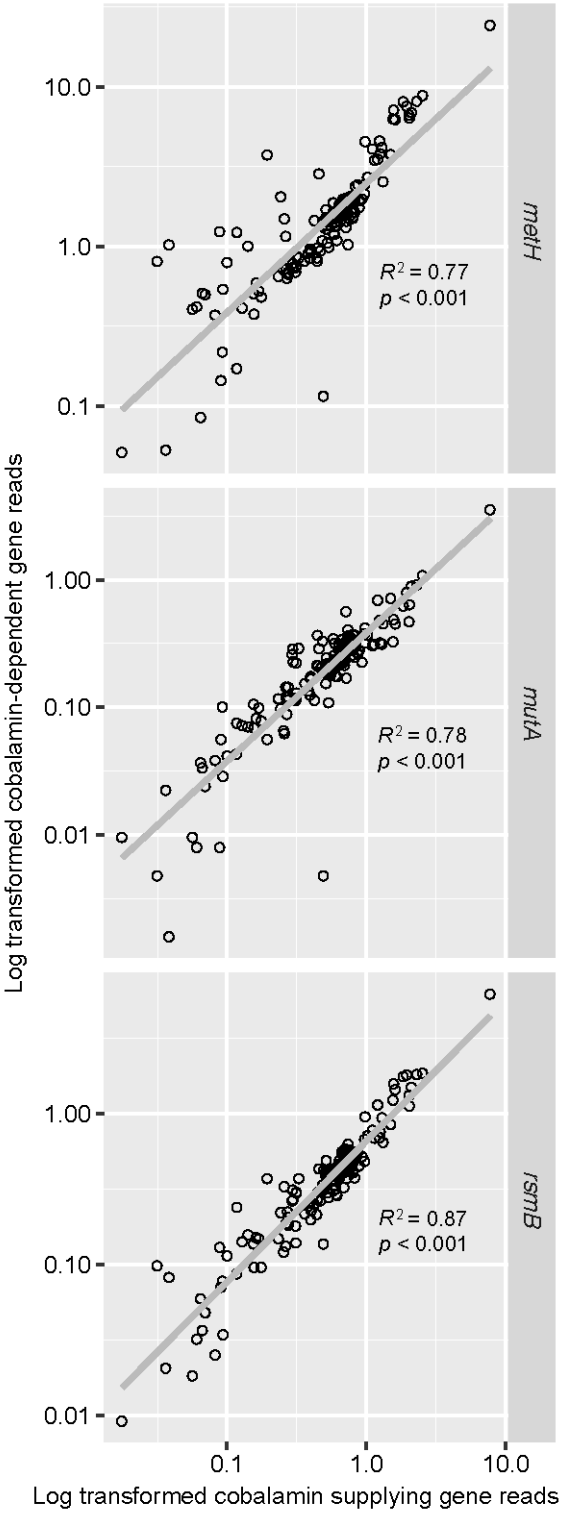

Figure 4.7 – Cobalamin-dependent genes and supplying genes

Correlation between HMM hits to cobalamin-dependent genes (*metH*, *mutA*, *rsmB*) and cobalamin supplying genes (*cob*/*cbi*, and *btuB*). Each point in the plots represents a soil metagenome with gene reads normalized to HMM length. The x-axis is the sum of both *cob*/*cbi* and *btuB* genes.

for a small proportion in all samples (10.1 ± 11.9%; Figure 4.10), indicating a strong association between cobalamin and soil mineral binding and/or microbial biomass (Figure 4.10).

Similar to total cobalamin, the cobalamin lower ligand (DMB) pool was also dominated by the non-water leachable form, with an average of 82.4 ± 31.8% of the total extractable DMB. The average concentration of DMB was higher than that of total cobalamin (Figures 4.9B and 4.10, Table 4.5); in one sample, the concentration of DMB was ~40 times that of total cobalamin (***rare*** IW soil, 15-30 cm). The presence of DMB concentration in excess of cobalamin in tested soil samples was consistent with soil metagenomics data showing that DMB biosynthesis (Group C *cob*/*cbi*) genes were more abundant than the other two *cob*/*cbi* gene groups. In general, OH-B_{12} was observed as the dominant cobalamin form based on its concentration in the total pool (sum of both water soluble and non-water leachable), followed by CN-, Ado-, and Me-B_{12}, consistent with previous work in marine systems (Heal *et al*, 2017).

Links between microbial diversity, biomass, and cobalamin concentrations were tested in the 40 soil samples analyzed for cobalamin chemistry (Table 4.2). Soil biomass, as indicated from extracted DNA concentrations, correlated positively with cobalamin concentration (Figure 4.11; $R^2 = 0.57$, $p < 0.01$).

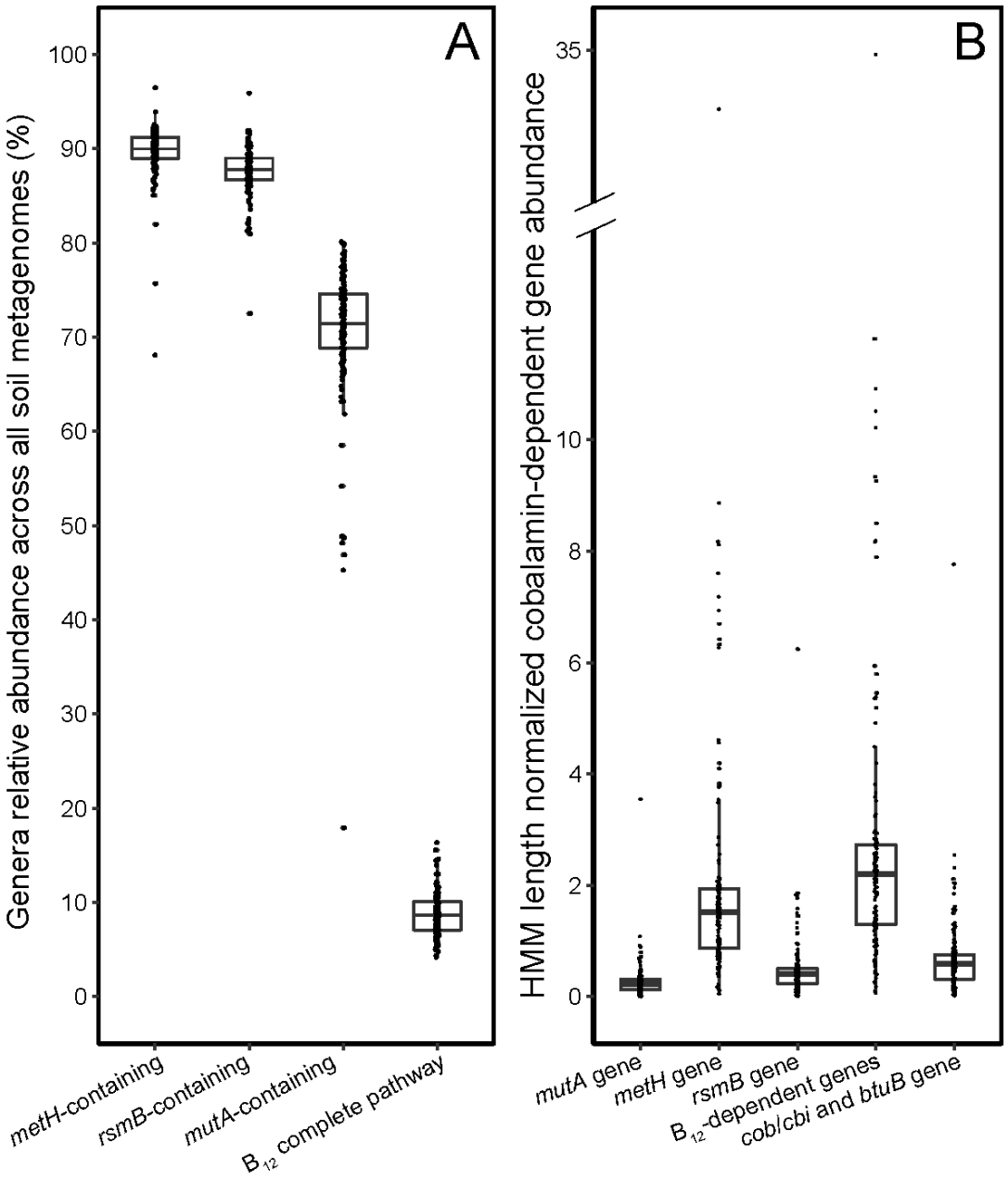

Figure 4.8 – cobalaminCobalamin producing and dependent gene abundance

Relative abundance of genera carrying the three cobalamin-dependent genes, *metH*, *mutA*, and *rsmB*, as well as the genera with complete cobalamin pathway (A). Relative abundances are calculated using *rpoB* gene abundance across all 155 soil metagenomes. (B) The abundance of each individual cobalamin-dependent genes (*metH*, *mutA*, and *rsmB*), sum of these three cobalamin-dependent genes (B_{12}-dependent genes), and cobalamin providing genes (*cob*/*cbi* and *btuB* genes). The reads for each gene are normalized to HMM length.

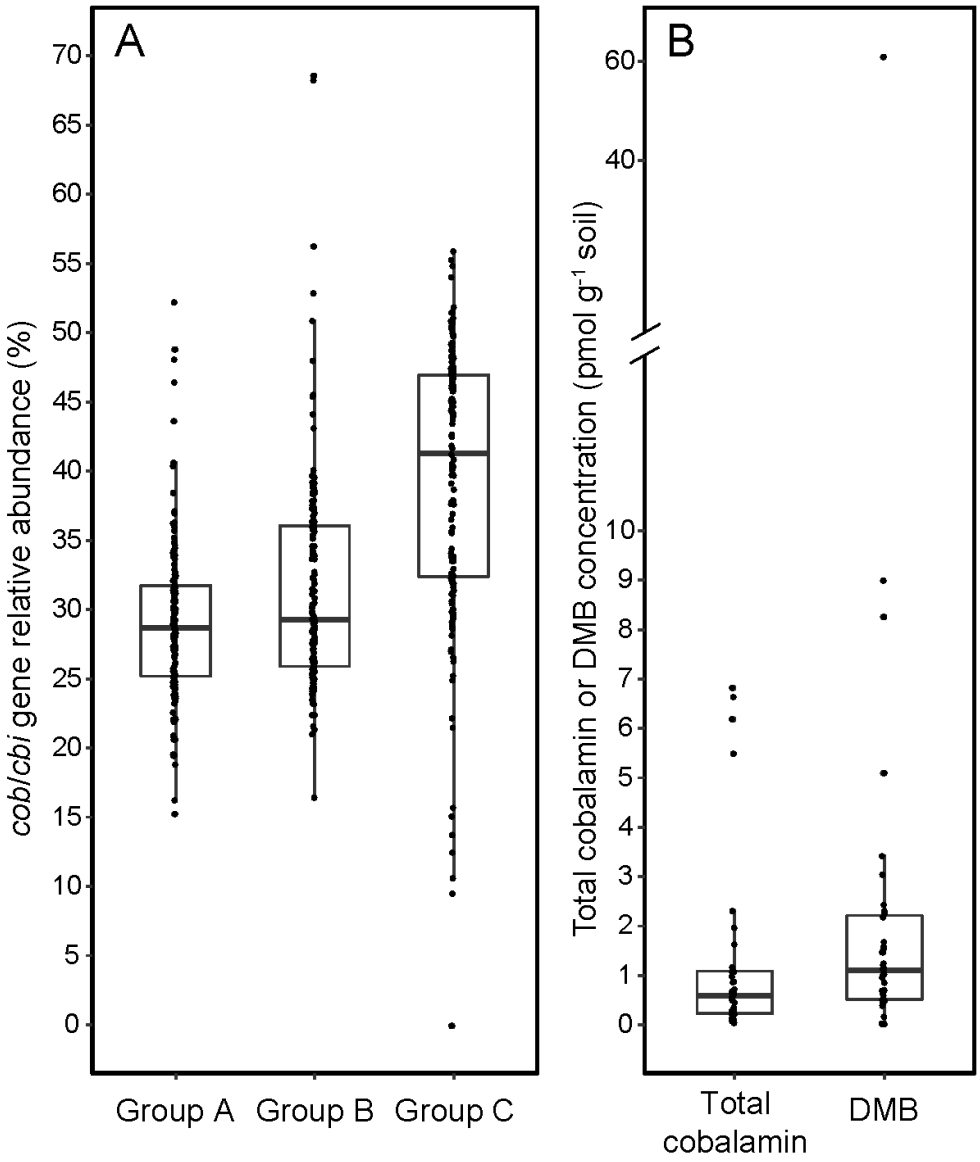

Figure 4.9 – Cobalamin biosynthesis gene relative abundance and cobalamin concentration

Cobalamin biosynthesis gene relative abundance of 155 soil metagenomes (A), and the measured total cobalamin (sum of Ado-, CN-, Me-, and OH-B_{12}) and 5,6-dimethylbenzimidazole (DMB) concentrations in 40 soil samples collected from CM^2BL, the ***rare*** Charitable Research Reserve, and the Craibstrone pH plots (B). Cobalamin producing genes in (A) were grouped as: Group A, corrin ring biosynthesis; Group B, final synthesis and repair; Group C, 5,6-dimethylbenzimidazole (DMB) synthesis.

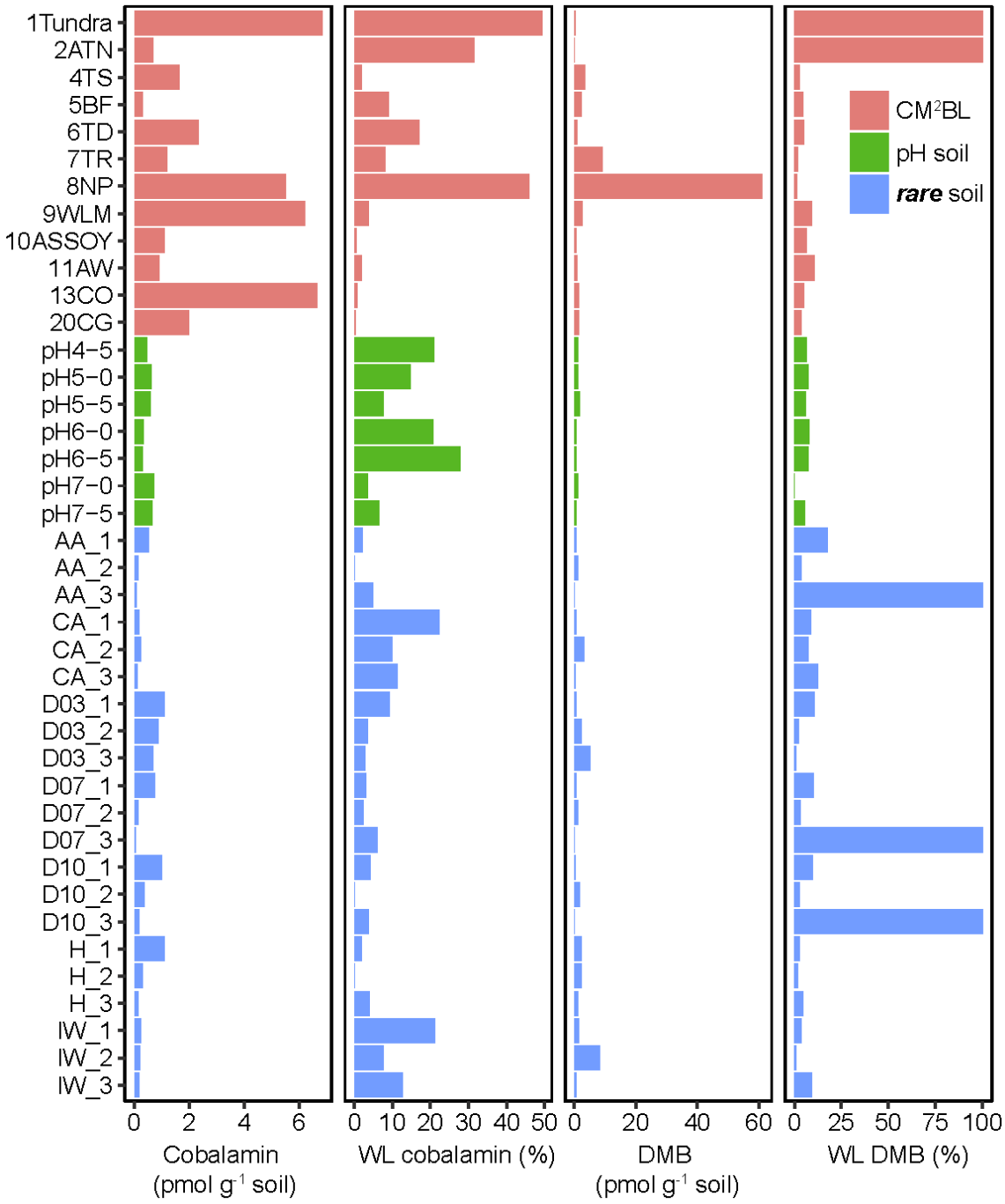

Figure 4.10 – Concentration of measured cobalamin and DMB

Concentration of total (sum of Ado-, CN-, Me-, and OH-) cobalamin and 5,6-dimethylbenzimidazole (DMB) measured in soils collected from CM^{2}BL (red), the ***rare*** Charitable Research Reserve (blue) and the Craibstone pH plots (green) projects. The proportion of water leachable (WL) cobalamin is shown on the right for each sample.

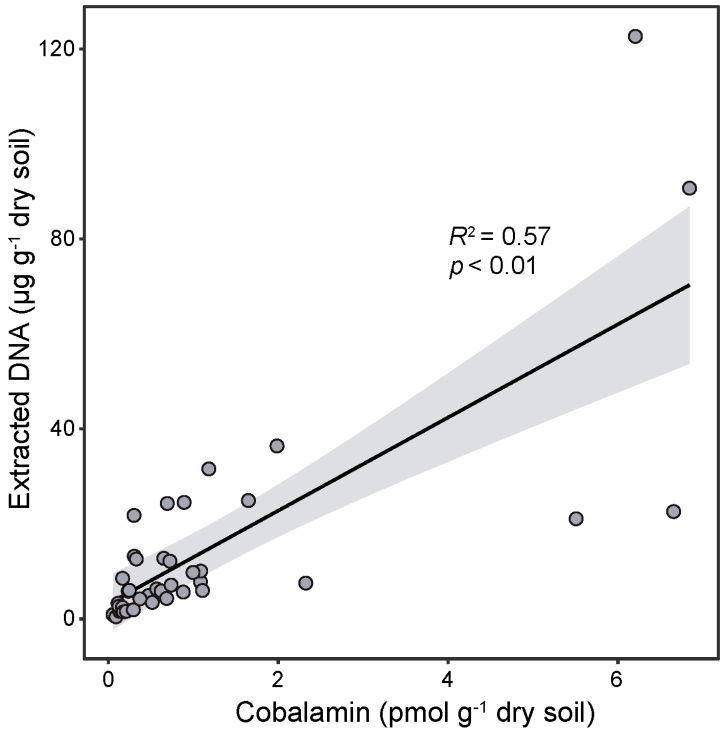

Figure 4.11 – Cobalamin concentration and microbial biomass

Scatter plot showing positive relationship between total cobalamin concentration and microbial biomass (i.e., DNA yield) across 40 soil samples collected for CM^2BL, ***rare*** Charitable Research Reserve, and Craibstone pH plots.

4.4 Discussion

The research demonstrated that *de novo* complete biosynthesis of soil cobalamin is a keystone function that is restricted to a relatively small cohort of bacteria and archaea (Figure 4.2), presumably supplying this essential nutrient to a much broader community. Global metagenomic analysis indicated the average proportion of complete cobalamin-producing taxa across all soils is less than 10% of the total community size, based on *rpoB* gene relative abundances. This is consistent with cobalamin producers serving as keystone species by shouldering the high metabolic cost of producing cobalamin (Mills, Soulé and Doak 1993; Giovannoni 2012; Lynch and Neufeld 2015; Mas *et al.* 2016).

Compared to the cobalamin-producing phyla identified previously in marine studies (Doxey *et al.* 2015; Heal *et al.* 2017), a relatively broad diversity of soil microorganisms possess the genomic potential for cobalamin biosynthesis. *Proteobacteria* are numerically abundant

cobalamin producers in both marine (Doxey *et al*. 2015) and soil environments. *Cyanobacteria*, and *Bacteroidetes*/*Chlorobi* are the most abundant cobalamin contributors in marine metagenomes (Doxey *et al*. 2015), but did not contribute a significant proportion of cobalamin synthesis genes in soils. Instead, *Actinobacteria*, *Firmicutes*, and *Acidobacteria* numerically dominated phyla in soil metagenomes that contained cobalamin genes. Despite being abundant cobalamin producers in marine environments (e.g., over 80% in some samples; Giovannoni 2012; Helliwell *et al*. 2016), thaumarchaeotal *cob*/*cbi* genes were relatively rare within sampled soil metagenomes (Figure 4.1). Nevertheless, because all known thaumarchaeotal cultures produce cobalamin (Qin *et al*. 2017), and the per cell cobalamin concentrations for members of the *Thaumarchaeota* growing in exponential phase is higher than for members of the *Proteobacteria* (Heal *et al*. 2017), *Thaumarchaeota* could nonetheless be a more important source of soil cobalamin than gene counts suggest (Heal *et al*. In press).

The research showed that, collectively, rare biosphere (0.1% relative abundance) and intermediate abundance (0.1-5.0% relative abundance) taxa are equally likely to be cobalamin producers (~50%) but the most abundant taxa (> 5% relative abundance) generally lack cobalamin synthesis genes (Table 4.4). Because rare taxa have been demonstrated to mediate nutrient cycle (Pester *et al.* 2010) and plant production (Hol *et al.* 2010), this research suggests that future experiments should investigate the importance of rare cobalamin-producing taxa to microbial community function more broadly.

The only known function of DMB in cells is as the lower ligand of cobalamin, and this component was detected at relatively high concentrations compared to cobalamin. Group C *cob*/*cbi* gene abundance were higher than group A and B *cob*/*cbi* genes (Figure 4.9), suggesting that greater biosynthesis of DMB could explain its elevated concentrations. Free DMB represents

the potential for pseudocobalamin, or other cobalamin-like compounds, present in terrestrial environments to be remodeled into cobalamin. Microorganisms capable of transforming cobalamin-like compounds to cobalamin play a critical role in maximizing the impact of cobalamin production. The cyanobacterium *Synechococcus* was hypothesized to be a major cobalamin source in some marine environments (Bonnet *et al.* 2010), yet has been demonstrated recently to produce pseudocobalamin (Helliwell *et al.* 2016; Heal *et al.* 2017), a less bioavailable cobalamin-like compound in which adenine replaces DMB. *Synechococcus* accounted for only 0.05% of soil metagenomes used in this study, but those detected also lacked HMM hits to the *bluB* gene that encodes for DMB synthesis, indicating they might also be a source of soil pseudocobalamin. Several marine microalgal species can remodel pseudocobalamin to increase its bioavailability when DMB is present (Helliwell *et al.* 2016). It is also possible that observed DMB concentrations are a result of cobalamin degradation. Nevertheless, this research suggests the possibility that DMB could be readily exchanged among different microorganisms via cross feeding, enabling subsequent remodeling within cells as has been hypothesized for the gut microbiome (Seth and Taga 2014).

Nitrospira spp., the most diverse and abundant nitrite-oxidizing bacteria (Daims *et al.* 2001), were detected in soil metagenomes with genetic capacity for complete cobalamin synthesis, in agreement with previous reports of cobalamin-producing genes in the *Candidatus* Nitrospira defluvii genome (Lücker *et al.* 2010). This research demonstrated that *Nitrospira* were associated with ~0.5% of all *cob*/*cbi* genes across 155 soil metagenomes (Figure 4.2), spanning cold desert, desert, forest, grassland, and other unclassified terrestrial environments. Genome analysis demonstrated the presence of cobalamin-dependent enzymes involved in porphyrin synthesis (HemE) and methyl-accepting chemotaxis (Mcp), suggesting a need for this cofactor

(Lücker *et al.* 2010; Romine *et al.* 2017). Another common nitrite-oxidizing bacterium, *Nitrobacter winogradskyi*, lacks the complete pathway encoding cobalamin biosynthesis, although cobalamin-dependent methionine synthase (MetH) is present (Starkenburg *et al.* 2006). Moreover, *Nitrospira defluvii* lacks genes coding for enzymes associated with detoxification of reactive oxygen species (Lücker *et al.* 2010), which are present in most other known aerobic microorganisms. Although manganese might function to protect *N. defluvii* cells from H_2O_2 (Horsburgh *et al.* 2002; Lücker *et al.* 2010), cobalamin synthesized by *Nitrospira* might also be a way to protect against oxidative stress, as demonstrated in *Leptospirillum* (Ferrer *et al.* 2016). Together with the potential for thaumarchaeotal production of NO_2-cobalamin (Qin *et al.* 2017b; Heal *et al*. 2018), the presence of these ammonia/nitrite oxidizers as cobalamin producers suggests links between cobalamin-production and the aerobic nitrogen cycle in diverse soil biomes.

Strong positive correlations between both soil microbial biomass and cobalamin concentrations (Figure 4.11), and microbial community cobalamin potential (*cob*/*cbi*) and community size (*rpoB*) (Figure 4.5), imply an importance for cobalamin in governing overall soil microbial community size. These observations contrast with measurements of intracellular cobalamin in marine samples, which do not appear to correlate with microbial biomass (Suffridge, Cutter and Sañudo-Wilhelmy 2017). The highest cobalamin concentration in a gram of soil can be two orders of magnitude greater than those measured in a liter of seawater (Heal *et al.* 2017), which is likely due to lower microbial biomass in marine relative to terrestrial habitats (Whitman, Coleman and Wiebe 1998). Lower water-leachable cobalamin concentrations in soils might suggest rapid scavenging of these compounds; thus, rates of cobalamin release from cells to the soil matrix may actually exceed those in the marine environment. Besides prokaryotes, soil

cobalamin might also be ingested by soil eukaryotes (e.g., nematodes), accelerating development and reducing mortality (Watson *et al.* 2014).

Combined metagenomic and biochemical perspectives provide strong evidence for an important role of cobalamin-producing taxa in relation to the much larger overall microbial community in terrestrial environments. Lower ligand remodeling mechanisms among soil microorganisms is likely given the presence of higher concentrations of free DMB and higher relative abundance of DMB synthesis genes in soil metagenomes. This study, by quantifying soil cobalamin and identifying the bacterial and archaeal contributions to cobalamin synthesis, transport, dependence and remodeling in soils, implicates cobalamin synthesis as a keystone role for maintaining an abundant and diverse terrestrial microbial community that, in turn, contributes to the broader functioning of terrestrial ecosystems.

Chapter 5

Conclusions

5.1 Summary

Recent research has changed the central dogma of nitrification dramatically. The discovery of ammonia-oxidizing archaea (AOA, *Thaumarchaeota*) addressed the gap between ammonia oxidation activity and AOB biomass in acidic (Lehtovirta-Morley *et al.* 2011; Li *et al.* 2018) and nitrogen-limited soils (Daebeler *et al.* 2015), triggering follow-up studies investigating the distributions (Angel *et al.* 2010; Nelson, Martiny and Martiny 2016) and relative contributions of AOA and AOB within diverse terrestrial habitats (Prosser and Nicol 2008; Jia and Conrad 2009; Gubry-Rangin, Nicol and Prosser 2010; Taylor *et al.* 2010, 2013; Zhang *et al.* 2012; Che *et al.* 2015; Giguere *et al.* 2015; Lu, Bottomley and Myrold 2015; Ouyang *et al.* 2016). The ubiquitous distribution and dominance of AOA in global soils (Leininger *et al.* 2006) implicated AOA as important contributors to nitrogen cycling in terrestrial biomes.

Although the ecology, physiology, and biochemistry of AOA have been investigated for more than a decade, their role in the nitrogen cycle remains an important area of research. My thesis project adds new understanding to the role of AOA in soil nitrogen cycling from the perspectives of depth-dependent biogeography (Chapter 2) and temperature-influenced activity (Chapter 3). Although previous research investigated thaumarchaeotal distributions in surface soils in relation to abiotic factors such as soil pH, moisture content, temperature, and ammonia availability (Nicol *et al.* 2008; Angel *et al.* 2010; Höfferle *et al.* 2010; Szukics *et al.* 2010; Gubry-Rangin *et al.* 2010, 2011), the influence of soil depth on thaumarchaeotal biogeography was overlooked. Soil bacterial communities are highly heterogeneous along soil depth profiles due to depth-dependent physicochemical characteristics (Fierer, Schimel and Holden 2003) and

my research targeted *Thaumarchaeota* to uncover their vertical soil distributions using the range of land uses available locally at the ***rare*** Charitable Research Reserve (Chapter 2).

With AOA representatives enriched and/or isolated from soils under diverse pH, temperature, nitrogen concentration, and agricultural practices (Jung *et al.* 2011, 2014b; Lehtovirta-Morley *et al.* 2011, 2016; Tourna *et al.* 2011; Kim *et al.* 2012), physiological characterization of these ammonia oxidizers revealed optimum growth temperatures that range from 25 to 74°C (De La Torre *et al.* 2008; Kim *et al.* 2012; Jung *et al.* 2014a; Lehtovirta-Morley *et al.* 2014; Stieglmeier *et al.* 2014a; Sauder *et al.* 2017; Abby *et al.* 2018; Daebeler *et al.* 2018). This relatively high temperature range may be useful for distinguishing activities of soil AOA from AOB given that AOB optimum temperatures typically range from 20 to 30°C (Groeneweg, Sellner and Tappe 1994; Jiang and Bakken 1999; Avrahami and Conrad 2005; Avrahami and Bohannan 2007). As a consequence of this potential for niche differentiation between AOA and AOB as a function of temperature, differential responses of ammonia oxidizers along soil vertical profiles under different land usages were studied at three different temperatures (Chapter 3). Using differential inhibition, this research shed light on how temperature, depth, and land use resulted in varying production of N_2O, and nitrite stimulation of N_2O production, providing evidence for N_2O derived from nitrifer denitrification.

Vitamin B_{12} (cobalamin) is the most structurally complex coenzyme known (Hodgkin *et al.* 1955), requiring approximately 30 enzymatic steps for *de novo* synthesis (Roth, Lawrence and Bobik 1996; Romine *et al.* 2017). Cobalamin is necessary for the growth of many microbial lineages and its availability is thought to influence microbial diversity and community composition. Inspired by the discovery of thaumarchaeotal contributions to cobalamin

production in the marine environment (Doxey *et al.* 2015; Heal *et al.* 2017), the research described in Chapter 4 originated as an effort to explore the role of soil thaumarchaeota to cobalamin production. The scope of this study encompassed global soil metagenomes and all known cobalamin-producing phyla when it became apparent that members of the *Thaumarchaeota* were among many other cobalamin-producing taxa (Doxey *et al*. 2015). In a broader context, this research provided first evidence for the potential regulating effect of cobalamin on soil microbial community composition and abundance. Accompanied by *in situ* soil cobalamin concentration measurements, this metagenomics research addressed a wide knowledge gap and served as important follow-up to research conducted many decades ago (Lochhead and Thexton 1951; Lochhead, Burton and Thexton 1952; Lochhead and Burton 1956).

5.2 AOA communities along soil depth profiles under different land use types

Previous reports indicate that AOA dominate ammonia-oxidizers in subsoils, showing that AOA to AOB ratios increase with soil depth. Indeed, AOA can be over three orders of magnitude more abundant than AOB in subsoils at 40-50 cm depth (Leininger *et al.* 2006). However, research on AOA community composition focused on only surface soils (Pesaro and Widmer 2002; Kemnitz, Kolb and Conrad 2007; Nicol *et al.* 2008; Angel *et al.* 2010; Höfferle *et al.* 2010; Gubry-Rangin *et al.* 2011, 2015), and their community composition along vertical soil profile remained poorly understood. Because agricultural and forest soils represent more than 30% of global land usage, and heavily rely on nitrogen, it is necessary to comprehensively characterize the dominant ammonia oxidizers within a deeper soil profile.

The data reported in my thesis demonstrate that thaumarchaeotal community composition varies along soil depth profiles and under contrasting land use types. The biogeography of AOA

was explored by high-throughput sequencing of thaumarchaeotal 16S rRNA genes. Diversity was higher in forest sites than field sites, and lower in surface soils than subsurface soils (Figure 2.2). Field sites were characterized by members of the Soil Crenarchaeote Group (SCG), whereas the forest sites were dominated by members of the Terrestrial Group (TG). My research showed that AOA communities showed distinct depth profiles for top (0-15 cm) and subsurface (30-45 cm) samples for all field sites, whereas AOA communities were more homogeneous across all depths in forest soils (Figure 2.7).

Soil pH is the major abiotic factor that separated thaumarchaeotal communities among field sites from those among forest sites (Figures 2.10, 2.11). Specifically, thaumarchaeota in forest samples were related to soil pH and NO_3^- concentrations, but not specifically to variables related to depth (Figures 2.10, 2.11). In terms of field soils, NO_3^-, NH_4^+, organic carbon, and gravel content variations along soil profiles likely drove the separation of thaumarchaeotal communities of topsoils from subsoils (Figures 2.10, 2.11), underlining the importance of nitrogen and carbon in shaping the niches of soil AOA. Previously, archaeal community changes with soil organic carbon were demonstrated in acidic forest soils (Pesaro and Widmer 2002; Kemnitz, Kolb and Conrad 2007), and here this trend was confirmed specifically for thaumarchaeota in agricultural soils. Data presented in this research suggested that soil mineral content was linked to thaumarchaeotal community differences (Figure 2.10). The impact of the soil matrix on microbial communities was observed five decades ago (Greenwood and Goodman 1967; Bales *et al.* 1989; Treves *et al.* 2003), but its effect on thaumarchaeotal community composition was overlooked before my research. Soil particle vectors linked to thaumarchaeotal community changes supported physical “filtering” for certain microbes, and suggested a potential soil matrix-associated nitrification activity, which needs further investigation.

5.3 Temperature effect on soil AOA and AOB

Because the observed differences of AOA communities in top (0-15 cm) and sub (30-45 cm) soils (Chapter 2), follow-up investigations on their ammonia oxidation activity was carried out, especially under environmental stress (e.g., temperature), which is not well understood. Temperature was identified as a key factor governing the relative activity of AOA and AOB, with AOA more active at high temperature. For example, AOA-associated activity in surface soils peaked at 40°C, whereas AOB-associated activity was highest at 30°C. (Figure 3.2). The overall AOA-associated relative activity ranged from 5 to 98% across all soil microcosms, and increased to over 50% in all soils when incubated at 40°C (Figure 3.3). AOB dominated activity in agricultural and subsurface forest samples collected in autumn when the incubation temperature was reduced to 20°C. However, AOA dominated in the same soils collected in summer (Figure 3.3). This general temperature trend agreed with that found by Taylor and colleagues (2017), demonstrating an average of 12°C higher optimum temperature for AOA compared to AOB in several soils. Overall, nitrification potential was significantly influenced by land use type (agricultural and forest), depth (0-15 and 30-45 cm), and temperature (20, 30, and 40°C).

Ammonia oxidation contributes to 80% of soil N_2O emissions (Gödde and Conrad 1999; Kool *et al.* 2011, 2011), yet relative contributions of AOA and AOB to N_2O production was not studied when this research started. Accompanying ammonia oxidation, N_2O was detected in soil microcosms only in surface agricultural soils incubated at 30°C, which indicates a land-use and temperature-sensitive N_2O production (Table 3.2). Importantly, no N_2O was detected with octyne-resistant activity, thus the N_2O produced during incubation was attributed to AOB-driven ammonia oxidation, suggesting AOB as major contributors to N_2O production. This pattern was

reported in Scottish agricultural soils, with the same incubation inhibitor (Hink, Nicol and Prosser 2017). Possible N_2O-producing mechanisms among ammonia oxidizers are not clear yet, but nitrifier-denitrification has been suggested as one pathway in AOB (Arp and Stein 2003). A significant correlation between NO_2^- accumulation and N_2O production was observed in summer soil samples (Figure 3.6). However, the inability to detect AOA-associated N_2O production in this study did not exclude the possibility of their contributions. A recently published study demonstrated NO_2^--dependent N_2O production during AOA-supported nitrification (Giguere *et al.* 2017), which pointed out the need for further study into N_2O producing mechanisms in AOA. For terrestrial environments, assessing AOA-associated greenhouse gas emissions, niche differentiation, and efficient nitrification inhibitors, might help reduce agriculture-associated N_2O production, and enhance fertilizer use efficiency.

5.4 Soil microbial cobalamin producing and consuming potential

Recently, marine cobalamin production has been investigated, where members of the *Thaumarchaeota* were identified as major cobalamin producers in marine habitats (Doxey *et al.* 2015; Heal *et al.* 2017), and currently all thaumarchaeotal cultures tested have been detected to produce cobalamin (Doxey *et al.* 2015; Heal *et al.* 2017). My research combined metagenomics and analytical chemistry to provide the first broad survey of soil cobalamin, "nature's most beautiful cofactor" (Hodgkin *et al.* 1955; Stubbe 1994). Soil microbial cobalamin producers were identified across 155 global soil metagenomes (Appendix A and B) and five predominant phyla were associated with cobalamin synthesis genes, among which, members of the *Thaumarchaeota* accounted for ~3% of all cobalamin gene abundances (Figure 4.1). Only a limited group of bacteria and archaea can biosynthesize cobalamin and data presented in this study identified genera that likely encoded complete cobalamin synthesis pathways. The results showed that

these genera accounted for less than 10% of the overall microbial community. Such small relative population sizes suggest that production of cobalamin is a disproportionally important function, consistent with a keystone role for cobalamin producers. Besides these genera with complete cobalamin synthesis pathways, many more genera were capable of 5,6-dimethylbenzimidazole (DMB) biosynthesis than those responsible for corrin ring biosynthesis or final assembly and repair (Table 4.2).

This research measured soil cobalamin (Me-, Ado-, OH-, and CN-B_{12}) concentrations (Table 4.5) in an independent investigation of 40 soil samples, representing a wide range of land use types (Table 4.2). Water-leachable cobalamin concentrations were lower than those of non-water-leachable cobalamin (Figure 4.9), suggesting that most cobalamin is associated with microbial biomass and/or soil mineral matrix. The biologically inactive form, OH-B_{12}, dominated the soil cobalamin pool, and thus is proposed to serve as a "currency" for cross-feeding among soil microbes, which requires further research to confirm. The lower-ligand, 5,6-dimethylbenzimidazole (DMB), was found in much higher concentration than cobalamin, consistent with the finding of more DMB biosynthesis gene reads than cobalamin synthesis gene reads (Figure 4.9), suggesting a possible lower-ligand remodeling in soils. Cobalamin concentrations positively correlated with microbial biomass in soil, consistent with a significant positive correlation between cobalamin producing gene abundance and microbial community size estimation. These results provide strong evidence that cobalamin constrains soil microbial community sizes. Interestingly, cobalamin concentrations and microbial biomass in marine samples did not follow the same trends (Suffridge, Cutter and Sañudo-Wilhelmy 2017), implying different cobalamin-producing and transferring mechanisms in terrestrial and marine habitats that are worthy of further study.

5.5 Future outlook

Overall, my thesis research suggests that pH is the key factor separating AOA communities in soils linked to agricultural activities from those in forest soils. Currently, cultivated soil AOA representatives are derived from acidic (Lehtovirta-Morley *et al.* 2011) or neutral (Tourna *et al.* 2011) soils, and no obligately alkalinophilic AOA have been obtained, although their presence has been detected in alkaline soil environments (Shen *et al.* 2008). A lack of AOA cultures from high pH soils prevents understanding of ammonia oxidation mechanisms under low H^+ concentrations, which might be different from low pH soils because ammonia/ammonium dynamics change with soil pH (Sigunga, Janssen and Oenema 2002). Obtaining high pH AOA cultures would help determine if AOA cultures from a wide range of pH values employ the same carbon assimilation pathways. Current knowledge is that AOB fix atmospheric CO_2 by the Calvin cycle, whereas AOA fix HCO_3^- with a more efficient hydroxypropionate-hydroxybutyrate cycle (Berg *et al.* 2007). Because the CO_2 and HCO_3^- equilibrium is pH dependent, the mechanisms and consequences for these differential substrate preferences for AOA and AOB are not clear.

This research has provided evidence demonstrating a significant stimulatory effect of NO_2^- on N_2O production in soil samples. Interesting topics for future research include NOB distributions in soils under diverse land use types, and along soil depth profiles, and their co-existence with AOA/AOB. Assessing a possible symbiosis between NOB and AOA/AOB could be achieved by tracking ^{15}N signature in soil AOA/AOB and NOB. This could be coupled with different environmental stresses (e.g., temperature, substrate forms, pH) to demonstrate NO_2^-, and nitrogen oxide gas (NO, NO_2, and N_2O) dynamics in nitrification under diverse environmental conditions.

Potentially important for soil nitrification, the biogeography and activity of bacteria that are linked to complete ammonia oxidation (comammox; Daims *et al.* 2015; van Kessel *et al.* 2015) may result in a reconsideration of their influence on the terrestrial nitrogen cycle. Recent metagenomic surveys demonstrate a widespread distribution of comammox bacteria in soils (Daims *et al.* 2015; van Kessel *et al.* 2015; Pinto *et al.* 2016), indicating a potentially significant role in soil nitrification. The only available comammox isolate, *Nitrospira inopinata*, demonstrates an extremely high substrate affinity compared to either AOA or AOB, and transient NO_2^- accumulation during ammonia oxidation (Kits *et al.* 2017). The NO_2^- accumulation detected in my research incubations might be attributed partially to comammox-associated *Nitrospira* present in those soils. It remains an open question whether or not comammox bacteria can produce N_2O. If so, N_2O yields may be comparable to those of AOA and AOB. More investigations of soil comammox bacteria would help estimate soil ammonia oxidation-related N_2O production more accurately, and be linked to solutions to reducing greenhouse gas emissions by identifying suitable inhibitors.

Resuming pioneering research initiated seven decades ago, my Chapter 4 research focused on soil cobalamin, the cofactor required by most microorganisms, elucidating its microbial production and consumption, and *in situ* concentration. Although evidence provided showed that the microbial cobalamin producers are potential keystone species among soil microbial communities, the cobalamin-dependent microbial dynamics must be confirmed by wet lab experimentation. It would be valuable to assess impacts of cobalamin additions on soil microbial community composition. With OH-B_{12} being the most abundant cobalamin form in soils, it might serve as a "currency" of exchange among cobalamin consumers in microbial communities, readily taken up and converted to biologically active forms such as Ado- and Me-

B_{12} by cells (Obeid, Fedosov and Nexo 2015). This hypothesis could be tested by developing OH-B_{12} probes (Romine *et al.* 2017) and tracking its uptake and transformation within microbial cells. Because soil is a complex system involving both prokaryotes and eukaryotes, and eukaryotes are incapable of cobalamin production, follow-up research should also focus on microbial cobalamin producers and their effects on soil eukaryotic community dynamics. Soil is home to both eukaryotes (e.g., earthworms, nematodes, and mites) and prokaryotes (bacteria and archaea) that benefit each other (Binet *et al.* 1998; Drake and Horn 2007).

5.6 Research significance

Soil is home to the most diverse microbial communities on Earth (Richter and Markewitz 1995; Daniel 2005; Roesch *et al.* 2007), feeding humans by supporting crop growth with microbially driven biogeochemical cycles (Kennedy and Smith 1995; Nannipieri *et al.* 2003), among which, nitrogen is one of several basic elements. This thesis research, combining both biogeochemical and bioinformatics techniques, has bridged gaps in our understanding of nitrogen cycling within terrestrial environments. Data presented in Chapter 2 and 3 contributed the first AOA biogeography survey along soil vertical profile under contrasting land use types, and the first report of AOA-associated N_2O responses to temperature gradients under contrasting land practices, respectively. Chapter 4 presents first evidence demonstrating the importance of cobalamin in governing soil microbial community composition, underlining the potential keystone function of cobalamin-producers, including but not limited to AOA. As the first quantitative and culture-independent large-scale investigation of cobalamin in terrestrial environments, data presented here laid important foundations for further studies connecting microbial community composition and activity with cofactor-associated biogeochemistry.

References

Aakra A, Utåker J, Pommerening-Röser A *et al.* Detailed phylogeny of ammonia-oxidizing bacteria determined by rDNA sequences and DNA homology values. *Int J Syst Evol Microbiol* 2001;**51**:2021–30.

Abby S, Melcher M, Kerou M *et al. Candidatus* Nitrosocaldus cavascurensis, an ammonia oxidizing, extremely thermophilic archaeon with a highly mobile genome. *Front Microbiol* 2018;**9**:28.

Adair K, Schwartz E. Evidence that ammonia-oxidizing archaea are more abundant than ammonia-oxidizing bacteria in semiarid soils of northern Arizona, USA. *Microb Ecol* 2008;**56**:420–6.

Alawi M, Lipski A, Sanders T *et al.* Cultivation of a novel cold-adapted nitrite oxidizing betaproteobacterium from the Siberian Arctic. *ISME J* 2007;**1**:256.

Albers S-V, Meyer BH. The archaeal cell envelope. *Nat Rev Microbiol* 2011;**9**:414–26.

Allison FE. The fate of nitrogen applied to soils. In: Norman AG (ed.). *Advances in Agronomy*. Vol 18. Academic Press, 1966, 219–58.

Allison SM, Prosser JI. Ammonia oxidation at low pH by attached populations of nitrifying bacteria. *Soil Biol Biochem* 1993;**25**:935–41.

Alves RJE, Wanek W, Zappe A *et al.* Nitrification rates in Arctic soils are associated with functionally distinct populations of ammonia-oxidizing archaea. *ISME J* 2013;**7**:1620–31.

Anderson MJ. A new method for non-parametric multivariate analysis of variance. *Austral Ecol* 2001;**26**:32–46.

Angel R, Soares MIM, Ungar ED *et al.* Biogeography of soil archaea and bacteria along a steep precipitation gradient. *ISME J* 2010;**4**:553–63.

Arp DJ, Bottomley PJ. Nitrifers: more than 100 years from isolation to genome sequences. *Microbe-Am Soc Microbiol* 2006;**1**:229–34.

Arp DJ, Stein LY. Metabolism of inorganic N compounds by ammonia-oxidizing bacteria. *Crit Rev Biochem Mol Biol* 2003;**38**:471–95.

Attard E, Poly F, Commeaux C *et al.* Shifts between *Nitrospira*- and *Nitrobacter*- like nitrite oxidizers underlie the response of soil potential nitrite oxidation to changes in tillage practices. *Environ Microbiol* 2010;**12**:315–26.

Auguet J-C, Barberan A, Casamayor EO. Global ecological patterns in uncultured Archaea. *ISME J* 2009;**4**:182–90.

Avrahami S, Bohannan BJM. Response of *Nitrosospira* sp. strain AF-like ammonia oxidizers to changes in temperature, soil moisture content, and fertilizer concentration. *Appl Environ Microbiol* 2007;**73**:1166–73.

Avrahami S, Conrad R. Patterns of community change among ammonia oxidizers in meadow soils upon long-term incubation at different temperatures. *Appl Environ Microbiol* 2003;**69**:6152–64.

Avrahami S, Conrad R. Cold-temperate climate: a factor for selection of ammonia oxidizers in upland soil? *Can J Microbiol* 2005;**51**:709–14.

Avrahami S, Liesack W, Conrad R. Effects of temperature and fertilizer on activity and community structure of soil ammonia oxidizers. *Environ Microbiol* 2003;**5**:691–705.

Bales RC, Gerba CP, Grondin GH *et al.* Bacteriophage transport in sandy soil and fractured tuff. *Appl Environ Microbiol* 1989;**55**:2061–7.

Bancroft K, Grant IF, Alexander M. Toxicity of NO_2: effect of nitrite on microbial activity in an acid soil. *Appl Environ Microbiol* 1979;**38**:940–4.

Banerjee R. *Chemistry and Biochemistry of B_{12}*. John Wiley & Sons, 1999.

Banerjee R. The Yin-Yang of cobalamin biochemistry. *Chem Biol* 1997;**4**:175–86.

Banerjee RV, Matthews RG. Cobalamin-dependent methionine synthase. *FASEB J* 1990;**4**:1450–9.

Bardgett RD, van der Putten WH. Belowground biodiversity and ecosystem functioning. *Nature* 2014;**515**:505–11.

Bartosch S, Hartwig C, Spieck E *et al.* Immunological detection of *Nitrospira*-like bacteria in various soils. *Microb Ecol* 2002;**43**:26–33.

Bartram AK, Jiang X, Lynch MDJ *et al.* Exploring links between pH and bacterial community composition in soils from the Craibstone Experimental Farm. *FEMS Microbiol Ecol* 2014;**87**:403–15.

Bartram AK, Lynch MDJ, Stearns JC *et al.* Generation of multimillion-sequence 16S rRNA gene libraries from complex microbial communities by assembling paired-end Illumina reads. *Appl Environ Microbiol* 2011;**77**:3846–52.

Bates ST, Berg-Lyons D, Caporaso JG *et al.* Examining the global distribution of dominant archaeal populations in soil. *ISME J* 2011;**5**:908–17.

Bédard C, Knowles R. Physiology, biochemistry, and specific inhibitors of CH_4, NH_4^+, and CO oxidation by methanotrophs and nitrifiers. *Microbiol Rev* 1989;**53**:68–84.

Begley TP, Downs DM, Ealick SE *et al.* Thiamin biosynthesis in prokaryotes. *Arch Microbiol* 1999;**171**:293–300.

Berg IA, Kockelkorn D, Buckel W *et al.* A 3-Hydroxypropionate/4-Hydroxybutyrate autotrophic carbon dioxide assimilation pathway in Archaea. *Science* 2007;**318**:1782–6.

Bertrand EM, Allen AE. Influence of vitamin B auxotrophy on nitrogen metabolism in eukaryotic phytoplankton. *Front Microbiol* 2012;**3**:375.

Bertrand EM, McCrow JP, Moustafa A *et al.* Phytoplankton–bacterial interactions mediate micronutrient colimitation at the coastal Antarctic sea ice edge. *Proc Natl Acad Sci USA* 2015;**112**:9938–43.

Bertrand EM, Saito MA, Jeon YJ *et al.* Vitamin B_{12} biosynthesis gene diversity in the Ross Sea: the identification of a new group of putative polar B_{12} biosynthesizers. *Environ Microbiol* 2011;**13**:1285–98.

Bier RL, Bernhardt ES, Boot CM *et al.* Linking microbial community structure and microbial processes: an empirical and conceptual overview. *FEMS Microbiol Ecol* 2015;**91**:fiv113.

Binet F, Fayolle L, Pussard M *et al.* Significance of earthworms in stimulating soil microbial activity. *Biol Fertil Soils* 1998;**27**:79–84.

Bintrim SB, Donohue TJ, Handelsman J *et al.* Molecular phylogeny of Archaea from soil. *Proc Natl Acad Sci USA* 1997;**94**:277–82.

Blackburne R, Vadivelu VM, Yuan Z *et al.* Kinetic characterisation of an enriched *Nitrospira* culture with comparison to *Nitrobacter*. *Water Res* 2007;**41**:3033–42.

Blakley RL. Cobamides and ribonucleotide reduction: I. Cobamide stimulation of ribonucleotide reduction in extracts of *Lactobacillus leichmannii*. *J Biol Chem* 1965;**240**:2173–80.

Blakley RL, Barker HA. Cobamide stimulation of the reduction of ribotides to deoxyribotides in *Lactobacillus leichmannii*. *Biochem Biophys Res Commun* 1964;**16**:391–7.

Blanche F, Cameron B, Crouzet J *et al.* Vitamin B_{12}: how the problem of its biosynthesis was solved. *Angew Chem Int Ed Engl* 1995;**34**:383–411.

Bock E, Wilderer PA, Freitag A. Growth of *Nitrobacter* in the absence of dissolved oxygen. *Water Res* 1988;**22**:245–50.

Bomberg M, Timonen S. Distribution of cren- and euryarchaeota in Scots pine mycorrhizospheres and boreal forest humus. *Microb Ecol* 2007;**54**:406–16.

Bomberg M, Timonen S. Effect of tree species and mycorrhizal colonization on the archaeal population of boreal forest rhizospheres. *Appl Environ Microbiol* 2009;**75**:308–15.

Bonnet S, Tovar-Sanchez A, Panzeca C *et al.* Geographical gradients of dissolved Vitamin B_{12} in the Mediterranean Sea. *Front Microbiol* 2013;**4**:126.

Bonnet S, Webb EA, Panzeca C *et al.* Vitamin B_{12} excretion by cultures of the marine cyanobacteria *Crocosphaera* and *Synechococcus*. *Limnol Oceanogr* 2010;**55**:1959–64.

Boyle-Yarwood S, Bottomley PJ, Myrold DD. Community composition of ammonia-oxidizing bacteria and archaea in soils under stands of red alder and Douglas fir in Oregon. *Environ Microbiol* 2008;**10**:2956–65.

Boysen AK, Heal KR, Carlson LT *et al.* Best-matched internal standard normalization in liquid chromatography–mass spectrometry metabolomics applied to environmental samples. *Anal Chem* 2018;**90**:1363–9.

Brochier-Armanet C, Boussau B, Gribaldo S *et al.* Mesophilic crenarchaeota: proposal for a third archaeal phylum, the Thaumarchaeota. *Nat Rev Microbiol* 2008;**6**:245–52.

Bruns MA, Stephen JR, Kowalchuk GA *et al.* Comparative diversity of ammonia oxidizer 16S rRNA gene sequences in native, tilled, and successional soils. *Appl Environ Microbiol* 1999;**65**:2994–3000.

Buckley DH, Graber JR, Schmidt TM. Phylogenetic analysis of nonthermophilic members of the kingdom Crenarchaeota and their diversity and abundance in soils. *Appl Environ Microbiol* 1998;**64**:4333–9.

Burns LC, Stevens RJ, Smith RV *et al.* The occurrence and possible sources of nitrite in a grazed, fertilized, grassland soil. *Soil Biol Biochem* 1995;**27**:47–59.

Burton E, Read H, Pellitteri M *et al.* Identification of acyl-homoserine lactone signal molecules produced by *Nitrosomonas europaea* strain Schmidt. *Appl Environ Microbiol* 2005;**71**:4906–9.

Burton SAQ, Prosser JI. Autotrophic ammonia oxidation at low pH through urea hydrolysis. *Appl Environ Microbiol* 2001;**67**:2952–7.

Cadieux N, Kadner RJ. Site-directed disulfide bonding reveals an interaction site between energy-coupling protein TonB and BtuB, the outer membrane cobalamin transporter. *Proc Natl Acad Sci USA* 1999;**96**:10673–8.

Campbell GR, Taga ME, Mistry K *et al. Sinorhizobium meliloti bluB* is necessary for production of 5, 6-dimethylbenzimidazole, the lower ligand of B_{12}. *Proc Natl Acad Sci USA* 2006;**103**:4634–9.

Cantera JJL, Stein LY. Role of nitrite reductase in the ammonia-oxidizing pathway of *Nitrosomonas europaea*. *Arch Microbiol* 2007;**188**:349–54.

Caporaso JG, Kuczynski J, Stombaugh J *et al.* QIIME allows analysis of high-throughput community sequencing data. *Nat Methods* 2010;**7**:335–6.

Carey CJ, Dove NC, Beman JM *et al.* Meta-analysis reveals ammonia-oxidizing bacteria respond more strongly to nitrogen addition than ammonia-oxidizing archaea. *Soil Biol Biochem* 2016;**99**:158–66.

Carnol M, Kowalchuk GA, De Boer W. *Nitrosomonas europaea*-like bacteria detected as the dominant β-subclass Proteobacteria ammonia oxidisers in reference and limed acid forest soils. *Soil Biol Biochem* 2002;**34**:1047–50.

Case RJ, Boucher Y, Dahllöf I *et al.* Use of 16S rRNA and *rpoB* genes as molecular markers for microbial ecology studies. *Appl Environ Microbiol* 2007;**73**:278–88.

Catão E, Castro AP, Barreto CC *et al.* Diversity of archaea in Brazilian savanna soils. *Arch Microbiol* 2013;**195**:507–12.

Chapman H, Liebig GF. Field and laboratory studies of nitrite accumulation in soils. *Soil Sci Soc Am J* 1952;**16**:276–82.

Che J, Zhao XQ, Zhou X *et al.* High pH-enhanced soil nitrification was associated with ammonia-oxidizing bacteria rather than archaea in acidic soils. *Appl Soil Ecol* 2015;**85**:21–9.

Chimento DP, Mohanty AK, Kadner RJ *et al.* Substrate-induced transmembrane signaling in the cobalamin transporter *btuB*. *Nat Struct Mol Biol* 2003;**10**:394–401.

Conrad R, Seiler W, Bunse G. Factors influencing the loss of fertilizer nitrogen into the atmosphere as N_2O. *J Geophys Res Oceans* 1983;**88**:6709–18.

Costa E, Pérez J, Kreft J-U. Why is metabolic labour divided in nitrification? *Trends Microbiol* 2006;**14**:213–9.

Court MN, Stephen RC, Waid JS. Toxic effect of urea on plants: nitrite toxicity arising from the use of urea as a fertilizer. *Nature* 1962;**194**:1263–5.

Coyotzi S, Doxey AC, Clark ID *et al.* Agricultural soil denitrifiers possess extensive nitrite reductase gene diversity. *Environ Microbiol* 2017;**19**:1189–208.

Daebeler A, Bodelier PL, Yan Z *et al.* Interactions between Thaumarchaea, *Nitrospira* and methanotrophs modulate autotrophic nitrification in volcanic grassland soil. *ISME J* 2014;**8**:2397.

Daebeler A, Bodelier PLE, Hefting MM *et al.* Ammonia-limited conditions cause of Thaumarchaeal dominance in volcanic grassland soil. *FEMS Microbiol Ecol* 2015;**91**:fiv014.

Daebeler A, Herbold C, Vierheilig J *et al.* Cultivation and genomic analysis of "*Candidatus* Nitrosocaldus islandicus", an obligately thermophilic, ammonia-oxidizing thaumarchaeon from a hot spring biofilm in Graendalur valley, Iceland. *Front Microbiol* 2018;**9**:193.

Dahllöf I, Baillie H, Kjelleberg S. *rpoB*-based microbial community analysis avoids limitations inherent in 16S rRNA gene intraspecies heterogeneity. *Appl Environ Microbiol* 2000;**66**:3376–80.

Daims H, Lebedeva EV, Pjevac P *et al.* Complete nitrification by *Nitrospira* bacteria. *Nature* 2015;**528:**504-9.

Daims H, Lücker S, Wagner M. A new perspective on microbes formerly known as nitrite-oxidizing bacteria. *Trends Microbiol* 2016;**24**:699–712.

Daims H, Nielsen JL, Nielsen PH *et al.* In situ characterization of *Nitrospira*-like nitrite-oxidizing bacteria active in wastewater treatment plants. *Appl Environ Microbiol* 2001;**67**:5273–84.

Daniel R. The metagenomics of soil. *Nat Rev Micro* 2005;**3**:470–8.

De Boer W, Gunnewiek PK, Veenhuis M *et al.* Nitrification at low pH by aggregated chemolithotrophic bacteria. *Appl Environ Microbiol* 1991;**57**:3600–4.

De La Torre JR, Walker CB, Ingalls AE *et al.* Cultivation of a thermophilic ammonia oxidizing archaeon synthesizing crenarchaeol. *Environ Microbiol* 2008;**10**:810–8.

DeLong EF. Everything in moderation: Archaea as 'non-extremophiles.' *Curr Opin Genet Dev* 1998;**8**:649–54.

Degnan PH, Barry NA, Mok KC *et al.* Human gut microbes use multiple transporters to distinguish vitamin B_{12} analogs and compete in the gut. *Cell Host Microbe* 2014;**15**:47–57.

Delgado-Baquerizo M, Oliverio AM, Brewer TE *et al.* A global atlas of the dominant bacteria found in soil. *Science* 2018;**359**:320–5.

DeLong EF. Archaea in coastal marine environments. *Proc Natl Acad Sci USA* 1992;**89**:5685–9.

Di HJ, Cameron KC, Shen J-P *et al.* Ammonia-oxidizing bacteria and archaea grow under contrasting soil nitrogen conditions. *FEMS Microbiol Ecol* 2010;**72**:386–94.

Dickman S. Ribonucleotide reduction and the possible role of cobalamin in evolution. *J Mol Evol* 1977;**10**:251–60.

Doxey AC, Kurtz DA, Lynch MD *et al.* Aquatic metagenomes implicate Thaumarchaeota in global cobalamin production. *ISME J* 2015b;**9**:461–71.

Drake HL, Horn MA. As the worm turns: the earthworm gut as a transient habitat for soil microbial biomes. *Annu Rev Microbiol* 2007;**61**:169–89.

Duan P, Wu Z, Zhang Q *et al.* Thermodynamic responses of ammonia-oxidizing archaea and bacteria explain N_2O production from greenhouse vegetable soils. *Soil Biol Biochem* 2018;**120**:37–47.

Dworkin M, Gutnick D. Sergei Winogradsky: a founder of modern microbiology and the first microbial ecologist. *FEMS Microbiol Rev* 2012;**36**:364–79.

Eddy SR. Profile hidden Markov models. *Bioinformatics* 1998;**14**:755–63.

Edgar RC. Search and clustering orders of magnitude faster than BLAST. *Bioinformatics* 2010;**26**:2460–1.

Edgar RC. UPARSE: highly accurate OTU sequences from microbial amplicon reads. *Nat Methods* 2013;**10**:996–8.

Edgar RC, Haas BJ, Clemente JC *et al.* UCHIME improves sensitivity and speed of chimera detection. *Bioinformatics* 2011;**27**:2194–200.

Ferrer A, Rivera J, Zapata C *et al.* Cobalamin protection against oxidative stress in the acidophilic iron-oxidizing bacterium *Leptospirillum* Group II CF-1. *Front Microbiol* 2016;**7**:748.

Fierer N, Carney KM, Horner-Devine mc *et al*. The biogeography of ammonia-oxidizing bacterial communities in soil. *Microb Ecol* 2009;**58**:435-45.

Fierer N, Jackson RB. The diversity and biogeography of soil bacterial communities. *Proc Natl Acad Sci USA* 2006;**103**:626–31.

Fierer N, Schimel JP, Holden PA. Variations in microbial community composition through two soil depth profiles. *Soil Biol Biochem* 2003;**35**:167–76.

Finn RD, Coggill P, Eberhardt RY *et al.* The Pfam protein families database: towards a more sustainable future. *Nucleic Acids Res* 2016;**44**:D279–85.

Fish J, Chai B, Wang Q *et al.* FunGene: the functional gene pipeline and repository. *Front Microbiol* 2013;**4**:291.

Frame CH, Casciotti KL. Biogeochemical controls and isotopic signatures of nitrous oxide production by a marine ammonia-oxidizing bacterium. *Biogeosciences* 2010;**7**:2695–709.

Freitag TE, Chang L, Clegg CD *et al.* Influence of inorganic nitrogen management regime on the diversity of nitrite-oxidizing bacteria in agricultural grassland soils. *Appl Environ Microbiol* 2005;**71**:8323–34.

Frey SD. Spatial distribution of soil organisms. In: Paul EA (ed.). *Soil Microbiology, Ecology and Biochemistry (Third Edition)*. San Diego: Academic Press, 2007, 283–300.

Frischkorn KR, Haley ST, Dyhrman ST. Coordinated gene expression between *Trichodesmium* and its microbiome over day–night cycles in the North Pacific Subtropical Gyre. *ISME J* 2018;**12**:997-1007.

Fuhrman JA, McCallum K, Davis AA. Novel major archaebacterial group from marine plankton. *Nature* 1992;**356**:148–9.

Galloway J, Winiwarter W, Leip A *et al.* Nitrogen footprints: past, present and future. *Environ Res Lett* 2014;**9**:115003.

Gao J, Ma A, Zhuang X *et al.* An *N*-acyl homoserine lactone synthase in the ammonia-oxidizing bacterium *Nitrosospira multiformis*. *Appl Environ Microbiol* 2014;**80**:951–8.

Giedyk M, Goliszewska K, Gryko D. Vitamin B_{12} catalysed reactions. *Chem Soc Rev* 2015;**44**:3391–404.

Giguere AT, Taylor AE, Myrold DD *et al.* Nitrification responses of soil ammonia-oxidizing archaea and bacteria to ammonium concentrations. *Soil Sci Soc Am J* 2015;**79**:1366–74.

Giguere AT, Taylor AE, Myrold DD *et al.* Nitrite-oxidizing activity responds to nitrite accumulation in soil. *FEMS Microbiol Ecol* 2018;**94**:fiy008.

Giguere AT, Taylor AE, Suwa Y *et al.* Uncoupling of ammonia oxidation from nitrite oxidation: Impact upon nitrous oxide production in non-cropped Oregon soils. *Soil Biol Biochem* 2017;**104**:30–8.

Giovannoni SJ. Vitamins in the sea. *Proc Natl Acad Sci USA* 2012;**109**:13888–9.

Gödde M, Conrad R. Immediate and adaptational temperature effects on nitric oxide production and nitrous oxide release from nitrification and denitrification in two soils. *Biol Fertil Soils* 1999;**30**:33–40.

Greenwood D, Goodman D. Direct measurements of the distribution of oxygen in soil aggregates and in columns of fine soil crumbs. *Eur J Soil Sci* 1967;**18**:182–96.

Groeneweg J, Sellner B, Tappe W. Ammonia oxidation in *Nitrosomonas* at NH_3 concentrations near K_m: effects of pH and temperature. *Water Res* 1994;**28**:2561–6.

Gubry-Rangin C, Nicol GW, Prosser JI. Archaea rather than bacteria control nitrification in two agricultural acidic soils. *FEMS Microbiol Ecol* 2010a;**74**:566–574.

Gubry-Rangin C, Hai B, Quince C *et al.* Niche specialization of terrestrial archaeal ammonia oxidizers. *Proc Natl Acad Sci USA* 2011;**108**:21206–11.

Gubry-Rangin C, Kratsch C, Williams TA *et al.* Coupling of diversification and pH adaptation during the evolution of terrestrial Thaumarchaeota. *Proc Natl Acad Sci USA* 2015;**112**:9370–5.

Gubry-Rangin C, Novotnik B, Mandič-Mulec I *et al.* Temperature responses of soil ammonia-oxidising archaea depend on pH. *Soil Biol Biochem* 2017;**106**:61–8.

Gülay A, Musovic S, Albrechtsen H-J *et al.* Ecological patterns, diversity and core taxa of microbial communities in groundwater-fed rapid gravity filters. *ISME J* 2016;**10**:2209–22.

Haft DH, Selengut JD, White O. The TIGRFAMs database of protein families. *Nucleic Acids Res* 2003;**31**:371–3.

Hansel CM, Fendorf S, Jardine PM *et al.* Changes in bacterial and archaeal community structure and functional diversity along a geochemically variable soil profile. *Appl Environ Microbiol* 2008;**74**:1620–33.

Hashsham SA, Freedman DL. Enhanced biotransformation of carbon tetrachloride by *Acetobacterium woodii* upon addition of hydroxocobalamin and fructose. *Appl Environ Microbiol* 1999;**65**:4537–42.

Hatzenpichler R. Diversity, physiology, and niche differentiation of ammonia-oxidizing archaea. *Appl Environ Microbiol* 2012;**78**:7501–10.

Hatzenpichler R, Lebedeva EV, Spieck E *et al.* A moderately thermophilic ammonia-oxidizing crenarchaeote from a hot spring. *Proc Natl Acad Sci USA* 2008;**105**:2134–9.

Hayatsu M, Tago K, Uchiyama I *et al.* An acid-tolerant ammonia-oxidizing γ-proteobacterium from soil. *ISME J* 2017;**11**:1130–41.

He J, Shen J, Zhang L *et al.* Quantitative analyses of the abundance and composition of ammonia-oxidizing bacteria and ammonia-oxidizing archaea of a Chinese upland red soil under long-term fertilization practices. *Environ Microbiol* 2007;**9**:2364–74.

Heal KR, Carlson LT, Devol AH *et al.* Determination of four forms of vitamin B_{12} and other B vitamins in seawater by liquid chromatography/tandem mass spectrometry. *Rapid Commun Mass Spectrom* 2014;**28**:2398–404.

Heal KR, Qin W, Ribalet F *et al.* Two distinct pools of B_{12} analogs reveal community interdependencies in the ocean. *Proc Natl Acad Sci USA* 2017;**114**:364–9.

Heal KR, Qin W, Amin SA et al. Accumulation of NO_2-cobalamin in nutrien-tstressed ammonia-oxidizing archaea and in the oxygen deficient zone of the Eastern Tropical North Pacific. *Environ Microbiol Rep* 2018 In press.

Helliwell KE, Lawrence AD, Holzer A *et al.* Cyanobacteria and eukaryotic algae use different chemical variants of vitamin B_{12}. *Curr Biol* 2016;**26**:999–1008.

Hershberger KL, Barns SM, Reysenbach A-L *et al.* Wide diversity of Crenarchaeota. *Nature* 1996;**384**:420.

Hink L, Gubry-Rangin C, Nicol GW *et al.* The consequences of niche and physiological differentiation of archaeal and bacterial ammonia oxidisers for nitrous oxide emissions. *ISME J* 2018;**12**:1084-93.

Hink L, Nicol GW, Prosser JI. Archaea produce lower yields of N_2O than bacteria during aerobic ammonia oxidation in soil. *Environ Microbiol* 2017;**19**:4829–37.

Hodgkin DC, Pickworth J, Robertson JH *et al.* The crystal structure of the hexacarboxylic acid derived from B12 and the molecular structure of the vitamin. *Nature* 1955;**176**:325–8.

Höfferle Š, Nicol GW, Pal L *et al.* Ammonium supply rate influences archaeal and bacterial ammonia oxidizers in a wetland soil vertical profile. *FEMS Microbiol Ecol* 2010;**74**:302–15.

Hol W, De Boer W, Termorshuizen AJ *et al.* Reduction of rare soil microbes modifies plant–herbivore interactions. *Ecol Lett* 2010;**13**:292–301.

Hommes NG, Sayavedra-Soto LA, Arp DJ. Chemolithoorganotrophic growth of *Nitrosomonas europaea* on fructose. *J Bacteriol* 2003;**185**:6809–14.

Hooper AB, Terry KR. Specific inhibitors of ammonia oxidation in *Nitrosomonas*. *J Bacteriol* 1973;**115**:480–5.

Horak REA, Qin W, Schauer AJ *et al.* Ammonia oxidation kinetics and temperature sensitivity of a natural marine community dominated by Archaea. *ISME J* 2013;**7**:2023–33.

Horsburgh MJ, Wharton SJ, Karavolos M *et al.* Manganese: elemental defence for a life with oxygen. *Trends Microbiol* 2002;**10**:496–501.

Hu H-W, He J-Z. Comammox—a newly discovered nitrification process in the terrestrial nitrogen cycle. *J Soils Sediments* 2017;**17**:2709–17.

Hu J, Inglett KS, Clark MW *et al.* Nitrous oxide production and consumption by denitrification in a grassland: Effects of grazing and hydrology. *Sci Total Environ* 2015;**532**:702–10.

Hughes MN. Relationships between nitric oxide, nitroxyl ion, nitrosonium cation and peroxynitrite. *Biochim Biophys Acta BBA - Bioenerg* 1999;**1411**:263–72.

Hyman MR, Wood PM. Suicidal inactivation and labelling of ammonia mono-oxygenase by acetylene. *Biochem J* 1985;**227**:719–25.

Janssen DB, Oppentocht JE, Poelarends GJ. Microbial dehalogenation. *Curr Opin Biotechnol* 2001;**12**:254–8.

Jia Z, Conrad R. Bacteria rather than Archaea dominate microbial ammonia oxidation in an agricultural soil. *Environ Microbiol* 2009;**11**:1658–71.

Jiang QQ, Bakken LR. Comparison of *Nitrosospira* strains isolated from terrestrial environments. *FEMS Microbiol Ecol* 1999;**30**:171–86.

Jones RD, Morita RY, Koops H-P *et al.* A new marine ammonium-oxidizing bacterium, *Nitrosomonas cryotolerans* sp. nov. *Can J Microbiol* 1988;**34**:1122–8.

Jordan FL, Cantera JJL, Fenn ME *et al.* Autotrophic ammonia-oxidizing bacteria contribute minimally to nitrification in a nitrogen-impacted forested ecosystem. *Appl Environ Microbiol* 2005;**71**:197–206.

Jung M-Y, Kim J-G, Sinninghe Damsté JS *et al.* A hydrophobic ammonia-oxidizing archaeon of the *Nitrosocosmicus* clade isolated from coal tar-contaminated sediment. *Environ Microbiol Rep* 2016;**8**:983–92.

Jung M-Y, Park S-J, Kim S-J *et al.* A mesophilic, autotrophic, ammonia-oxidizing archaeon of thaumarchaeal group I.1a cultivated from a deep oligotrophic soil horizon. *Appl Environ Microbiol* 2014a;**80**:3645–55.

Jung M-Y, Park S-J, Min D *et al.* Enrichment and characterization of an autotrophic ammonia-oxidizing archaeon of mesophilic crenarchaeal group I.1a from an agricultural soil. *Appl Environ Microbiol* 2011;**77**:8635–47.

Jung M-Y, Well R, Min D *et al.* Isotopic signatures of N_2O produced by ammonia-oxidizing archaea from soils. *ISME J* 2014b;**8**:1115–25.

Jurgens G, Lindström K, Saano A. Novel group within the kingdom Crenarchaeota from boreal forest soil. *Appl Environ Microbiol* 1997;**63**:803–5.

Juzeniene A, Nizauskaite Z. Photodegradation of cobalamins in aqueous solutions and in human blood. *J Photochem Photobiol B* 2013;**122**:7–14.

Kembel SW, Wu M, Eisen JA *et al.* Incorporating 16S gene copy number information improves estimates of microbial diversity and abundance. *PLoS Comput Biol* 2012;**8**:e1002743.

Kemnitz D, Kolb S, Conrad R. High abundance of Crenarchaeota in a temperate acidic forest soil. *FEMS Microbiol Ecol* 2007;**60**:442–8.

Kemp JS, Paterson E, Gammack SM *et al.* Leaching of genetically modified *Pseudomonas fluorescens* through organic soils: Influence of temperature, soil pH, and roots. *Biol Fertil Soils* 1992;**13**:218–24.

Kennedy AC, Smith KL. Soil microbial diversity and the sustainability of agricultural soils. *Plant Soil* 1995;**170**:75–86.

van Kessel MA, Speth DR, Albertsen M *et al.* Complete nitrification by a single microorganism. *Nature* 2015;**528**:555–9.

Kim J-G, Jung M-Y, Park S-J *et al.* Cultivation of a highly enriched ammonia-oxidizing archaeon of thaumarchaeotal group I.1b from an agricultural soil. *Environ Microbiol* 2012;**14**:1528–43.

Kits KD, Sedlacek CJ, Lebedeva EV *et al.* Kinetic analysis of a complete nitrifier reveals an oligotrophic lifestyle. *Nature* 2017;**549**:269–72.

Koch H, Lücker S, Albertsen M *et al.* Expanded metabolic versatility of ubiquitous nitrite-oxidizing bacteria from the genus *Nitrospira*. *Proc Natl Acad Sci USA* 2015;**112**:11371–6.

Könneke M, Bernhard AE, De La Torre JR *et al.* Isolation of an autotrophic ammonia-oxidizing marine archaeon. *Nature* 2005;**437**:543–66.

Kool DM, Dolfing J, Wrage N *et al.* Nitrifier denitrification as a distinct and significant source of nitrous oxide from soil. *Soil Biol Biochem* 2011;**43**:174–8.

Koops H, Pommerening- Röser A. Distribution and ecophysiology of the nitrifying bacteria emphasizing cultured species. *FEMS Microbiol Ecol* 2001;**37**:1–9.

Koops H-P, Purkhold U, Pommerening-Röser A *et al.* The lithoautotrophic ammonia-oxidizing bacteria. *The Prokaryotes*. Springer, 2006, 778–811.

Kowalchuk GA, Stephen JR. Ammonia-oxidizing bacteria: a model for molecular microbial ecology. *Annu Rev Microbiol* 2001;**55**:485–529.

Kozlowski JA, Price J, Stein LY. Revision of N_2O-producing pathways in the ammonia-oxidizing bacterium *Nitrosomonas europaea* ATCC 19718. *Appl Environ Microbiol* 2014;**80**:4930–5.

Kozlowski JA, Stieglmeier M, Schleper C *et al.* Pathways and key intermediates required for obligate aerobic ammonia-dependent chemolithotrophy in bacteria and Thaumarchaeota. *ISME J* 2016;**10**:1836–45.

Kumar S, Nicholas DJD, Williams EH. Definitive ^{15}N NMR evidence that water serves as a source of 'O' during nitrite oxidation by *Nitrobacter agilis*. *FEBS Lett* 1983;**152**:71–4.

De La Torre JR, Walker CB, Ingalls AE *et al.* Cultivation of a thermophilic ammonia oxidizing archaeon synthesizing crenarchaeol. *Environ Microbiol* 2008;**10**:810–8.

Laverman AM, Speksnijder AGCL, Braster M *et al.* Spatiotemporal stability of an ammonia-oxidizing community in a nitrogen-saturated forest soil. *Microb Ecol* 2001;**42**:35–45.

Le Roux X, Bouskill NJ, Niboyet A *et al.* Predicting the responses of soil nitrite-oxidizers to multi-factorial global change: a trait-based approach. *Front Microbiol* 2016;**7**:628.

Lebedeva EV, Hatzenpichler R, Pelletier E *et al.* Enrichment and genome sequence of the group I.1a ammonia-oxidizing Archaeon "*Ca*. Nitrosotenuis uzonensis" representing a clade globally distributed in thermal habitats. *PLoS ONE* 2013;**8**:e80835.

Lehtovirta LE, Prosser JI, Nicol GW. Soil pH regulates the abundance and diversity of Group 1.1c Crenarchaeota. *FEMS Microbiol Ecol* 2009;**70**:367–76.

Lehtovirta-Morley LE. Ammonia oxidation: ecology, physiology, biochemistry and why they must all come together. *FEMS Microbiol Lett* 2018;**365**:fny058.

Lehtovirta-Morley LE, Ge C, Ross J *et al.* Characterisation of terrestrial acidophilic archaeal ammonia oxidisers and their inhibition and stimulation by organic compounds. *FEMS Microbiol Ecol* 2014;**89**:542–52.

Lehtovirta-Morley LE, Ross J, Hink L *et al.* Isolation of '*Candidatus* Nitrosocosmicus franklandus', a novel ureolytic soil archaeal ammonia oxidiser with tolerance to high ammonia concentration. *FEMS Microbiol Ecol* 2016;**92**:fiw057.

Lehtovirta-Morley LE, Stoecker K, Vilcinskas A *et al.* Cultivation of an obligate acidophilic ammonia oxidizer from a nitrifying acid soil. *Proc Natl Acad Sci USA* 2011;**108**:15892–7.

Lehtovirta-Morley LE, Verhamme DT, Nicol GW *et al.* Effect of nitrification inhibitors on the growth and activity of *Nitrosotalea devanaterra* in culture and soil. *Soil Biol Biochem* 2013;**62**:129–33.

Leininger S, Urich T, Schloter M *et al.* Archaea predominate among ammonia-oxidizing prokaryotes in soils. *Nature* 2006;**442**:806–9.

Levičnik-Höfferle Š, Nicol GW, Ausec L *et al.* Stimulation of thaumarchaeal ammonia oxidation by ammonia derived from organic nitrogen but not added inorganic nitrogen. *Microb Ecol* 2012;**80**:114–23.

Li J, Nedwell DB, Beddow J *et al. amoA* gene abundances and nitrification potential rates suggest that benthic ammonia-oxidizing bacteria and not archaea dominate N cycling in the Colne estuary, United Kingdom. *Appl Environ Microbiol* 2015;**81**:159–65.

Li PN, Herrmann JR, PB Poitevin F *et al.* Cryo electron tomography and reaction-diffusion simulations reveal a molecular and evolutionary basis for charged archaeal surface layer proteins. *Biophys J* 2018;**114**:495.

Li Y, Chapman SJ, Nicol GW *et al.* Nitrification and nitrifiers in acidic soils. *Soil Biol Biochem* 2018;**116**:290–301.

Lochhead AG, Burton M. Soil as a habitat of vitamin-requiring bacteria. *Nature* 1956;**178**:144–5.

Lochhead AG, Burton MO, Thexton RH. A bacterial growth-factor synthesized by a soil bacterium. *Nature* 1952;**170**:282.

Lochhead AG, Thexton RH. Vitamin B_{12} as a growth factor for soil bacteria. *Nature* 1951;**167**:1034.

Löscher C, Kock A, Könneke M *et al.* Production of oceanic nitrous oxide by ammonia-oxidizing archaea. *Biogeosciences* 2012;**9**:2419–29.

Louca S, Parfrey LW, Doebeli M. Decoupling function and taxonomy in the global ocean microbiome. *Science* 2016;**353**:1272–7.

Lu L, Han W, Zhang J *et al.* Nitrification of archaeal ammonia oxidizers in acid soils is supported by hydrolysis of urea. *ISME J* 2012;**6**:1978–84.

Lu X, Bottomley PJ, Myrold DD. Contributions of ammonia-oxidizing archaea and bacteria to nitrification in Oregon forest soils. *Soil Biol Biochem* 2015;**85**:54–62.

Lu X, Nicol GW, Neufeld JD. Differential responses of soil ammonia-oxidizing archaea and bacteria to temperature and depth under two different land uses. *Soil Biol Biochem* 2018;**120**:272–82.

Lu X, Seuradge BJ, Neufeld JD. Biogeography of soil Thaumarchaeota in relation to soil depth and land usage. *FEMS Microbiol Ecol* 2017;**93**:fiw246.

Lücker S, Wagner M, Maixner F *et al.* A *Nitrospira* metagenome illuminates the physiology and evolution of globally important nitrite-oxidizing bacteria. *Proc Natl Acad Sci USA* 2010;**107**:13479–84.

Lynch M, Masella A, Hall M *et al.* AXIOME: automated exploration of microbial diversity. *GigaScience* 2013;**2**:3.

Lynch MDJ, Neufeld JD. Ecology and exploration of the rare biosphere. *Nat Rev Micro* 2015;**13**:217–29.

Ma L, Shan J, Yan X. Nitrite behavior accounts for the nitrous oxide peaks following fertilization in a fluvo-aquic soil. *Biol Fertil Soils* 2015;**51**:563–72.

MacDonald JA, Skiba U, Sheppard LJ *et al.* The effect of nitrogen deposition and seasonal variability on methane oxidation and nitrous oxide emission rates in an upland spruce plantation and moorland. *Atmos Environ* 1997;**31**:3693–706.

MacGregor BJ, Moser DP, Alm EW *et al.* Crenarchaeota in Lake Michigan sediment. *Appl Environ Microbiol* 1997;**63**:1178–81.

Maharjan B, Venterea RT. Nitrite intensity explains N management effects on N_2O emissions in maize. *Soil Biol Biochem* 2013;**66**:229–38.

Martens J-H, Barg H, Warren M *et al.* Microbial production of vitamin B_{12}. *Appl Microbiol Biotechnol* 2002;**58**:275–85.

Martens-Habbena W, Qin W, Horak REA *et al.* The production of nitric oxide by marine ammonia-oxidizing archaea and inhibition of archaeal ammonia oxidation by a nitric oxide scavenger. *Environ Microbiol* 2015;**17**:2261–74.

Martin M. Cutadapt removes adapter sequences from high-throughput sequencing reads. *EMBnet J* 2011;**17**:10–2.

Marusenko Y, Garcia-Pichel F, Hall SJ. Ammonia-oxidizing archaea respond positively to inorganic nitrogen addition in desert soils. *FEMS Microbiol Ecol* 2015;**91**:1-11.

Mas A, Jamshidi S, Lagadeuc Y *et al.* Beyond the black queen hypothesis. *ISME J* 2016;**10**:2085–91.

Masella A, Bartram A, Truszkowski J *et al.* PANDAseq: paired-end assembler for illumina sequences. *BMC Bioinformatics* 2012;**13**:31.

Matejek B, Huber C, Dannenmann M *et al.* Microbial nitrogen-turnover processes within the soil profile of a nitrogen-saturated spruce forest and their relation to the small-scale pattern of seepage-water nitrate. *J Plant Nutr Soil Sci* 2010;**173**:224–36.

McMurdie PJ, Holmes S. phyloseq: an R package for reproducible interactive analysis and graphics of microbiome census data. *PLoS ONE* 2013;**8**:e61217.

Meinhardt KA, Bertagnolli A, Pannu MW *et al.* Evaluation of revised polymerase chain reaction primers for more inclusive quantification of ammonia-oxidizing archaea and bacteria. *Environ Microbiol Rep* 2015;**7**:354–63.

Mellbye BL, Bottomley PJ, Sayavedra-Soto LA. Nitrite-oxidizing bacterium *Nitrobacter winogradskyi* produces *N*-acyl-homoserine lactone autoinducers. *Appl Environ Microbiol* 2015;**81**:5917–26.

Mellbye BL, Spieck E, Bottomley PJ *et al.* Acyl-homoserine lactone production in nitrifying bacteria of the genera *Nitrosospira*, *Nitrobacter*, and *Nitrospira* identified via a survey of putative quorum-sensing genes. *Appl Environ Microbiol* 2017;**83**:e01540-17.

Mendum T, Sockett R, Hirsch P. Use of molecular and isotopic techniques to monitor the response of autotrophic ammonia-oxidizing populations of the β subdivision of the class Proteobacteria in arable soils to nitrogen fertilizer. *Appl Environ Microbiol* 1999;**65**:4155–62.

Mills LS, Soulé ME, Doak DF. The keystone-species concept in ecology and conservation. *BioScience* 1993;**43**:219–24.

Miranda KM, Espey MG, Wink DA. A Rapid, simple spectrophotometric method for simultaneous detection of nitrate and nitrite. *Nitric Oxide* 2001;**5**:62–71.

Mogge B, Kaiser E-A, Munch J-C. Nitrous oxide emissions and denitrificationN-losses from forest soils in the Bornhöved Lake region (Northern Germany). *Soil Biol Biochem* 1998;**30**:703–10.

Mogge B, Kaiser E-A, Munch J-C. Nitrous oxide emissions and denitrification N-losses from agricultural soils in the Bornhöved Lake region: influence of organic fertilizers and land-use. *Soil Biol Biochem* 1999;**31**:1245–52.

Mørkved PT, Dörsch P, Bakken LR. The N_2O product ratio of nitrification and its dependence on long-term changes in soil pH. *Soil Biol Biochem* 2007;**39**:2048–57.

Mosier AC, Lund MB, Francis CA. Ecophysiology of an ammonia-oxidizing archaeon adapted to low-salinity habitats. *Microb Ecol* 2012;**64**:955–63.

Müller C, Laughlin RJ, Spott O *et al.* Quantification of N_2O emission pathways via a ^{15}N tracing model. *Soil Biol Biochem* 2014;**72**:44–54.

Müller C, Stevens R, Laughlin R. Sources of nitrite in a permanent grassland soil. *Eur J Soil Sci* 2006;**57**:337–43.

Nannipieri P, Ascher J, Ceccherini MT *et al.* Microbial diversity and soil functions. *Eur J Soil Sci* 2003;**54**:655–70.

Nelson DW. Gaseous losses of nitrogen other than through denitrification. *Nitrogen Agric Soils* 1982:327–63.

Nelson DW, Sommers LE. Total carbon, organic carbon, and organic matter. In: Pages AL (ed.). *Methods of Soil Analysis*: *Part 2—Chemical and Microbiological Properties*. Madison, WI: American Society of Agronomy, Inc., Soil Science Society of America, Inc., 1982, 549–52.

Nelson MB, Martiny AC, Martiny JBH. Global biogeography of microbial nitrogen-cycling traits in soil. *Proc Natl Acad Sci USA* 2016;**113**:8033–40.

Neufeld J, Engel K, Cheng J *et al.* Open resource metagenomics: a model for sharing metagenomic libraries. *Stand Genomic Sci* 2011;**5**:203.

Nicol GW, Leininger S, Schleper C *et al.* The influence of soil pH on the diversity, abundance and transcriptional activity of ammonia oxidizing archaea and bacteria. *Environ Microbiol* 2008;**10**:2966–2978.

Nicol GW, Tscherko D, Embley TM *et al.* Primary succession of soil *Crenarchaeota* across a receding glacier foreland. *Environ Microbiol* 2005;**7**:337–47.

Norton JM. Diversity and environmental distribution of ammonia-oxidizing bacteria. In: Ward BB. and Arp DJ. and Klotz MG.(ed). *Nitrification*. Washington, DC: American Society of Microbiology, Inc., 2011, 39-55.

Nowka B, Daims H, Spieck E. Comparison of oxidation kinetics of nitrite-oxidizing bacteria: nitrite availability as a key factor in niche differentiation. *Appl Environ Microbiol* 2015;**81**:745–53.

Nugroho RA, Röling WFM, van Straalen NM *et al.* Changes in nitrification and bacterial community structure upon cross-inoculation of Scots pine forest soils with different initial nitrification rates. *Soil Biol Biochem* 2009;**41**:243–50.

Obeid R, Fedosov SN, Nexo E. Cobalamin coenzyme forms are not likely to be superior to cyano- and hydroxyl- cobalamin in prevention or treatment of cobalamin deficiency. *Mol Nutr Food Res* 2015;**59**:1364–72.

Ochsenreiter T, Selezi D, Quaiser A *et al.* Diversity and abundance of Crenarchaeota in terrestrial habitats studied by 16S RNA surveys and real time PCR. *Environ Microbiol* 2003;**5**:787–97.

Offre P, Prosser JI, Nicol GW. Growth of ammonia-oxidizing archaea in soil microcosms is inhibited by acetylene. *FEMS Microbiol Ecol* 2009;**70**:99–108.

Okbamichael M, Sañudo-Wilhelmy SA. A new method for the determination of vitamin B_{12} in seawater. *Anal Chim Acta* 2004;**517**:33–8.

O'Leary NA, Wright MW, Brister JR *et al.* Reference sequence (RefSeq) database at NCBI: current status, taxonomic expansion, and functional annotation. *Nucleic Acids Res* 2016;**44**:D733–45.

Ortiz-Guerrero JM, Polanco MC, Murillo FJ *et al.* Light-dependent gene regulation by a coenzyme B_{12}-based photoreceptor. *Proc Natl Acad Sci USA* 2011;**108**:7565–70.

Ouyang Y, Norton JM, Stark JM *et al.* Ammonia-oxidizing bacteria are more responsive than archaea to nitrogen source in an agricultural soil. *Soil Biol Biochem* 2016;**96**:4–15.

Ouyang Y, Norton JM, Stark JM. Ammonium availability and temperature control contributions of ammonia oxidizing bacteria and archaea to nitrification in an agricultural soil. *Soil Biol Biochem* 2017;**113**:161–72.

Palatinszky M, Herbold C, Jehmlich N *et al.* Cyanate as an energy source for nitrifiers. *Nature* 2015;**524**:105–8.

Panzeca C, Tovar-Sanchez A, Agustí S *et al.* B vitamins as regulators of phytoplankton dynamics. *EOS Trans Am Geophys Union* 2006;**87**:593–6.

Peng X, Fuchsman CA, Jayakumar A *et al.* Revisiting nitrification in the Eastern Tropical South Pacific: A focus on controls. *J Geophys Res Oceans* 2016;**121**:1667–84.

Pesaro M, Widmer F. Identification of novel Crenarchaeota and Euryarchaeota clusters associated with different depth layers of a forest soil. *FEMS Microbiol Ecol* 2002;**42**:89–98.

Pester M, Bittner N, Deevong P *et al.* A 'rare biosphere' microorganism contributes to sulfate reduction in a peatland. *ISME J* 2010;**4**:1591–602.

Pester M, Maixner F, Berry D *et al. NxrB* encoding the beta subunit of nitrite oxidoreductase as functional and phylogenetic marker for nitrite-oxidizing *Nitrospira*. *Environ Microbiol* 2014;**16**:3055–71.

Pester M, Rattei T, Flechl S *et al. amoA*-based consensus phylogeny of ammonia-oxidizing archaea and deep sequencing of amoA genes from soils of four different geographic regions. *Environ Microbiol* 2012;**14**:525–39.

Petersen DG, Blazewicz SJ, Firestone M *et al.* Abundance of microbial genes associated with nitrogen cycling as indices of biogeochemical process rates across a vegetation gradient in Alaska. *Environ Microbiol* 2012;**14**:993–1008.

Petrenko P, Lobb B, Kurtz DA *et al.* MetAnnotate: function-specific taxonomic profiling and comparison of metagenomes. *BMC Biol* 2015;**13**:1–8.

Pinto AJ, Marcus DN, Ijaz UZ *et al.* Metagenomic evidence for the presence of comammox *Nitrospira*-like bacteria in a drinking water system. *mSphere* 2016;**1**:e00054-15.

Pjevac P, Schauberger C, Poghosyan L *et al. AmoA*-targeted polymerase chain reaction primers for the specific detection and quantification of comammox *Nitrospira* in the environment. *Front Microbiol* 2017;**8**:1508.

Poly F, Wertz S, Brothier E *et al.* First exploration of *Nitrobacter* diversity in soils by a PCR cloning-sequencing approach targeting functional gene *nxrA*. *FEMS Microbiol Ecol* 2008;**63**:132–40.

Presant EW. *The Soils of Waterloo County*. Research Branch, Canada Dept. of Agriculture, 1971.

Prosser JI. Autotrophic nitrification in bacteria. In: Rose AH, Tempest DW (ed.). *Advances in Microbial Physiology*. Volume 30. Academic Press, 1990, 125–81.

Prosser JI, Nicol GW. Relative contributions of archaea and bacteria to aerobic ammonia oxidation in the environment. *Environ Microbiol* 2008;**10**:2931–41.

Prosser JI, Nicol GW. Archaeal and bacterial ammonia oxidisers in soil: the quest for niche specialisation and differentiation. *Trends Microbiol* 2012;**20**:523–31.

Purkhold U, Pommerening-Röser A, Juretschko S *et al.* Phylogeny of all recognized species of ammonia oxidizers based on comparative 16S rRNA and *amoA* sequence analysis: implications for molecular diversity surveys. *Appl Environ Microbiol* 2000;**66**:5368–82.

Qin W, Heal KR, Ramdasi R *et al. Nitrosopumilus maritimus* gen. nov., sp. nov., *Nitrosopumilus cobalaminigenes* sp. nov., *Nitrosopumilus oxyclinae* sp. nov., and *Nitrosopumilus*

ureiphilus sp. nov., four marine ammonia-oxidizing archaea of the phylum *Thaumarchaeota*. *Int J Syst Evol Microbiol* 2017a;**67**:5067–79.

Qin W, Meinhardt KA, Moffett JW *et al.* Influence of oxygen availability on the activities of ammonia-oxidizing archaea. *Environ Microbiol Rep* 2017b;**9**:250–6.

Raun W, Johnson G. Improving nitrogen use efficiency for cereal production. *Agron J* 1999;**91**:357–63.

Raux E, Schubert HL, Roper JM *et al.* Vitamin B_{12}: Insights into biosynthesis's mount improbable. *Bioorganic Chem* 1999;**27**:100–18.

Ravishankara AR, Daniel JS, Portmann RW. Nitrous oxide (N_2O): the dominant ozone-depleting substance emitted in the 21st century. *Science* 2009;**326**:123–5.

Renz P. Biosynthesis of the 5, 6-dimethylbenzimidazole moiety of cobalamin and of the other bases found in natural corrinoids. *Chem Biochem B* 1999;**12**:557–75.

Richter DD, Markewitz D. How deep is soil? *BioScience* 1995;**45**:600–9.

Robertson GP, Groffman PM. Nitrogen transformations. In: Paul EA (ed.). *Soil Microbiology, Ecology and Biochemistry (Third Edition)*. San Diego: Academic Press, 2007, 341–64.

Rodionov DA, Vitreschak AG, Mironov AA *et al.* Comparative genomics of the vitamin B_{12} metabolism and regulation in prokaryotes. *J Biol Chem* 2003;**278**:41148–59.

Roesch LFW, Fulthorpe RR, Riva A *et al.* Pyrosequencing enumerates and contrasts soil microbial diversity. *ISME J* 2007;**1**:283–90.

Romine MF, Rodionov DA, Maezato Y *et al.* Elucidation of roles for vitamin B_{12} in regulation of folate, ubiquinone, and methionine metabolism. *Proc Natl Acad Sci USA* 2017;**114**:E1205–14.

Roth J, Lawrence J, Bobik T. Cobalamin (coenzyme B_{12}): synthesis and biological significance. *Annu Rev Microbiol* 1996;**50**:137–81.

Roth JR, Lawrence JG, Rubenfield M *et al.* Characterization of the cobalamin (vitamin B_{12}) biosynthetic genes of *Salmonella typhimurium*. *J Bacteriol* 1993;**175**:3303–16.

Rotthauwe JH, Witzel KP, Liesack W. The ammonia monooxygenase structural gene *amoA* as a functional marker: molecular fine-scale analysis of natural ammonia-oxidizing populations. *Appl Environ Microbiol* 1997;**63**:4704–12.

Santoro AE, Buchwald C, McIlvin MR *et al.* Isotopic signature of N_2O produced by marine ammonia-oxidizing archaea. *Science* 2011;**333**:1282–5.

Sañudo-Wilhelmy SA, Gómez-Consarnau L, Suffridge C *et al.* The role of B vitamins in marine biogeochemistry. *Annu Rev Mar Sci* 2014;**6**:339–67.

Sauder LA, Albertsen M, Engel K *et al.* Cultivation and characterization of *Candidatus* Nitrosocosmicus exaquare, an ammonia-oxidizing archaeon from a municipal wastewater treatment system. *ISME J* 2017;**11**:1142–57.

Sauder LA, Ross AA, Neufeld JD. Nitric oxide scavengers differentially inhibit ammonia oxidation in ammonia-oxidizing archaea and bacteria. *FEMS Microbiol Lett* 2016;**363**:fnw052.

Schleper C. Ammonia oxidation: different niches for bacteria and archaea? *ISME J* 2010;**4**:1092–4.

Schleper C, Holben W, Klenk HP. Recovery of crenarchaeotal ribosomal DNA sequences from freshwater-lake sediments. *Appl Environ Microbiol* 1997;**63**:321–3.

Schleper C, Jurgens G, Jonuscheit M. Genomic studies of uncultivated archaea. *Nat Rev Microbiol* 2005;**3**:479–88.

Schlesinger WH. On the fate of anthropogenic nitrogen. *Proc Natl Acad Sci USA* 2008;**106**:203-8.

Schmidt CS, Hultman KA, Robinson D *et al.* PCR profiling of ammonia-oxidizer communities in acidic soils subjected to nitrogen and sulphur deposition. *FEMS Microbiol Ecol* 2007;**61**:305–16.

Schmidt I, Steenbakkers PJ, op den Camp HJ *et al.* Physiologic and proteomic evidence for a role of nitric oxide in biofilm formation by *Nitrosomonas europaea* and other ammonia oxidizers. *J Bacteriol* 2004;**186**:2781–8.

Schmidt S, Nemergut D, Miller A *et al.* Microbial activity and diversity during extreme freeze–thaw cycles in periglacial soils, 5400 m elevation, Cordillera Vilcanota, Perú. *Extremophiles* 2009;**13**:807–16.

Schreiber F, Wunderlin P, Udert K *et al.* Nitric oxide and nitrous oxide turnover in natural and engineered microbial communities: biological pathways, chemical reactions, and novel technologies. *Front Microbiol* 2012;**3**:372.

Seth EC, Taga ME. Nutrient cross-feeding in the microbial world. *Front Microbiol* 2014;**5**:350.

Seuradge BJ, Oelbermann M, Neufeld JD. Depth-dependent influence of different land-use systems on bacterial biogeography. *FEMS Microbiol Ecol* 2017;**93**:fiw239.

Shaw LJ, Nicol GW, Smith Z *et al. Nitrosospira spp*. can produce nitrous oxide via a nitrifier denitrification pathway. *Environ Microbiol* 2006;**8**:214–22.

Shen J, Zhang L, Zhu Y *et al.* Abundance and composition of ammonia- oxidizing bacteria and ammonia- oxidizing archaea communities of an alkaline sandy loam. *Environ Microbiol* 2008;**10**:1601–11.

Shen Q, Ran W, Cao Z. Mechanisms of nitrite accumulation occurring in soil nitrification. *Chemosphere* 2003;**50**:747–53.

Shen T, Stieglmeier M, Dai J *et al.* Responses of the terrestrial ammonia-oxidizing archaeon *Ca*. Nitrososphaera viennensis and the ammonia-oxidizing bacterium *Nitrosospira multiformis* to nitrification inhibitors. *FEMS Microbiol Lett* 2013;**344**:121–9.

Shi X, Hu H-W, Zhu-Barker X *et al.* Nitrifier-induced denitrification is an important source of soil nitrous oxide and can be inhibited by a nitrification inhibitor 3,4-dimethylpyrazole phosphate. *Environ Microbiol* 2017;**19**:4851–65.

Sigunga D, Janssen B, Oenema O. Ammonia volatilization from Vertisols. *Eur J Soil Sci* 2002;**53**:195–202.

Slemr F, Conrad R, Seiler W. Nitrous oxide emissions from fertilized and unfertilized soils in a subtropical region (Andalusia, Spain). *J Atmospheric Chem* 1984;**1**:159–69.

Smith C, Chalk P. Gaseous nitrogen evolution during nitrification of ammonia fertilizer and nitrite transformations in soils. *Soil Sci Soc Am J* 1980;**44**:277–82.

Smith Z, McCaig AE, Stephen JR *et al.* Species diversity of uncultured and cultured populations of soil and marine ammonia oxidizing bacteria. *Microb Ecol* 2001;**42**:228–37.

Spang A, Hatzenpichler R, Brochier-Armanet C *et al.* Distinct gene set in two different lineages of ammonia-oxidizing archaea supports the phylum Thaumarchaeota. *Trends Microbiol* 2010;**18**:331–40.

Spieck E, Bock E. The lithoautotrophic nitrite-oxidizing bacteria. In: Garrity G, Brenner DJ, Krieg NR, Staley JR (ed.). *Bergey's Manual of Systematic Bacteriology*. Springer, 2005, 149–53.

Spott O, Russow R, Stange CF. Formation of hybrid N_2O and hybrid N_2 due to codenitrification: First review of a barely considered process of microbially mediated N-nitrosation. *Soil Biol Biochem* 2011;**43**:1995–2011.

Starkenburg SR, Arp DJ, Bottomley PJ. Expression of a putative nitrite reductase and the reversible inhibition of nitrite- dependent respiration by nitric oxide in *Nitrobacter winogradskyi* Nb- 255. *Environ Microbiol* 2008;**10**:3036–42.

Starkenburg SR, Chain PS, Sayavedra-Soto LA *et al.* Genome sequence of the chemolithoautotrophic nitrite-oxidizing bacterium *Nitrobacter winogradskyi* Nb-255. *Appl Environ Microbiol* 2006;**72**:2050–63.

Stein LY. Surveying N_2O-producing pathways in bacteria. In: Klotz MG (ed.). *Methods in Enzymology*. Volume 486. Academic Press, 2011a, 131–52.

Stein LY. Heterotrophic nitrification and nitrifier denitrification. In: Ward BB, Arp DJ, Klotz MG (ed.). *Nitrification*. American Society of Microbiology, 2011b, 95–114.

Stein LY, Arp DJ. Loss of ammonia monooxygenase activity in *Nitrosomonas europaea* upon exposure to nitrite. *Appl Environ Microbiol* 1998;**64**:4098–102.

Stempfhuber B, Richter-Heitmann T, Regan KM *et al.* Spatial interaction of archaeal ammonia-oxidizers and nitrite-oxidizing bacteria in an unfertilized grassland soil. *Front Microbiol* 2016;**6**:1567.

Stephen JR, Kowalchuk GA, Bruns M-AV *et al.* Analysis of β-subgroup proteobacterial ammonia oxidizer populations in soil by denaturing gradient gel electrophoresis analysis and hierarchical phylogenetic probing. *Appl Environ Microbiol* 1998;**64**:2958–65.

Stephen JR, McCaig AE, Smith Z *et al.* Molecular diversity of soil and marine 16S rRNA gene sequences related to beta-subgroup ammonia-oxidizing bacteria. *Appl Environ Microbiol* 1996;**62**:4147–54.

Stieglmeier M, Klingl A, Alves RJE *et al. Nitrososphaera viennensis* gen. nov., sp. nov., an aerobic and mesophilic, ammonia-oxidizing archaeon from soil and a member of the archaeal phylum Thaumarchaeota. *Int J Syst Evol Microbiol* 2014a;**64**:2738–52.

Stieglmeier M, Mooshammer M, Kitzler B *et al.* Aerobic nitrous oxide production through N-nitrosating hybrid formation in ammonia-oxidizing archaea. *ISME J* 2014b;**8**:1135–46.

Stopnišek N, Gubry-Rangin C, Höfferle Š *et al.* Thaumarchaeal ammonia oxidation in an acidic forest peat soil is not influenced by ammonium amendment. *Appl Environ Microbiol* 2010;**76**:7626–34.

Stres B, Danevčič T, Pal L *et al.* Influence of temperature and soil water content on bacterial, archaeal and denitrifying microbial communities in drained fen grassland soil microcosms. *FEMS Microbiol Ecol* 2008;**66**:110–22.

Stubbe J. Binding site revealed of nature's most beautiful cofactor. *Science* 1994;**266**:1663–4.

Subbarao GV, Ito O, Sahrawat KL *et al.* Scope and strategies for regulation of nitrification in agricultural systems—challenges and opportunities. *Crit Rev Plant Sci* 2006;**25**:303–35.

Suffridge C, Cutter L, Sañudo-Wilhelmy SA. A new analytical method for direct measurement of particulate and dissolved B-vitamins and their congeners in seawater. *Front Mar Sci* 2017;**4**:11.

Sundermeyer-Klinger H, Meyer W, Warninghoff B *et al.* Membrane-bound nitrite oxidoreductase of *Nitrobacter*: evidence for a nitrate reductase system. *Arch Microbiol* 1984;**140**:153–8.

Suzuki I, Dular U, Kwok SC. Ammonia or ammonium ion as substrate for oxidation by *Nitrosomonas europaea* cells and extracts. *J Bacteriol* 1974;**120**:556–8.

Syakila A, Kroeze C. The global nitrous oxide budget revisited. *Greenhouse Gas Measurement Management* 2011;**1**:17–26.

Szukics U, Abell GCJ, Hödl V *et al.* Nitrifiers and denitrifiers respond rapidly to changed moisture and increasing temperature in a pristine forest soil. *FEMS Microbiol Ecol* 2010;**72**:395–406.

Tang YZ, Koch F, Gobler CJ. Most harmful algal bloom species are vitamin B_1 and B_{12} auxotrophs. *Proc Natl Acad Sci USA* 2010;**107**:20756–61.

Taylor AE, Giguere AT, Zoebelein CM *et al.* Modeling of soil nitrification responses to temperature reveals thermodynamic differences between ammonia-oxidizing activity of archaea and bacteria. *ISME J* 2017;**11**:896–908.

Taylor AE, Taylor K, Tennigkeit B *et al.* Inhibitory effects of C2 to C10 1-alkynes on ammonia oxidation in two *Nitrososphaera* species. *Appl Environ Microbiol* 2015;**81**:1942–8.

Taylor AE, Vajrala N, Giguere AT *et al.* Use of aliphatic n-alkynes to discriminate soil nitrification activities of ammonia-oxidizing thaumarchaea and bacteria. *Appl Environ Microbiol* 2013;**79**:6544–51.

Taylor AE, Zeglin LH, Dooley S *et al.* Evidence for different contributions of archaea and bacteria to the ammonia-oxidizing potential of diverse Oregon soils. *Appl Environ Microbiol* 2010;**76**:7691–8.

Taylor AE, Zeglin LH, Wanzek TA *et al.* Dynamics of ammonia-oxidizing archaea and bacteria populations and contributions to soil nitrification potentials. *ISME J* 2012;**6**:2024–32.

Thompson KA, Bent E, Abalos D *et al.* Soil microbial communities as potential regulators of in situ N_2O fluxes in annual and perennial cropping systems. *Soil Biol Biochem* 2016;**103**:262–73.

Tiedje JM, Asuming-Brempong S, Nüsslein K *et al.* Opening the black box of soil microbial diversity. *Appl Soil Ecol* 1999;**13**:109–22.

Tourna M, Freitag TE, Nicol GW *et al.* Growth, activity and temperature responses of ammonia-oxidizing archaea and bacteria in soil microcosms. *Environ Microbiol* 2008;**10**:1357–64.

Tourna M, Stieglmeier M, Spang A *et al. Nitrososphaera viennensis*, an ammonia oxidizing archaeon from soil. *Proc Natl Acad Sci USA* 2011;**108**:8420–5.

Treusch AH, Leininger S, Kletzin A *et al.* Novel genes for nitrite reductase and Amo-related proteins indicate a role of uncultivated mesophilic crenarchaeota in nitrogen cycling. *Environ Microbiol* 2005;**7**:1985–95.

Treves DS, Xia B, Zhou J *et al.* A two-species test of the hypothesis that spatial isolation influences microbial diversity in soil. *Microb Ecol* 2003;**45**:20–8.

Tringe SG, Von Mering C, Kobayashi A *et al.* Comparative metagenomics of microbial communities. *Science* 2005;**308**:554–7.

Tripathi BM, Kim M, Tateno R *et al.* Soil pH and biome are both key determinants of soil archaeal community structure. *Soil Biol Biochem* 2015;**88**:1–8.

Ueda T, Suga Y, Matsuguchi T. Molecular phylogenetic analysis of a soil microbial community in a soybean field. *Eur J Soil Sci* 1995;**46**:415–21.

Vajrala N, Martens-Habbena W, Sayavedra-Soto LA *et al.* Hydroxylamine as an intermediate in ammonia oxidation by globally abundant marine archaea. *Proc Natl Acad Sci USA* 2013;**110**:1006–11.

Van Cleemput O, Samater AH. Nitrite in soils: accumulation and role in the formation of gaseous N compounds. *Fertil Res* 1995;**45**:81–9.

Venter JC, Remington K, Heidelberg JF *et al.* Environmental genome shotgun sequencing of the Sargasso Sea. *Science* 2004;**304**:66–74.

Venterea RT. Nitrite-driven nitrous oxide production under aerobic soil conditions: kinetics and biochemical controls. *Glob Change Biol* 2007;**13**:1798–809.

Venterea RT, Clough TJ, Coulter JA *et al.* Ammonium sorption and ammonia inhibition of nitrite-oxidizing bacteria explain contrasting soil N_2O production. *Sci Rep* 2015;**5**:12153.

Verhamme DT, Prosser JI, Nicol GW. Ammonia concentration determines differential growth of ammonia-oxidising archaea and bacteria in soil microcosms. *ISME J* 2011;**5**:1067–71.

Vieten B, Conen F, Seth B *et al.* The fate of N_2O consumed in soils. *Biogeosciences* 2008;**5**:129–32.

Walker CB, De La Torre JR, Klotz MG *et al. Nitrosopumilus maritimus* genome reveals unique mechanisms for nitrification and autotrophy in globally distributed marine crenarchaea. *Proc Natl Acad Sci USA* 2010;**107**:8818–23.

Walworth NG, Lee MD, Suffridge C *et al.* Functional genomics and phylogenetic evidence suggest genus-wide cobalamin production by the globally distributed marine nitrogen fixer *Trichodesmium*. *Front Microbiol* 2018;**9**:189.

Wang Q, Garrity GM, Tiedje JM *et al.* Naïve Bayesian classifier for rapid assignment of rRNA sequences into the new bacterial taxonomy. *Appl Environ Microbiol* 2007;**73**:5261–7.

Wang Q, Zhang L-M, Shen J-P *et al.* Nitrogen fertiliser-induced changes in N_2O emissions are attributed more to ammonia-oxidising bacteria rather than archaea as revealed using 1-octyne and acetylene inhibitors in two arable soils. *Biol Fertil Soils* 2016;**52**:1163–71.

Ward BB, Jensen MM. The microbial nitrogen cycle. *Front Microbiol* 2014;**5**:553.

Warren MJ, Raux E, Schubert HL *et al.* The biosynthesis of adenosylcobalamin (vitamin B_{12}). *Nat Prod Rep* 2002;**19**:390–412.

Watanabe T, Wang G, Taki K *et al.* Vertical changes in bacterial and archaeal communities with soil depth in Japanese paddy fields. *Soil Sci Plant Nutr* 2010;**56**:705–15.

Watson E, MacNeil LT, Ritter AD *et al.* Interspecies systems biology uncovers metabolites affecting *C. elegans* gene expression and life history traits. *Cell* 2014;**156**:759–70.

Watson SW. Characteristics of a marine nitrifying bacterium, *Nitrosocystis oceanus* sp. n. *Limnol Oceanogr* 1965;**10**.

Weber EB, Lehtovirta-Morley LE, Prosser JI *et al.* Ammonia oxidation is not required for growth of Group 1.1c soil *Thaumarchaeota*. *FEMS Microbiol Ecol* 2015;**91**:274–89.

Wertz S, Leigh AK, Grayston SJ. Effects of long-term fertilization of forest soils on potential nitrification and on the abundance and community structure of ammonia oxidizers and nitrite oxidizers. *FEMS Microbiol Ecol* 2012;**79**:142–54.

Wertz S, Poly F, Le Roux X *et al.* Development and application of a PCR-denaturing gradient gel electrophoresis tool to study the diversity of *Nitrobacter*-like *nxrA* sequences in soil. *FEMS Microbiol Ecol* 2008;**63**:261–71.

Whitman WB, Coleman DC, Wiebe WJ. Prokaryotes: The unseen majority. *Proc Natl Acad Sci USA* 1998;**95**:6578–83.

Winkler MKH, Bassin JP, Kleerebezem R *et al.* Unravelling the reasons for disproportion in the ratio of AOB and NOB in aerobic granular sludge. *Appl Microbiol Biotechnol* 2012;**94**:1657–66.

Winogradsky, S. Contributions a la morphologie des organismes de la nitrification. *Arch Sci Biol* 1892;**1**:86-137.

Woese CR, Weisburg WG, Hahn CM *et al.* The phylogeny of purple bacteria: The gamma subdivision. *Syst Appl Microbiol* 1985;**6**:25–33.

Woese CR, Weisburg WG, Paster BJ *et al.* The phylogeny of purple bacteria: The beta subdivision. *Syst Appl Microbiol* 1984;**5**:327–36.

Wrage N, Velthof G., van Beusichem M. *et al.* Role of nitrifier denitrification in the production of nitrous oxide. *Soil Biol Biochem* 2001;**33**:1723–32.

Wu Y, Ke X, Hernández M *et al.* Autotrophic growth of bacterial and archaeal ammonia oxidizers in freshwater sediment microcosms incubated at different temperatures. *Appl Environ Microbiol* 2013;**79**:3076-84.

Wuchter C, Abbas B, Coolen MJL *et al.* Archaeal nitrification in the ocean. *Proc Natl Acad Sci USA* 2006;**103**:12317–22.

Xia W, Zhang C, Zeng X *et al.* Autotrophic growth of nitrifying community in an agricultural soil. *ISME J* 2011;**5**:1226–36.

Yao H, Campbell CD, Chapman SJ *et al.* Multi-factorial drivers of ammonia oxidizer communities: evidence from a national soil survey. *Environ Microbiol* 2013;**15**:2545–2556.

Zeglin LH, Taylor AE, Myrold DD *et al.* Bacterial and archaeal *amoA* gene distribution covaries with soil nitrification properties across a range of land uses. *Environ Microbiol Rep* 2011a;**3**:717–26.

Zhang CL, Ye Q, Huang Z *et al.* Global occurrence of archaeal *amoA* genes in terrestrial hot springs. *Appl Environ Microbiol* 2008;**74**:6417–26.

Zhang L-M, Hu H-W, Shen J-P *et al.* Ammonia-oxidizing archaea have more important role than ammonia-oxidizing bacteria in ammonia oxidation of strongly acidic soils. *ISME J* 2012;**6**:1032–45.

Zhang Y, Rodionov DA, Gelfand MS *et al.* Comparative genomic analyses of nickel, cobalt and vitamin B_{12} utilization. *BMC Genomics* 2009;**10**:78.

Zhong W, Bian B, Gao N *et al.* Nitrogen fertilization induced changes in ammonia oxidation are attributable mostly to bacteria rather than archaea in greenhouse-based high N input vegetable soil. *Soil Biol Biochem* 2016;**93**:150–9.

Zhu X, Burger M, Doane TA *et al.* Ammonia oxidation pathways and nitrifier denitrification are significant sources of N_2O and NO under low oxygen availability. *Proc Natl Acad Sci USA* 2013;**110**:6328–33.

Appendix A

All 155 soil metagenomes used in this study. Sample accession number and soil type are included.

Sample	Biome	Source
4477873	Desert	MG-RAST
4477900	Cold Desert	MG-RAST
4492602	Desert	MG-RAST
4497370	Agriculture	MG-RAST
4497385	Forest	MG-RAST
4508942	Forest	MG-RAST
4509398	Agriculture	MG-RAST
4510219	Wetland	MG-RAST
4511180	Grassland	MG-RAST
4539063	Grassland	MG-RAST
4539575	Grassland	MG-RAST
4539580	Grassland	MG-RAST
4539582	Grassland	MG-RAST
4539593	Grassland	MG-RAST
4541647	Grassland	MG-RAST
4541649	Grassland	MG-RAST
4541650	Grassland	MG-RAST
4543021	Desert	MG-RAST
4547279	Agriculture	MG-RAST
4554764	Pasture	MG-RAST
4554769	Pasture	MG-RAST
4554770	Pasture	MG-RAST
4554771	Pasture	MG-RAST
4573680	Lawn	MG-RAST
4573682	Lawn	MG-RAST
4578924	Grassland	MG-RAST
4582238	Forest	MG-RAST
4582244	Forest	MG-RAST
4582254	Forest	MG-RAST
4582263	Forest	MG-RAST
4582273	Forest	MG-RAST
4582275	Forest	MG-RAST
4582277	Forest	MG-RAST
4582792	Forest	MG-RAST
4582796	Forest	MG-RAST

4582799	Forest	MG-RAST
4582800	Forest	MG-RAST
4597444	Agriculture	MG-RAST
4623639	Grassland	MG-RAST
4626747	Agriculture	MG-RAST
4631724	Agriculture	MG-RAST
4635904	Lawn	MG-RAST
4654023	Grassland	MG-RAST
4667212	Agriculture	MG-RAST
4667213	Agriculture	MG-RAST
4637810	Grassland	MG-RAST
4637811	Grassland	MG-RAST
4637814	Grassland	MG-RAST
4637816	Grassland	MG-RAST
4637818	Grassland	MG-RAST
4637819	Grassland	MG-RAST
4637820	Grassland	MG-RAST
4637821	Grassland	MG-RAST
4637822	Grassland	MG-RAST
4637825	Grassland	MG-RAST
4637826	Grassland	MG-RAST
4637828	Grassland	MG-RAST
4637829	Grassland	MG-RAST
4637830	Grassland	MG-RAST
4637832	Grassland	MG-RAST
4637833	Grassland	MG-RAST
4637834	Grassland	MG-RAST
4637838	Pasture	MG-RAST
4637840	Pasture	MG-RAST
4637841	Pasture	MG-RAST
4637842	Pasture	MG-RAST
4637843	Pasture	MG-RAST
4637844	Pasture	MG-RAST
4637845	Pasture	MG-RAST
4637847	Pasture	MG-RAST
4637848	Pasture	MG-RAST
4637849	Pasture	MG-RAST
4637850	Forest	MG-RAST
4637852	Forest	MG-RAST
4637853	Forest	MG-RAST
4637855	Forest	MG-RAST
4637857	Grassland	MG-RAST
4637859	Grassland	MG-RAST

4637860	Grassland	MG-RAST
4637861	Grassland	MG-RAST
4637862	Grassland	MG-RAST
4637864	Grassland	MG-RAST
4637866	Grassland	MG-RAST
4637868	Grassland	MG-RAST
4664851	Forest	MG-RAST
4664852	Forest	MG-RAST
4664853	Forest	MG-RAST
4664854	Forest	MG-RAST
4664855	Grassland	MG-RAST
4664856	Forest	MG-RAST
4664857	Forest	MG-RAST
4664860	Forest	MG-RAST
4664862	Forest	MG-RAST
4664863	Forest	MG-RAST
4664864	Forest	MG-RAST
4664865	Pasture	MG-RAST
4664867	Pasture	MG-RAST
4664868	Forest	MG-RAST
4664869	Forest	MG-RAST
4664870	Pasture	MG-RAST
4664871	Grassland	MG-RAST
4664874	Forest	MG-RAST
4664875	Grassland	MG-RAST
4664876	Forest	MG-RAST
4664877	Forest	MG-RAST
4664878	Grassland	MG-RAST
4664880	Grassland	MG-RAST
4664881	Forest	MG-RAST
4664884	Forest	MG-RAST
4664885	Grassland	MG-RAST
4664889	Grassland	MG-RAST
4664890	Grassland	MG-RAST
4664891	Grassland	MG-RAST
4664892	Forest	MG-RAST
4664893	Forest	MG-RAST
4664895	Forest	MG-RAST
4664896	Forest	MG-RAST
4664898	Grassland	MG-RAST
4664899	Grassland	MG-RAST
4664900	Forest	MG-RAST
4664901	Grassland	MG-RAST

4664905	Forest	MG-RAST
4664907	Pasture	MG-RAST
4664908	Wetland	MG-RAST
4664909	Forest	MG-RAST
4664910	Pasture	MG-RAST
4664911	Forest	MG-RAST
4664912	Pasture	MG-RAST
4664913	Forest	MG-RAST
4664915	Pasture	MG-RAST
4664916	Forest	MG-RAST
4664919	Wetland	MG-RAST
4664922	Pasture	MG-RAST
4664924	Grassland	MG-RAST
4664925	Pasture	MG-RAST
4664926	Pasture	MG-RAST
4664927	Grassland	MG-RAST
4664930	Forest	MG-RAST
4664931	Grassland	MG-RAST
AND11f	Forest	LTER (courtesy of Noah Fierer)
AND11h	Herb	LTER (courtesy of Noah Fierer)
BNZ11f	Forest	LTER (courtesy of Noah Fierer)
BNZ11h	Herb	LTER (courtesy of Noah Fierer)
CDR11f	Forest	LTER (courtesy of Noah Fierer)
CDR11h	Herb	LTER (courtesy of Noah Fierer)
CWT11f	Forest	LTER (courtesy of Noah Fierer)
CWT11h	Herb	LTER (courtesy of Noah Fierer)
HBR11f	Forest	LTER (courtesy of Noah Fierer)
HFR11f	Forest	LTER (courtesy of Noah Fierer)
HFR11h	Herb	LTER (courtesy of Noah Fierer)
KBS11h	Herb	LTER (courtesy of Noah Fierer)
KNZ11f	Forest	LTER (courtesy of Noah Fierer)
KNZ11h	Herb	LTER (courtesy of Noah Fierer)
LUQ11f	Forest	LTER (courtesy of Noah Fierer)
NWT11h	Herb	LTER (courtesy of Noah Fierer)

Appendix B

Presence/absence of Groups A, B, and C *cob*/*cbi* genes at genus level for 155 soil metagenomes. Complete cobalamin pathway genera were selected when all of the 12 *cob*/*cbi* genes were present within the same taxa in the same soil metagenome, and annotated with "Y". Otherwise, "N" means absence of the group gene for that genus. Group A is corrin ring biosynthesis, Group B is final synthesis and repair, and Group C is 5,6-dimethylbenzimidazole (DMB) synthesis. The genera with three *cob*/*cbi* gene groups are highlighted if they are also the known cobalamin producing species in Perlman (1959).

Genus	Group A	Group B	Group C	Complete cobalamin pathway in the same metagenome
[Clostridium] ultunense	N	N	Y	
Acetobacter	N	Y	Y	
Acetobacteraceae bacterium AT-5844	N	N	Y	
Acetomicrobium	N	N	Y	
Acidianus	N	N	Y	
Acidibacillus	N	N	Y	
Acidimicrobium	N	N	Y	
Acidiphilium	N	N	Y	
Acidisphaera	N	N	Y	
Acidobacteriaceae bacterium KBS 83	N	N	Y	
Acidobacteriaceae bacterium KBS 89	N	N	Y	
Acidobacteriaceae bacterium TAA166	N	N	Y	
Acidobacteriaceae bacterium URHE0068	N	Y	N	
Acidobacterium	N	N	Y	
Acidocella	N	N	Y	
Acidovorax	N	N	Y	
Actibacterium	N	N	Y	
Actinobacteria bacterium IMCC26207	N	N	Y	
Actinobacteria bacterium IMCC26256	N	N	Y	
Actinobacteria bacterium OK006	N	N	Y	
actinobacterium LLX17	N	N	Y	
Actinocatenispora	N	N	Y	
Actinokineospora	N	N	Y	
Actinomadura	Y	Y	Y	
Actinomycetospora	N	N	Y	
Actinophytocola	N	N	Y	
Actinoplanes	Y	Y	Y	
Actinopolymorpha	N	N	Y	
Actinopolyspora	N	N	Y	
Actinospica	N	N	Y	
Actinosynnema	N	N	Y	

Actinotalea	N	N	Y
Acuticoccus	N	N	Y
Aeromicrobium	N	N	Y
Aestuariimicrobium	N	N	Y
Afipia	N	N	Y
Agarivorans	N	N	Y
Agrobacterium	N	N	Y
Agromyces	N	N	Y
Ahrensia	N	N	Y
Alcanivorax	N	N	Y
Algiphilus	N	N	Y
Algoriphagus	N	N	Y
Alicyclobacillus	N	N	Y
Aliihoeflea	N	N	Y
Aliiroseovarius	N	N	Y
Alloactinosynnema	N	N	Y
Allokutzneria	N	N	Y
alpha proteobacterium AAP81b	N	N	Y
alpha proteobacterium BAL199	N	N	Y
alpha proteobacterium Mf 1.05b.01	N	N	Y
Alteromonas	N	N	Y
Aminiphilus	N	N	Y
Aminobacter	N	N	Y
Aminomonas	N	N	Y
Ammonifex	N	N	Y
Amycolatopsis	N	Y	Y
Anaerolinea	N	N	Y
Anaerosphaera	N	N	Y
Ancylobacter	N	N	Y
Andreprevotia	N	N	Y
Aneurinibacillus	N	N	Y
Aquimarina	N	N	Y
Archangium	N	N	Y
Arcobacter	N	N	Y
Ardenticatena	N	N	Y
Arenimonas	N	N	Y
Arhodomonas	N	N	Y
Aromatoleum	N	N	Y
Arsenicicoccus	N	N	Y
Asaia	N	N	Y
Asinibacterium	N	N	Y

Aureimonas	Y	Y	Y		
Austwickia	N	N	Y		
Azoarcus	N	N	Y		
Azohydromonas	N	N	Y		
Azonexus	N	N	Y		
Azorhizobium	N	N	Y		
Azospira	N	N	Y		
Azospirillum	N	Y	Y		
Azotobacter	N	N	Y		
Azovibrio	N	N	Y		
Bacillus	Y	Y	Y		Y
bacterium JKG1	N	N	Y		
bacterium L21-Spi-D4	N	N	Y		
Balneola	N	N	Y		
Barnesiella	N	N	Y		
Bdellovibrio	N	N	Y		
Beijerinckia	N	N	Y		
Belnapia	Y	N	Y		
beta proteobacterium AAP51	N	N	Y		
Blastochloris	N	N	Y		
Blastococcus	N	N	Y		
Blastomonas	N	N	Y		
Bordetella	N	N	Y		
Bosea	Y	Y	Y		Y
Bradyrhizobium	Y	Y	Y		Y
Brevibacillus	N	N	Y		
Bryobacter	N	N	Y		
Burkholderia	Y	Y	Y		
Burkholderiales bacterium GJ-E10	N	N	Y		
Caballeronia	Y	N	Y		
Caenispirillum	N	N	Y		
Caldanaerobacter	N	N	Y		
Caldanaerobius	N	N	Y		
Caldanaerovirga	N	N	Y		
Caldicoprobacter	N	N	Y		
Caldilinea	N	N	Y		
Caloramator	N	N	Y		
Candidatus Brocadia	N	N	Y		
Candidatus Competibacter	N	N	Y		
Candidatus Contendobacter	N	N	Y		
Candidatus Desulforudis	N	N	Y		

Candidatus Glomeribacter	N	N	Y	
Candidatus Jettenia	N	N	Y	
Candidatus Korarchaeum	N	N	Y	
Candidatus Marispirochaeta	N	N	Y	
Candidatus Methanoperedens	N	N	Y	
Candidatus Microthrix	N	N	Y	
Candidatus Nitrosoarchaeum	N	N	Y	
Candidatus Nitrosopelagicus	N	N	Y	
Candidatus Nitrosotenuis	N	N	Y	
Carboxydothermus	N	N	Y	
Catelliglobosispora	N	N	Y	
Catenulispora	N	N	Y	
Caulobacter	N	Y	Y	
Caulobacteraceae bacterium OTSz_A_272	N	N	Y	
Celeribacter	N	N	Y	
Cellulosimicrobium	N	N	Y	
Chelatococcus	N	N	Y	
Chloracidobacterium	N	N	Y	
Chlorobaculum	N	N	Y	
Chlorobium	N	N	Y	
Chloroflexus	N	N	Y	
Chloroherpeton	N	N	Y	
Chromobacterium	N	N	Y	
Chthonomonas	N	N	Y	
Clostridiales bacterium DRI-13	N	N	Y	
Clostridiales bacterium VE202-09	N	N	Y	
Clostridioides	N	N	Y	
Clostridium	Y	Y	Y	Y
Comamonadaceae bacterium CCH4-C5	N	N	Y	
Comamonas	N	N	Y	
Commensalibacter	N	N	Y	
Corynebacterium	N	N	Y	
Couchioplanes	N	N	Y	
Cupriavidus	N	N	Y	
Curvibacter	N	N	Y	
Cutibacterium	N	N	Y	
Cyanothece	Y	N	N	
Cylindrospermum	N	N	Y	
Cystobacter	N	N	Y	
Dactylosporangium	N	N	Y	
Dasania	N	N	Y	

Dechloromonas	N	N	Y	
Deefgea	N	N	Y	
Deferrisoma	N	N	Y	
Defluviimonas	N	N	Y	
Dehalococcoides	N	Y	N	
Dehalogenimonas	N	Y	Y	
Deinococcus	N	Y	Y	
Delftia	N	N	Y	
delta proteobacterium NaphS2	Y	Y	Y	Y
Dermacoccus	N	N	Y	
Desulfarculus	Y	N	N	
Desulfatibacillum	Y	Y	Y	
Desulfatiglans	N	N	Y	
Desulfatirhabdium	Y	Y	N	
Desulfatitalea	N	N	Y	
Desulfitobacterium	N	N	Y	
Desulfobacca	Y	N	N	
Desulfobacter	N	Y	N	
Desulfobacterium	Y	N	Y	
Desulfobacula	Y	Y	Y	
Desulfobulbus	Y	N	Y	
Desulfocapsa	Y	N	N	
Desulfocarbo	Y	N	Y	
Desulfococcus	Y	Y	Y	
Desulfocurvus	N	N	Y	
Desulfofustis	Y	N	Y	
Desulfomicrobium	N	N	Y	
Desulfomonile	Y	Y	N	
Desulfonatronospira	N	N	Y	
Desulfonatronovibrio	N	N	Y	
Desulfonatronum	N	N	Y	
Desulfopila	Y	Y	Y	
Desulfosarcina	Y	Y	Y	
Desulfospira	N	N	Y	
Desulfosporosinus	N	Y	Y	
Desulfotignum	Y	N	Y	
Desulfotomaculum	Y	N	Y	
Desulfovermiculus	N	N	Y	
Desulfovibrio	Y	N	Y	
Desulfovirgula	N	N	Y	
Desulfuribacillus	N	N	Y	

Desulfurivibrio	Y	N	N
Desulfurococcus	N	N	Y
Desulfuromonas	Y	Y	Y
Dethiobacter	N	N	Y
Dethiosulfatarculus	N	N	Y
Devosia	Y	Y	Y
Dialister	N	N	Y
Dictyoglomus	N	N	Y
Dietzia	N	N	Y
Dinoroseobacter	N	N	Y
Domibacillus	N	N	Y
Donghicola	N	N	Y
Dongia	N	Y	Y
Draconibacterium	N	Y	Y
Duganella	N	N	Y
Dyella	N	Y	Y
Ectothiorhodospira	N	N	Y
Edaphobacter	Y	Y	Y
Effusibacillus	N	N	Y
Eggerthellaceae bacterium AT8	N	N	Y
Elusimicrobium	N	N	Y
Endozoicomonas	N	N	Y
Ensifer	Y	N	Y
Epsilonproteobacteria bacterium LFT 1.7	N	N	Y
Erythrobacteraceae bacterium CCH12-C2	N	N	Y
Ferrimicrobium	N	N	Y
Ferrimonas	N	N	Y
Ferriphaselus	N	N	Y
Ferrithrix	N	N	Y
Fervidicella	N	N	Y
Fervidicola	N	N	Y
Fibrisoma	N	N	Y
Fictibacillus	N	N	Y
Filomicrobium	N	N	Y
Fischerella	N	N	Y
Flammeovirga	N	N	Y
Flavisolibacter	N	N	Y
Flavobacterium	N	N	Y
Fodinicurvata	N	N	Y
Frankia	Y	Y	Y
Fulvimarina	N	N	Y

Fusobacterium	N	Y	N
gamma proteobacterium HdN1	N	N	Y
gamma proteobacterium HTCC2207	N	N	Y
Geitlerinema	N	N	Y
Geminicoccus	N	N	Y
Gemmatimonas	N	N	Y
Gemmobacter	N	N	Y
Geobacter	Y	Y	Y
Geodermatophilaceae bacterium URHB0048	N	N	Y
Geodermatophilaceae bacterium URHB0062	N	N	Y
Geodermatophilus	Y	Y	Y
Geosporobacter	N	N	Y
Gluconacetobacter	N	N	Y
Gluconobacter	N	N	Y
Gordonia	N	N	Y
Gracilimonas	N	N	Y
Granulibacter	N	N	Y
Granulicella	N	N	Y
Granulicoccus	N	N	Y
Hahella	N	N	Y
Halanaerobium	N	N	Y
Haliangium	N	N	Y
Halioglobus	N	N	Y
Haloarcula	N	N	Y
Halobacteroides	N	N	Y
Halocynthiibacter	N	N	Y
Halodesulfovibrio	N	N	Y
Haloferax	N	N	Y
Halofilum	N	N	Y
Haloglycomyces	N	N	Y
Halomonas	N	N	Y
Halonatronum	N	N	Y
Halopiger	N	N	Y
Halotalea	N	N	Y
Haloterrigena	N	N	Y
Heliobacterium	N	N	Y
Herbaspirillum	N	N	Y
Herbidospora	N	N	Y
Herbinix	N	N	Y
Herminiimonas	N	N	Y
Herpetosiphon	N	N	Y

Hoeflea	N	N	Y
Humibacillus	N	N	Y
Hyalangium	N	N	Y
Hydrocarboniphaga	N	N	Y
Hydrococcus	N	N	Y
Hydrogenibacillus	N	N	Y
Hydrogenophaga	N	N	Y
Hyphomicrobium	N	Y	Y
Ilumatobacter	N	Y	Y
Ilyobacter	N	N	Y
Immundisolibacter	N	N	Y
Inquilinus	N	N	Y
Intrasporangiaceae bacterium URHB0013	N	N	Y
Intrasporangium	N	Y	Y
Isoptericola	N	N	Y
Janibacter	N	Y	Y
Jannaschia	N	N	Y
Janthinobacterium	N	N	Y
Jatrophihabitans	Y	N	Y
Jiangella	N	N	Y
Kibdelosporangium	N	N	Y
Kiloniella	N	N	Y
Kineosphaera	N	N	Y
Kitasatospora	N	N	Y
Klebsiella	N	Y	N
Knoellia	N	N	Y
Komagataeibacter	N	N	Y
Kordiimonas	N	N	Y
Kribbella	Y	N	Y
Kribbia	N	N	Y
Ktedonobacter	N	Y	Y
Kushneria	N	N	Y
Kutzneria	Y	N	Y
Kyrpidia	N	N	Y
Labrenzia	N	N	Y
Labrys	N	N	Y
Lachnoclostridium	N	N	Y
Lachnospiraceae bacterium 3_1_57FAA_CT1	N	N	Y
Lachnospiraceae bacterium 6_1_63FAA	N	N	Y
Leadbetterella	N	N	Y
Lechevalieria	N	N	Y

Leisingera	N	N	Y
Lentimicrobium	N	N	Y
Lentisphaera	N	N	Y
Lentzea	N	N	Y
Leptolinea	N	N	Y
Leptolyngbya	N	N	Y
Leptospira	N	N	Y
Leptospirillum	N	N	Y
Litoreibacter	N	N	Y
Loktanella	Y	N	Y
Longispora	N	N	Y
Luteipulveratus	N	N	Y
Lyngbya	N	N	Y
Lysinibacillus	N	N	Y
Lysobacter	N	N	Y
Magnetococcus	N	N	Y
Magnetospira	N	N	Y
Magnetospirillum	Y	N	Y
Magnetovibrio	N	N	Y
Mameliella	N	N	Y
Maribacter	N	N	Y
Maribius	N	N	Y
Maricaulis	N	N	Y
Marichromatium	N	N	Y
marine gamma proteobacterium HTCC2143	N	N	Y
Marinobacter	N	N	Y
Marinobacterium	N	N	Y
Marinomonas	N	N	Y
Marinovum	N	N	Y
Marivirga	N	N	Y
Marmoricola	N	N	Y
Massilia	N	N	Y
Mastigocladopsis	N	N	Y
Megasphaera	N	N	Y
Melioribacter	N	N	Y
Mesorhizobium	Y	Y	Y
Metallosphaera	N	N	Y
Methanobacterium	Y	N	Y
Methanobrevibacter	N	N	Y
Methanocella	N	N	Y
Methanoculleus	N	Y	N

Methanosarcina	N	Y	Y
Methylibium	N	N	Y
Methylobacillus	N	N	Y
Methylobacter	N	N	Y
Methylobacterium	Y	Y	Y
Methylocaldum	N	N	Y
Methylocapsa	N	N	Y
Methyloceanibacter	Y	Y	Y
Methylocella	N	N	Y
Methylococcus	N	N	Y
Methylocystis	N	Y	Y
Methyloferula	N	N	Y
Methyloglobulus	N	N	Y
Methyloligella	N	N	Y
Methylomarinum	N	N	Y
Methylomicrobium	N	N	Y
Methylomonas	N	N	Y
Methylophaga	N	N	Y
Methylophilus	N	N	Y
Methylopila	N	N	Y
Methylosarcina	N	N	Y
Methylosinus	N	N	Y
Methylotenera	N	N	Y
Methyloversatilis	N	N	Y
Methylovorus	N	N	Y
Methylovulum	N	N	Y
Microbispora	N	N	Y
Microbulbifer	N	N	Y
Microcoleus	Y	N	Y
Micromonospora	Y	Y	Y
Microtetraspora	N	N	Y
Microvirga	N	Y	Y
Mitsuokella	N	N	Y
Mobilicoccus	N	N	Y
Modestobacter	N	N	Y
Moorella	N	N	Y
Moritella	N	N	Y
Mycobacterium	Y	Y	Y
Myxosarcina	Y	N	N
Natrialba	N	N	Y
Natrinema	N	N	Y

Natronohydrobacter	N	N	Y
Natronolimnobius	N	N	Y
Natronorubrum	N	N	Y
Neokomagataea	N	N	Y
Neorhizobium	N	N	Y
Neptuniibacter	N	N	Y
Neptunomonas	N	N	Y
Nevskia	N	N	Y
Niastella	N	N	Y
Nioella	N	N	Y
Nisaea	N	N	Y
Nitratireductor	Y	N	Y
Nitrolancea	N	N	Y
Nitrosomonas	N	N	Y
Nitrosopumilus	N	N	Y
Nitrososphaera	Y	Y	Y
Nitrospina	N	Y	Y
Nitrospira	Y	Y	Y
Niveispirillum	N	N	Y
Nocardia	Y	N	Y
Nocardioides	Y	Y	Y
Nocardiopsis	Y	Y	Y
Nonomuraea	N	N	Y
Noviherbaspirillum	N	N	Y
Novispirillum	N	N	Y
Novosphingobium	N	N	Y
Numidum	N	N	Y
Oblitimonas	N	N	Y
Oceanimonas	N	N	Y
Oceanithermus	N	N	Y
Oceanospirillum	N	N	Y
Ochrobactrum	N	N	Y
Octadecabacter	N	N	Y
Oleiagrimonas	N	N	Y
Oleiphilus	N	N	Y
Opitutus	N	N	Y
Orenia	N	N	Y
Ornatilinea	N	N	Y
Oscillatoria	N	N	Y
Oxalobacteraceae bacterium AB_14	N	N	Y
Paenibacillus	Y	Y	Y

Paenirhodobacter	N	N	Y
Paludibacterium	N	N	Y
Pandoraea	N	N	Y
Pannonibacter	N	N	Y
Paraburkholderia	Y	Y	Y
Paracoccus	N	Y	Y
Paramesorhizobium	N	N	Y
Paraprevotella	N	N	Y
Pararhizobium	N	N	Y
Patulibacter	N	N	Y
Pelobacter	Y	Y	N
Pelodictyon	N	N	Y
Pelosinus	N	N	Y
Peptococcaceae bacterium CEB3	N	N	Y
Phaeobacter	N	N	Y
Phaeospirillum	N	N	Y
Phenylobacterium	N	N	Y
Phormidesmis	N	Y	N
Photobacterium	N	N	Y
Phycicoccus	N	N	Y
Phyllobacterium	N	N	Y
Pimelobacter	N	N	Y
Piscicoccus	N	N	Y
Planctomycetaceae bacterium FC18	N	N	Y
Planomonospora	N	N	Y
Pleomorphobacterium	N	N	Y
Pleomorphomonas	N	N	Y
Pleurocapsa	Y	Y	N
Polaromonas	N	N	Y
Polycyclovorans	N	N	Y
Polymorphum	N	N	Y
Porphyrobacter	N	N	Y
Porphyromonadaceae bacterium FC4	N	N	Y
Porphyromonas	N	N	Y
Prauserella	N	N	Y
Propionibacterium	N	N	Y
Propionimicrobium	N	N	Y
Prosthecochloris	N	N	Y
Prosthecomicrobium	N	N	Y
Pseudaminobacter	N	N	Y
Pseudoalteromonas	N	N	Y

Pseudodonghicola	N	N	Y
Pseudoduganella	N	N	Y
Pseudogulbenkiania	N	N	Y
Pseudomonas	Y	Y	Y
Pseudonocardia	Y	Y	Y
Pseudooceanicola	N	N	Y
Pseudopelagicola	N	N	Y
Pseudorhodobacter	N	N	Y
Pseudorhodoferax	N	N	Y
Pseudothermotoga	N	N	Y
Pseudovibrio	N	N	Y
Psychromonas	N	N	Y
Pyrinomonas	N	N	Y
Ralstonia	N	N	Y
Raoultella	N	Y	N
Reinekea	N	N	Y
Reyranella	N	Y	Y
Rhizobiales bacterium CCH10-E5	N	N	Y
Rhizobiales bacterium CCH11-D2	N	N	Y
Rhizobiales bacterium CCH3-A5	N	N	Y
Rhizobiales bacterium HL-109	N	N	Y
Rhizobium	Y	Y	Y
Rhodobacter	N	N	Y
Rhodobacteraceae bacterium CY02	N	N	Y
Rhodobacteraceae bacterium EhC02	N	N	Y
Rhodobacteraceae bacterium HTCC2083	N	N	Y
Rhodobacteraceae bacterium KLH11	N	N	Y
Rhodobacteraceae bacterium PD-2	N	N	Y
Rhodococcus	Y	Y	Y
Rhodocyclaceae bacterium Paddy-1	N	N	Y
Rhodoferax	N	N	Y
Rhodomicrobium	N	N	Y
Rhodoplanes	Y	Y	Y
Rhodopseudomonas	Y	Y	Y
Rhodospirillaceae bacterium CCH5-H10	N	N	Y
Rhodospirillales bacterium URHD0088	Y	Y	Y
Rhodospirillum	N	N	Y
Rhodothermaceae bacterium RA	N	N	Y
Rhodovibrio	N	N	Y
Rhodovulum	N	Y	Y
Robiginitomaculum	N	N	Y

Roseateles	N	N	Y
Roseibium	N	N	Y
Roseiflexus	Y	N	Y
Roseimaritima	N	N	Y
Roseivirga	N	N	Y
Roseobacter	N	N	Y
Roseomonas	N	N	Y
Roseovarius	N	Y	Y
Rubritalea	N	N	Y
Rubrivivax	N	N	Y
Rubrobacter	Y	Y	Y
Ruegeria	N	N	Y
Ruminiclostridium	N	Y	Y
Saccharomonospora	N	N	Y
Saccharopolyspora	N	N	Y
Saccharothrix	N	N	Y
Sagittula	N	N	Y
Salinispora	N	N	Y
Salipiger	N	N	Y
Sciscionella	N	N	Y
Sedimenticola	N	N	Y
Sediminispirochaeta	N	N	Y
Selenomonas	Y	N	N
Serinicoccus	N	N	Y
Shewanella	N	N	Y
Shimia	N	N	Y
Silvibacterium	N	N	Y
Simiduia	N	N	Y
Singulisphaera	Y	Y	Y
Sinorhizobium	Y	N	Y
Skermanella	N	N	Y
Smaragdicoccus	N	N	Y
Solirubrobacter	Y	Y	Y
Sorangium	Y	Y	Y
Sphaerobacter	N	N	Y
Sphaerochaeta	N	N	Y
Sphingobium	N	Y	Y
Sphingomonadales bacterium EhC05	N	N	Y
Sphingomonas	N	Y	Y
Sphingopyxis	N	N	Y
Spirillospora	N	N	Y

Spirochaeta	N	N	Y
Spongiibacter	N	N	Y
Sporosarcina	N	N	Y
Stappia	N	N	Y
Starkeya	N	N	Y
Streptacidiphilus	Y	N	Y
Streptoalloteichus	N	N	Y
Streptomonospora	N	N	Y
Streptomyces	Y	Y	Y
Streptosporangium	Y	N	Y
Sulfitobacter	N	N	Y
Sulfobacillus	N	N	Y
Sulfolobus	N	N	Y
Sulfurimonas	N	N	Y
Sulfurospirillum	N	N	Y
Symbiobacterium	N	N	Y
Syntrophothermus	N	N	Y
Tangfeifania	N	N	Y
Tardiphaga	N	N	Y
Tateyamaria	N	N	Y
Tenacibaculum	N	N	Y
Tepidicaulis	N	N	Y
Tepidimonas	N	N	Y
Tepidiphilus	N	N	Y
Terasakiella	N	N	Y
Terrabacter	N	N	Y
Tessaracoccus	N	N	Y
Thalassobacter	N	N	Y
Thalassobius	N	N	Y
Thalassolituus	N	N	Y
Thalassospira	N	N	Y
Thauera	N	N	Y
Thaumarchaeota archaeon N4	N	N	Y
Thermacetogenium	N	N	Y
Thermoactinomyces	N	Y	Y
Thermoanaerobacter	N	N	Y
Thermobifida	N	N	Y
Thermococcus	N	N	Y
Thermodesulfatator	N	N	Y
Thermodesulfobacterium	N	N	Y
Thermofilum	N	N	Y

Thermogemmatispora	N	N	Y
Thermomicrobium	N	N	Y
Thermomonospora	Y	N	Y
Thermonema	N	N	Y
Thermopetrobacter	N	N	Y
Thermoproteus	N	N	Y
Thermorudis	N	N	Y
Thermosediminibacter	N	N	Y
Thermosulfidibacter	N	N	Y
Thermotoga	N	N	Y
Thermovenabulum	N	N	Y
Thermus	N	Y	Y
Thioalkalivibrio	N	N	Y
Thiobacillus	N	N	Y
Thiocapsa	N	N	Y
Thioclava	N	N	Y
Thiomonas	N	N	Y
Tistrella	N	N	Y
Trichodesmium	N	N	Y
Tropicibacter	N	N	Y
Tyzzerella	N	N	Y
Variovorax	N	N	Y
Verrucosispora	N	N	Y
Vibrio	N	N	Y
Vogesella	N	N	Y
Wenxinia	Y	N	N
Williamsia	N	N	Y
Woeseia	N	N	Y
Xanthobacter	N	N	Y
Xylanimonas	N	N	Y
Xylophilus	N	N	Y
Zetaproteobacteria bacterium TAG-1	N	N	Y
Zhongshania	N	N	Y
Zooshikella	N	N	Y